ANALYZING THE COMBINED IMPACT OF CLIMATE AND LAND USE LAND COVER CHANGE ON THE HYDROLOGICAL RESPONSE OF JHELUM RIVER BASIN IN KASHMIR

A THESIS SUBMITTED TO
THE BOARD OF GRADUATE PROGRAMS
OF
MIDDLE EAST TECHNICAL UNIVERSITY, NORTHERN CYPRUS CAMPUS

BY

INJILA HAMID

IN PARTIAL FULFILLMENT OF THE REQUIREMENTS
FOR
THE DEGREE OF MASTER OF SCIENCE
IN SUSTAINABLE ENVIRONMENT AND ENERGY SYSTEMS PROGRAM

JULY 2022

Approval of the Board of Graduate Programs

Prof. Dr. Cumali SABAH
Chairperson

I certify that this thesis satisfies all the requirements as a thesis for the degree of Master of Science

Assoc. Prof. Dr. Ceren İNCE DEROGAR
Program Coordinator

This is to certify that we have read this thesis and that in our opinion it is fully adequate, in scope and quality, as a thesis for the degree of Master of Science.

Asst. Prof. Dr. Bertuğ AKINTUĞ
Supervisor

Examining Committee Members

Assoc. Prof. Dr. Yeliz Yeşilada YILMAZ	METU NCC/ Computer Engineering Program	
Asst. Prof. Dr. İbrahim BAY	European University of Lefke/ Civil Engineering Department	
Asst. Prof. Dr. Bertuğ AKINTUĞ	METU NCC/ Civil Engineering Program	

I hereby declare that all information in this document has been obtained and presented in accordance with academic rules and ethical conduct. I also declare that, as required by these rules and conduct, I have fully cited and referenced all material and results that are not original to this work.

Name, Last name: Injila, Hamid

Signature:

ABSTRACT

ANALYZING THE COMBINED IMPACT OF CLIMATE AND LAND USE LAND COVER CHANGE ON THE HYDROLOGICAL RESPONSE OF JHELUM RIVER BASIN IN KASHMIR

Hamid, Injila
Master of Science, Sustainable Environment and Energy Systems Program
Supervisor: Asst. Prof. Dr. Bertuğ Akıntuğ

July 2022, 120 pages

In terms of efficient and sustainable management of water resources of a basin, land use land cover (LULC) and climate change impact studies hold utmost importance. Land use change dynamics along with the climate change owing to greenhouse gas emissions are altering the hydrological response of river basins. This study therefore focuses on quantifying the combined impact of LULC and climate change on the water balance components of the Jhelum river basin using Soil and Water Assessment Tool (SWAT) hydrological model. In the analysis, SWAT-CUP (SUFI-2 algorithm) was employed to calibrate and validate the model using Nash-Sutcliffe Efficiency (NSE) as the objective function. Model performance was evaluated using statistical parameters such as R^2, NSE, PBIAS and KGE that demonstrated satisfactory results. Future projections of climate change using bias corrected NorESM1-M model have also been utilized in this study under medium emission RCP 4.5 and high emission RCP 8.5 radiative forcing to estimate the changes in mean annual temperature and precipitation during mid (2041 – 2070) and end of the

21st century (2071 – 2100) in the Jhelum river basin. Moreover, projected future hydrological response of the basin as a result of this climate change has been quantified in terms of the changes exhibited by the water balance components of the basin using SWAT model.

Keywords:, LULC, Hydrological Modeling, SWAT, SUFI-2, Jhelum River Basin

ÖZ

İKLİM VE ARAZİ KULLANIMI ARAZİ ÖRTÜSÜ DEĞİŞİKLİĞİNİN KAŞMİR'DEKİ JHELUM NEHİR HAVZASININ HİDROLOJİK TEPKİSİ ÜZERİNDEKİ BİRLEŞİK ETKİSİNİN ANALİZİ

Hamid, Injila
Yüksek Lisans, Sürdürülebilir Çevre ve Enerji Sistemleri
Tez Yöneticisi: Dr. Öğr. Üyesi Bertuğ Akıntuğ

Temmuz 2022, 120 sayfa

Bir havzanın su kaynaklarının verimli ve sürdürülebilir yönetimi için, arazi kullanımı arazi örtüsü (AKAÖ) ve iklim değişikliği etkisi çalışmaları en üst düzeyde önem taşımaktadır. İklim değişikliği ile birlikte arazi kullanım değişikliği dinamikleri de sera gazı emisyonlarını artırdığından nehir havzalarının hidrolojik tepkisini tkilemektedir. Bu nedenle bu çalışmada, SWAT hidrolojik modeli kullanılarak Jhelum nehir havzasının su dengesi bileşenlerinde arazi kullanımı arazi örtüsü ve iklim değişikliğinin birleşik etkisinin ölçülmesine odaklanılmaktadır. Modelin kalibrasyonu ve doğrulanması için SWAT-CUP (SUFI-2 Algoritması) Nash-Sutcliffe Efficiency amaç fonksiyonuyla birlikte kullanıldı. Tatmin edici sonuçlar alınan modelin performansı R^2, NSE, PBIAS ve KGE gibi istatistiksel parametreler kullanılarak değerlendirildi. Bu çalışmada, Jhelum nehir havzasında 2041-2070 ve 2071-2100 dönemlerine ait yıllık ortalama sıcaklık ve toplam yağış değerleri orta emisyon (RCP-4.5) ve yüksek emisyon (RCP-8.5) durumlarındaki gelecek iklim

değişikliği projeksiyonlarına göre NorESM1-M Modeli kullanılarak elde edilmiştir. Ayrıca, iklim değişikliğinin sonucu olarak havzanın gelecekteki tahmini hidrolojik tepkisi, havzanın su dengesi bileşenlerinin sergilediği değişiklikler açısından dikkate alınarak açısından SWAT modeli kullanılarak belirlenmiştir.

Anahtar Kelimeler: Arazi Kullanımı Arazi Örtüsü, Hidrolojik Modelleme, SWAT, SUFI-2, Jhelum Nehri Havzası

Dedication

I would like to dedicate this work to my parents, Mr. Abdul Hamid Rather and Ms. Ishrat Hamid, for being the backbone of my life and prioritizing our needs even before their own.

ACKNOWLEDGMENTS

I would humbly like to thank Allah (SWT), the most High and the most Honoured for guiding me during the course of this journey through various people. The conception, execution and compilation of this work is a result of the contribution of precious time and efforts of some people who I would like to mention and thank generously.

Firstly, I would like to thank my supervisor, Assist. Prof. Dr. Bertuğ Akıntuğ, for helping and encouraging me during this study period through his valuable experience and extensive knowledge of the subject. I am also grateful to him for providing me with the free learning atmosphere that also allowed for critical analysis of the different aspects of this research work.

I would also like to mention the generosity of Irrigation and Flood Control Department, Kashmir Division and Indian Meteorological Department, Kashmir for providing me access to the hydrological and meteorological data of the Kashmir valley. Additionally, I would like to thank Mr. Lateef Ahmad Dar and Mr. Shahid Gulzar for helping me acquiring the data.

I am also especially grateful to my family members who have stood with me throughout. I am thankful to my parents, Mr. Abdul Hamid Rather and Ms. Ishrat Hamid for encouraging, supporting, motivating and teaching me that there is always room for improvement. I thank my siblings Ms. Haiqa Hamid, Mr. Muhammad Umaid Rather and Ms. Maira Hamid for their genuine love, encouragement and help at every stage of my life.

Last but not the least; I would like to extend my appreciation to the Chemistry Department of METU, NCC for offering me the position of a Teaching Assistant during my time on campus as a scholarship that taught me some of the valuable lessons of life to carry ahead with me.

TABLE OF CONTENTS

LIST OF TABLES

TABLES

LIST OF FIGURES

FIGURES

LIST OF ABBREVIATIONS

ABBREVIATIONS

LULC	Land Use Land Cover
RS	Remote Sensing
GIS	Geographic Information System
SWAT	Soil and Water Assessment Tool
SWAT-CUP	SWAT Calibration and Uncertainty Program
CMhyd	Climate Model data for Hydrologic Modeling
GCM	General Circulation Model
RCP	Representative Concentration Pathway
RCM	Regional Climate Model
HEC-HMS	Hydrologic Engineering Center's Hydraulic Modeling System
MIKE SHE	MIKE Systeme Hydrologique Europeen
ANN	Artificial Neural Network

CHAPTER 1

INTRODUCTION

1.1 Introduction

Global climate change phenomenon is acknowledged as a threat in the social and environmental domains by the scientific community worldwide [Lee et. al. 2015]. Apart from the economic losses suffered on a global scale, which have reportedly surged from an average of US$7 billion per year in 1980's to around US$24 billion per year for the 2001-2011 period, thousands of human lives are claimed annually on an average to flood calamity with South and Southeast Asia having a major share [Kundzewicz et. al. 2014]. The frequent instances of extreme weather events unfolding have impelled the researchers to develop models that can predict and assess the influence of global warming on recurring floods and heatwaves [Schiermeier 2018]. Consequently, the research community revved up, more so in the last two decades to investigate trends depicted by the meteorological variables as a response to changing climate both at the global as well as the regional levels. These researches provide sufficient evidence that natural causes alone are not to be attributed as the sole reason inciting climate change but also the consequences of human activities have a major role [Kadioglu 1997, Tabari et. al. 2011, Gocic and Trajkovic 2013]. Analyzing the trend of rainfall time series holds more importance for countries like India whose major share of economy and food security rely on the appropriate availability of water resources. Climate change studies have been reported far and wide in literature acknowledging the bearing it has on water resource hydrology and the implications thereof. The proper management of water resources and the prediction of probable occurrence of deviations from the expected river discharge in the form of floods or droughts demands detailed investigation into the response of the watershed. Aligning with this thought, various studies have been

undertaken reporting the impact of climate change on water resource regimes utilizing numerous statistical and hydrological modelling techniques. A modified method of two-parameter climate elasticity index was applied to two basins namely, the Spokane river basin in the USA and the Yellow River basin in China by Fu et. al. (2007) who reported that the runoff regionally generated depends critically on the temperature, however a non-linear relation was revealed for the response of streamflow to variations in temperature and precipitation. The impact of climate change was projected on the future streamflow of Bernam river basin in Malaysia and Yarlung Tsangpo-Brahmaputra River basin in China for predicting the changes in water resources as a response to climate change [Ismail et. al. 2020, Xu et. al. 2018]. Such studies can be helpful for the case of Jhelum River basin also where the temporal shifting of runoff and fluctuations in its quantity on account of snow and glacial melt in the Himalayan region have potential implications on the availability of water for agricultural requirements in summer [Jeelani et. al. 2012].

Although there exists a complex nature of relationship between the basin response and the climate extremes, yet such studies enhance our understanding of the climate trends and aid in projecting the probable future events. A study examining the existing trends demonstrated by climatological variables and simulating future extreme climate events suggested increased intensity and frequency of extreme precipitation and maximum-minimum temperature events in future in the valley of Kashmir attributed to climate change [Gujree et. al. 2017]. Of the diverse climate change impacts on the river hydrology, a serious concern is the recession of glacial area for the Jhelum river basin whose streamflow is predominantly snow-fed through its tributaries. A major tributary feeding River Jhelum – the Lidder catchment area has witnessed 27.47% reduction in its glacier area within 51 years from 1962 to 2013 [Romshoo et. al. 2015]. More importance has been ascribed to the natural storage of fossil water in the form of glaciers than that available in the snowpack as a seasonal storage. Consequently, the glacial retreat caters to the threat imposed in the critical region of Himalayas feeding the rivers during the summer months implying that their shortage might arrive abruptly ceasing the water supply to the region [Barnett et. al.

2005]. Although there is no concrete evidence suggesting increased frequency of extreme weather events unfolding in the Kashmir valley that has endured 30 major floods in its recorded history. However, the 2014 major flooding of the Jhelum river bearing similar magnitude (3,254.50 m^3/s) of 1903 and 1959 floods insinuated the flood event as one having 50-year return period [Meraj et al. 2015a]. Nonetheless, increased human population and unplanned urbanization around the river banks, encroached wetlands that used to soak the outpours of the river and minor water channels along with the silting of the river has intensified and exacerbated the response and management of extreme weather events – like floods occurring in the valley claiming more human lives apart from damaging economy and infrastructure [Meraj et. al. 2015b, Romshoo et. al. 2017, Zaz et. al. 2019]. Srinagar has recorded a significant surge per decade of 0.07 ^oC for its annual mean temperature from 1894-2000 [Fowler and Archer 2005].

In the past two decades, with the rapid expansion of population and increasing human exploitation of the available natural resources to meet their ever growing needs, the land use land cover change studies using Remote Sensing (RS) and Geographic Information System (GIS) has received much importance. Tracing such changes in the land use patterns in space and time plays a crucial role in understanding the implications of natural and man induced changes on the environment. Altering land cover patterns has been a chief contributor to the global environmental change. It is estimated that 20% of the global carbon dioxide emissions are a consequence of the degraded forest cover [Van Der Werf et al. 2009]. Unplanned urbanization especially at the cost of over exploiting natural resources renders the human and other lives alike, more vulnerable to natural disasters. Analyzing the land cover changes act as a crucial step towards curtailing further damage to the biosphere through poorly managed and unchecked utilization of the natural resources. However, analyzing these LULC changes manually on a large scale are time consuming, arduous and economically impractical. The LULC analysis has been simplified essentially by making the remotely sensed satellite data available for free use.

LULC change studies have been utilized for wide range of objectives ranging from monitoring their impact on risk of soil erosion, increasing land surface temperature, to assessing the change in watershed characteristics. LULC change when incorporated in hydrological models can further be used for ground water level and water quality assessment [Grecchi et al. 2014]. Land cover classification has also been employed for observing the non-point source pollutants using the remote sensing satellite imagery by developing a relation between the changing LULC patterns with the water quality [Abdulkareem et al. 2018a]. Effect of LULC changes on the groundwater recharge rates and surface response studies are also based on land use land cover change studies.

Various techniques available for monitoring the LULC changes include supervised classification, unsupervised classification and object-oriented/based classification techniques [Enderle and Weih 2005, Weih and Riggan 2010]. An important prerequisite of employing the supervised classification technique demands prior understanding and knowledge of the area to be classified [Campbell and Wynne 2011]. The analyst defines numerous land classes by assigning pixels to each land class with the help of ground truth data and analyst's acquaintance with the geographical area to be classified. Spectral signatures are then formed for the specific spectral reflectance of each land class. Maximum likelihood classification technique, which is a type of supervised classification, is the most commonly used method for classifying remotely sensed satellite data [Jensen 1986, Purkis and Klemas 2011]. Of the other available techniques adopted for classification, the main advantage offered by maximum likelihood is that the whole range of spectral variability is taken into consideration and not only the mean. It then considers the band of spectral signatures provided for a particular land class to be normally distributed and allots a specific pixel to that land class which finds the maximum probability of being a part of it [Kantakumar and Neelamsetti 2015]. In this study, the maximum likelihood classification technique was utilized to classify the raw satellite imagery.

Water forms the central most necessity of human and other lives alike. Quantifying the importance of water in our day-to-day life is almost impossible as nearly

everything we need directly or indirectly uses water. Societies depend on sufficient availability of quality water for drinking, irrigation, sanitation, cleaning, industrial and other purposes. However, with the passage of time, the dependence and pressure on this natural resource has seen a constant escalation because of increasing population, climate change and urbanization. Its accessibility is more important for areas whose major share of economy is dependent on agriculture like India [Bolch, 2017]. In addition to other negative impacts on the biosphere, changes in the climate are affecting the streamflow of river basins. Marked changes in temperature and precipitation that have direct impact on the streamflow of the river basin have been reported in numerous studies.

Due to the increased emission of greenhouse gasses in the atmosphere, rising temperatures affect the precipitation patterns and also interfere with the natural balance of the hydrological cycle. As a result, the surface moisture conditions get altered because of increased temperature. Such changes lead to hydrological droughts and affect the vegetative cover of the basin [Tripathi and Mishra 2017, Dai et al. 2018]. Therefore, LULC changes form another major factor to which the water balance components of a basin show sensitivity. The LULC of a watershed has huge impact on the infiltration as well as the potential evapotranspiration (PET) characteristics of the area. While as the canopy cover of a vegetation has buffering impact on the quick evaporation of soil moisture; barren and urbanised lands hasten this process and also stimulate increased surface runoff owing to their impervious nature [Metzger et al. 2014]. Nonetheless, the hydrology of each watershed is unique because of its varying sensitivity to natural and man induced changes. This makes the analysis of a watershed more complex as it is difficult to predict and study the hydrological response of a watershed using physical based models given the range of different factors, huge amount of input data, long computational time during calibration and skill of the modeller that can affect quality of the model generated [Belvederesi et al. 2020]. Despite that, recent studies have attempted to estimate the response of streamflow to the combined impact of LULC and climate change through hydrological modelling by using different tools. These different tools include HEC-

HMS, SWAT, MIKE SHE and ANN's [Abdulkareem et al. 2018b]. Amongst these, one of the most popular and extensively used software is the Soil and Water Assessment Tool (SWAT) because of its flexibility to be used for different types of watersheds and generating reliable results [Neitsch et al. 2011, Gassman et al. 2014]. SWAT has the ability to incorporate all the measurable parameters in a watershed that have an impact on the catchment response including land cover, soil, slope and weather characteristics. Therefore, various studies have been conducted utilizing SWAT to identify the streamflow changes in a basin because of the altered land cover patterns and the increased frequency of experiencing peak flood events. While some have reported more erratic streamflow patterns owing to deforestation in the catchments, certain other studies have concluded that climate change is a major driver of changes in annual and seasonal discharge. Subsequently, it becomes imperative for the effective management of water resources and sustainability of an area to study the combined impact of LULC and climate change at the basin level.

Furthermore, predicting the streamflow response under the future climate scenarios based on a reliable developed model is a significant study in terms of preparedness, planning and management policies. Several Global Circulation Models (GCM's) have been utilized in SWAT after downscaling for projecting the probable future water balance components. The most commonly used future climate scenarios have been Representative Concentration Pathways RCP 4.5 and RCP 8.5 [Buras and Menzel 2019]. Across different basins, the future predictions for annual mean temperature project an increasing trend throughout with variable projections for future precipitation and streamflow until the end of 21st century [Haider et al. 2020].

The Jhelum river basin in India is of utmost importance not only for the inhabitants of Kashmir valley but also because it is a transboundary river flowing into Pakistan. River Jhelum and its tributaries drain the densely populated valley of Kashmir providing livelihood to its inhabitants and is also harnessed for hydroelectric power generation. However, insufficient data is available in the public domain because of limited number of meteorological stations located in the plains and only 3 hydrological stations on the Jhelum river under Irrigation & Flood Control

Department (I&FC) Kashmir. Hydrological impact studies using modelling require high quality data and sufficient number of hydro-meteorological stations depicting the true hydrological and climatological characteristics of the study area. In view of these limitations, a comprehensive analysis comprising the LULC and climate change impact on the hydrological response of the Jhelum river basin has not been carried out so far.

Therefore, the first part of this study is aimed to investigate in detail the statistical trends shown by hydro-meteorological parameters namely temperature, precipitation and streamflow for the Jhelum River basin in Kashmir valley over the past forty-one years (1980-2020) using Mann-Kendall and Sen's Slope Estimator tests. The effect of change in these meteorological parameters on the catchment response i.e. river discharge of Jhelum was also analyzed. Bravais-Pearson correlation coefficient was used to find correlations between various hydro-meteorological parameters to analyse the interrelationship between these parameters.

Due to the lack of proper governance and management of natural resources in the Kashmir valley, land use land cover has experienced remarkable changes over the past three decades. So far, the LULC change analysis for the whole Kashmir valley has not been carried out. As a result, the second part of this study is aimed to analyze changing land use patterns and quantify the transforming land cover for the whole valley of Kashmir over a three decade period spanning (1992 to 2020) using RS and GIS technology. Three decade period was selected for LULC change analysis instead of using the 4 decade period which was utilized in the trend analysis because of the availability of quality satellite images for the Kashmir valley. The satellite images available for the study area before 1992 lacked clarity to be classified using GIS software.

Finally, in the last part of this study the aim is to 1) develop a SWAT model using a detailed LULC, soil map and gridded weather data of the basin, 2) study the combined impact of LULC and climate on the water balance components of the

Jhelum river basin from 1984 – 2013 and 3) use bias corrected Regional Climate Model (RCM) to predict the future hydro-meteorological response of the basin under RCP 4.5 and RCP 8.5 till the end of 21st century

The motivation of this study stems from the fact that there exists a dearth in literature of a comprehensive analysis of the combined impact of land use land cover change on the hydrological response of the Jhelum river basin in Kashmir valley. Such studies hold immense significance for the hydrologists and even the common masses to be aware of the changing streamflow patterns because of the climate and LULC change. Water is a basic need of every life present on this planet, as a result it is important to be fully aware of the changes in this natural resource and its proper management and judicious use.

1.2 Objectives of the Study

The objectives or goals of this study have been listed below:

1. Trend analysis of the hydro-meteorological parameters of the Jhelum river basin in Kashmir.
2. Analyzing the changing land use land cover dynamics over the past 3 decades [1992 – 2020] in Kashmir valley using GIS.
3. Observing the combined effect of land use land cover and climate change on the hydrological response of Jhelum river basin in Kashmir for the past 4 decades using SWAT model.
4. Predicting the future hydrological response of the basin till the end of 21st century using the developed SWAT model.

1.3 Content of the Thesis

The first chapter of this study includes the introduction. In the 2nd chapter, literature review has been discussed. Thereafter, in the 3rd chapter study area is explained in

detail and the data that is required for achieving the goals of this study. In the 4th chapter, methodology has been explained. Subsequently, in the 5th chapter results obtained from this study have been discussed in detail. And finally, in the 6th chapter concluding remarks have been enumerated.

CHAPTER 2

LITERATURE REVIEW

Climate change impact studies have been reported extensively in literature. Studies that have focused on trend analysis of hydro-meteorological parameters, along with land use land cover changes in the river basins have been discussed briefly in the subsequent section. Additionally, research papers throwing light upon hydrological modeling using SWAT to incorporate the combined impact of land use land cover and climate change impact on the hydrological response of different river basins have also been discussed.

2.1 Trend Analysis

Various studies have been conducted utilizing the trend analysis to find out the patterns followed by the meteorological parameters and streamflow in different parts of the world. Some of such studies have been discussed as under.

Gajbhiye et al. (2015) carried out the trend analysis of rainfall time series of the Sindh river basin in India using Mann-Kendall and Sen's Slope Estimator tests. A significant increase in the seasonal as well as the annual rainfall was observed from 1901 to 2002 for the basin.

Wani (2014) conducted a historical trend analysis of the climatic variables and streamflow response in the upper Jhelum catchment to the varying climate. Temperature data for six meteorological stations was analyzed using Student's t test for a period spanning 1975 to 2009. Kendall's correlation was used to explore the relation between the seasonal and annual temperature and precipitation. While as winter temperature showed significant increase, the precipitation of the basin

exhibited a declining trend with significant correlation between precipitation and discharge.

Mahmood and Jia (2017) observed trends in climatic variables like temperature and precipitation in the transboundary Jhelum river basin using Mann-Kendal and Sen's Slope Estimator tests. Minimum and maximum temperature showed an overall increase in the basin while as precipitation exhibited variable trends. However, a decreasing trend for seasonal and annual precipitation dominated in the basin.

Ashraf and Hanif-ur-Rehman (2019) studied the response of water resource regimes in the upstream and downstream Indus river basin to changing climate. They also developed correlation to find the variation of changing temperature and precipitation with the streamflow of the basin.

Shafiq et al. (2020) carried out a trend analysis of the hydro-meteorological parameters in the Jhelum river basin from 1980 to 2015 and also tried to correlate the different climate parameters with the discharge of the river basin. Their study revealed rising mean maximum and mean minimum temperature 0.05 °C/year and 0.01 °C/year respectively. While the precipitation showed a substantial decline of 4.2 mm/year.

Fu et al. (2007) developed a two-parameter climate elasticity index in relation with both temperature and precipitation to find out the relation between the meteorological parameters of the Spokane basin and the streamflow and assess at the same time the impact of changing climate on the streamflow of the river basin. A 20% increase in the precipitation changed the climate elasticity for streamflow for an increase in the temperature from 1 °C to 1.8°C.

Ismail et al. (2020) studied the climate change impact on the future streamflow of the Bernam river basin in Malaysia. 10 Global Climate Models were used for this

study and a 9.14 % decline in the streamflow for the worst case scenario of RCP 8.5 was projected.

Xu et al. (2018) projected the future climate change impact on the streamflow of the Yarlung Tsangpo-Brahmaputra River (YBR) with the help of a hydrological model and regional climate projections fom CORDEX. The results showed an increasing trend with greater magnitude under the RCP 8.5 scenario as compared to the RCP 4.5 scenario.

Tan et al. (2019) observed the trends in temperature and precipitation extremes over the Muda river basin from 1985 to 2015. They employed Mann-Kendal and Sen's slope estimator tests to carry out the analysis. Overall the annual temperature showed increasing trend while as the total precipitation showed decreasing trend in the basin with variable trends for monthly parameters.

Gujree et al. (2017) evaluated the trends and variability in the exreme climate events using PRECIS RCM simulations in the Kashmir valley. Trend analysis was conducted using Mann-Kendall test and Theil-Sen estimator test. An increasing trend was observed by using the future climate scenarios in extreme hot events from 1990 to 2098.

Romshoo et al. (2015a) analyzed the impact of shrinking snow and ice cover under changing climate on the discharge of Lidder catchment in the upper Indus river basin. Their results suggested a 27.47% reduction in the glacier cover in the basin due to climate change.

Croitoru and Minea (2014) studied the impact of climate change on the river discharge in Eastern Romania from 1950 to 2006 using Mann-Kendall and Sen's slope estimator tests. Bravais Pearson correlation was employed to find the relation

between the precipitation and the river discharge of the basin. An increase in the temperature as well as precipitation was observed in the catchment.

Tabari et al. (2011a) evaluated the trends in temperature and precipitation for Iran from 1966 to 2005 using Mann–Kendall, Mann–Whitney and Mann–Kendall rank statistic tests. While as temperature showed increasing trend all across the stations annually however, precipitation exhibited varibale trends.

It is observed from these studies that the temperature has shown an increasing trend while as precipitation and streamflow have shown a decreasing trend in most of the places.

2.2 Land Use Land Cover Change Analysis

Various research studies have reported LULC change to analyse the changing dynamics of land patterns and understand how the increasing population is affecting the usage of this natural resource. Some of such studies have been discussed as follows:

Guler et al. (2007) assessed the land use land cover changes using Landsat data in Samsun, Turkey from 1980 to 1999. The area of dense forests reportedly reduced from 41.09% to 29.64% of the total area according to their study and the urban areas increased from 0.77% to 2.47% of the total area.

Diallo et al. (2009) studied the changes in land use land cover in Puer and Simao Counties of Yunnan Province from 1990 to 1999. Their study suggested increase in urban areas (16.72%) and reduction in forest areas (18.77%) amongst other changes that affect the environment and lead to climate change.

Nie et al. (2011) evaluated the impact of land use land cover changes on the hydrology of the upper San Pedro catchment using hydrological modeling and multiple regression technique. They concluded that urban area increase is the most important factor that leads to increased runoff in the basin.

Elmahdy et al. (2020) studied the impact of land use land cover change on the groundwater quality and its level in the northern area of the United Arab Emirates from 1990 to 2018. Changes were reported as increase in the urban areas and vegetative cover that directly linked with the changes in the groundwater quality and level.

Gazi et al. (2020) evaluated the changes occuring in the land use land cover in Chittagong metropolitan area of Bangladesh from 1989 to 2018 and linked its impact with the raising land surface temperature. According to their study the mean annual temperature incresaed by 6.5 ℃ through the time period of study owing to changes in the land cover patterns.

Basnyat et al. (2000) studied the non-point source of pollution for the watershed using RS and GIS techniques. A model was developed to identify the various sources of pollution to the watershed in terms of contribution of nitrate from urban, residential or other forested areas.

Owuor et al. (2016) evaluated the response of groundwater recharge rate as well as surface runoff to the changes in land use land cover for semi arid areas. The study revealed an increase in the surface runoff from 1 to 14.1% by the conversion of forest land to other LULC.

It has been observed from literature review of LULC change, that in most of the places urbanization is accompanied with deforestation and reductions in the cover of water bodies. Glacier cover has also gone down and such changes have harmful

impacts on the natural balance between man and environment which can be observed by the increased frequency of floods and droughts in different parts of the world.

2.3 Climate Change Scenarios

Climate along with LULC change impact studies through hydrological modelling are of utmost importance for understanding the dynamics of changing streamflow in any basin as water is a basic necessity for one and all alike. Therefore, research studies reporting results from such analysis have been discussed in this section.

Drogue et al. (2004) studied the response of streamflow to climate change scenarios in Alzette watershed by developing a continuous time scale hydrological model. Variations in the streamflow along with changes in precipitation patterns and potential evapotranspiration were reported as the impact of climate change for the basin.

Azari et al. (2016) evaluated the effect of cliamte change on the streamflow and sediment yield of Gorganroud watershed in Northern Iran using SWAT hydrological model and general circulation model data. They concluded that sediment yield had more influence of climate change than streamflow of the basin.

Asadieh and Krakauer (2017) studied the global changes in streamflow because of climate change till the end of 21st century. Their study suggested increasing streamflow near the Arctic circle and reductions in discharge in arid tropical areas under the high emission RCP 8.5 scenario.

Jiang et al. (2020) studied the impact of climate change on the streamflow of Nicolet river basin in Quebec in terms of melting snow. SWAT hydrological model was set up for the basin for eleven future climate model data and the results suggested flooding during winter season. Future peak flows showed earlier occurance due to

the increased temperature accompanied with enhanced magnitude owing to increasing precipitation.

Deng et al. (2015) evaluated the influence of land use land cover change on the surface energy and water balance components of the Heihe catchment in China from 2000 to 2010. The impact was measured in terms of changes in precipitation, runoff and evapotranspiration.

Yifru et al. (2021) studied the effect of land use land cover and climate change on the water yield and groundwater recharge in East African Rift valley. Their results pointed towards increasing mean annual temperature and precipitation apart from water scarcity arising mostly because of changes in climate.

Olivera and DeFee (2007) studied the influence of growing urbanization on the runoff of Whiteoak Bayou watershed in Texas from 1949 to 2000. Their findings suggested that post 1970 the annual runoff depth and peak flow has witnessed a surge of 146% and 159% respectively in the basin owing to urbanization.

Guo et al. (2008) studied the seasonal as well as annual discharge response to land use land cover and climate change on the Poyang Lake watershed in China. Their study reported that climate change has a dominant effect on the streamflow of the basin while as land use land cover change only moderately influences it. However, land use land cover change has a major impact on the seasonal variation of the basin.

Mango et al. (2010) evaluated the impact of land use land cover and climate change on the water flux of upper Mara river basin. They reported from their study that land cover changes lead to more unexpected changes in the discharge of the river basin while as the climate change parameters exhibit a more predictable response.

Jodar-Abellan et al. (2019) studied the impact of land use land cover and climate change on the prediction of flas floods in five Mediterranean watersheds of Spain using SWAT hydrological model. Their findings suggested an increment by two or three times in the peak flow of the basin because of changes in the land cover patterns mostly in the form of urbanization from 1990 to 2012.

Nilawar and Waikar (2019) evaluated the impact of climate change on the streamflow and sediment yield of Purna river watershed in India under RCP 4.5 and RCP 8.5 emission scenarios. Seasonal temperature and precipitation are expected to increase under both radiative forcings untill the end of 21st century. The streamflow exhibited a more pronounced increasing trend under the high emission scenario RCP 8.5.

Shah et al. (2020) studied the impact of climate change on the hydrological response in the glaciered region of the upper Indus river basin using climate change scenarios. Their results suggested and increase in the temperature, precipitation and streamflow of the basin ranging from 2 to 5 ^{o}C, 2.4% to 4.6% and 15.86% to 20.13% under two emission scenarios of RCP 4.5 and RCP 8.5. respectively untill the end of 21st century.

Chanapathi and Thatikonda (2020) studied the impact of land use land cover and climate change on the hydrological response of the Krishna river basin in India under present and future climate scenarios. Contrasting response of the streamflow was observed to changes in climate and land use land cover changes in the basin. The importance of incorporating water storage structures was also highlighted in the study.

Yaseen et al. (2020) projected the future streamflow of the basin using SWAT and global climate models on the transboundary river of Mangla catchment in Pakistan.

15% increase in the streamflow was projected by the end of 21st century owing to increase in the temperature and melting glacier in the basin.

Future projections across different study areas have reported an increasing and decreasing trend in the temperature and precipitation respectively by the end of 21st century utilizing different climate models. Most of the studies have also found out significant surge in the peak flow of rivers for future streamflow projections which is a serious issue and needs immediate remediation.

2.4 Research Gap

This study utilizes hydrological modelling to analyze the combined impact of climate and land use land cover change on the hydrological response of the Jhelum river basin in Kashmir using SWAT model. From literature review it was found out that no such studies have been conducted for the basin as of yet using this methodology. Therefore, this study was conducted with the above-mentioned aim to provide a comprehensive analysis of the hydrological scenarios in the basin in terms of impact assessment study for changing climate and land use land cover change as a valuable contribution to the hydrologists for proper management of water resources in the basin.

CHAPTER 3

STUDY AREA AND DATA

3.1 Hydro-Meteorological Data

The study area comprises the valley of Kashmir bordered by the Pir Panjal range in the South and Western side, the Zanskar range in the East and the Karakoram range from the Northern side which constitute the Western Himalayan range. Covering an area of approximately over 15,900 km^2 extending from 33°40' N to 34°30' N latitude and 73°47 E to 75°30' E longitude, the valley of Kashmir harbours river Jhelum which originates from the Verinag spring in the South Eastern part of the valley. Before leaving the valley through a gorge to enter Pakistan, the Jhelum river is joined by various tributaries such as Rambiara, Bringi, Vishaw, Aripal, Lidder, Romshi, Doodhganga, Sindh, Pohru etc. This river feeds a number of lakes such as Dal, Nigeen, Anchar, Manasbal, Wular etc with Wular lake in Bandipora being one of the largest fresh water lakes in Asia. From 1850 m above sea level at Verinag in Anantnag and 1592 m above sea level at Srinagar to 1578 m above sea level for the farther end of Wular lake in Bandipora, the Jhelum shows a fall of 265 m in the first 85 kilometers, and 14 m only in the next 60 kilometers. The study area along with the location of meteorological and hydrological stations in the Jhelum river basin are shown in Figure 3.1. Categorizing mainly into four fairly discernable seasons: Winter (December-February), Spring (March-May), Summer (June-August) and Autumn (September-November) coupled with the average elevation ranging from 1550 to 1800 m above the sea level, the valley of Kashmir endures a considerably temperate climate with distinct temperature variations throughout the year.

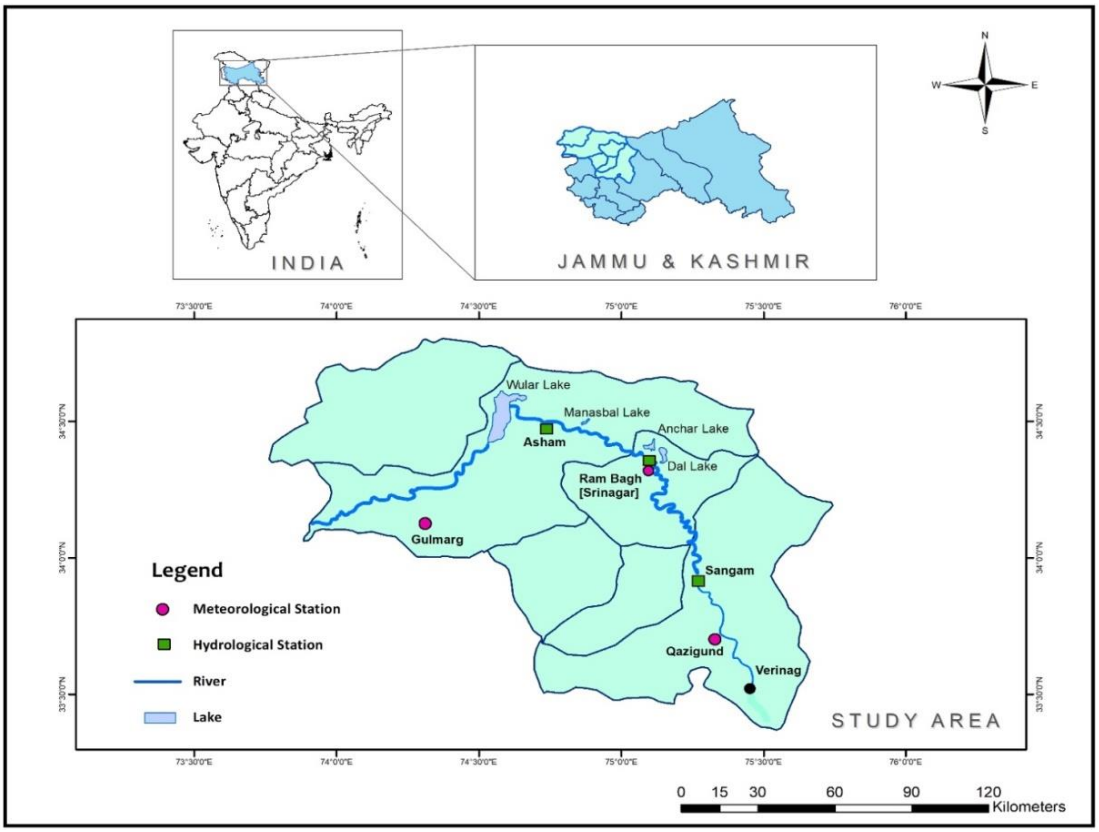

Figure 3.1. Location Map of the study area illustrating meteorological stations, hydrological stations and course of the river in Jhelum River Basin.

The average monthly values of temperature and precipitation were acquired from the Indian Meteorological Department IMD – Srinagar for three stations: Qazigund, Rambagh and Gulmarg premised at the closest proximity of the stations from which discharge data was availed for Jhelum River. Average monthly values were computed from the daily discharge data obtained from the Irrigation and Flood Control Department, I&FC – Srinagar for three hydrological stations at upstream, central and downstream sites stationed at Sangam, Ram Munshi Bagh and Asham respectively for the time spanning from 1980 – 2020. For the purpose of observing the seasonal trends, average monthly values were noted down grouping December – February as Winter, March – April for Spring, June – August as Summer and

September – November as Autumn seasons respectively. The elevation and co-ordinates along with the mean temperature, precipitation and streamflow of the stations in the Jhelum River basin have been illustrated in Table 3.1.

Table 3.1. Coordinates, Elevation and Mean Annual Temperature, Precipitation and Streamflow of the Hydro-Meteorological Stations Located in the Jhelum River Basin for the record period from 1980 to 2020

S no	Station	Latitude (^{o} N)	Longitude (^{o} E)	Altitude (m)	Mean Annual Temperature (^{o}C)	Total Annual Precipitation (mm)	Mean Annual Streamflow (m^3/s)
1	Qazigund	33.59	75.17	1670	12.80	1198.70	–
2	RamBagh	34.05	74.80	1583	13.80	717.70	–
3	Gulmarg	34.05	74.38	2650	7.10	1454.70	–
4	Sangam	33.83	75.07	1597	–	–	117.60
5	RamMunshiBagh [Srinagar]	34.06	74.84	1592	–	–	131.98
6	Asham	34.26	74.64	1576	–	–	197.75

3.2 Land Use Land Cover Change

The valley of Kashmir is located between 33.36º to 34.70º North Latitude and 73.74º to 75.60º East Longitude, surrounded by the Karakoram Range beyond the Southern foothills of Himalayas from the North East side and the Pir Panjal Range from the South West direction as shown in Figure 3.2. The geographical expanse of the valley assumes an inclined orientation towards North West with the minimum and maximum elevation ranging from 1152 m to 5370 m above sea level and covering an expanse of approximately 12955.79 sq. km. The study area mainly comprises of loamy soil with a wide variety of vegetative cover ranging from meadows to Poplar (Fraest), Willow (Vir), Deodar (Devdor), Pine (Yaari kul), Nettle (Bremij), Chinar (Booen), Birch (Burze`), Silver fir (Budul) trees to apple, walnut, saffron, apricot, cherry, peach, almond, strawberry, grapes, pear, vegetables, mustard, maize, wheat and marshy lands. Other locally known soils found in the study area include Peaty soil (Nambal), mountain soil (Tand), alkaline (Zabelzamin), Karewas (Wudur), Clayey (Gurut), Loamy soil (Behil), Sandy loam (Sekil) and sandy silt (Dazanlad). Rice being the staple food of the population occupies an important part of the agricultural sector. The land forms identified in the study area range from fertile valley plains to Karewas, meadows, forested barren and glaciated mountains and hills.

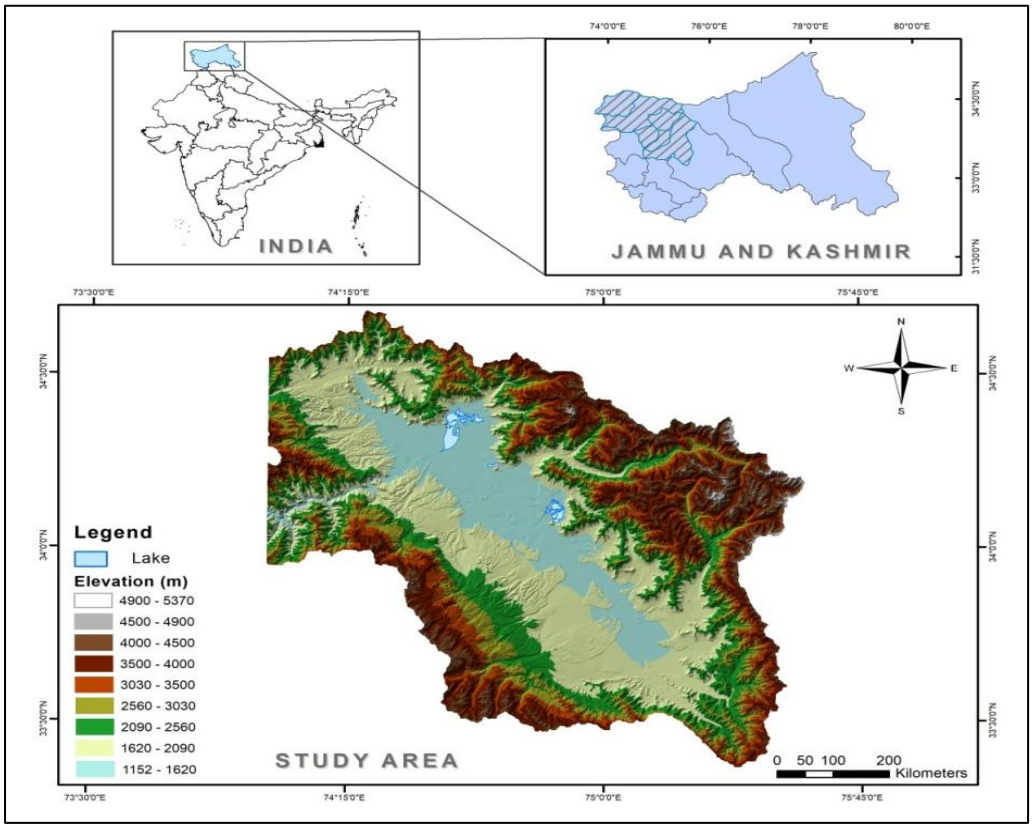

Figure 3.2. Location Map of the Study Area Illustrating Shuttle Radar Topography Mission Digital Elevation Model (SRTM-DEM) of the Kashmir valley

For the purpose of analyzing the changes in land use patterns and transforming land cover, RS technology which has gained special prominence in the past two decades was utilized in the present study. The RS and GIS technology has immensely simplified the complex process of observing large scale changing LULC over a long period of time. In the present study, three satellite images were downloaded from the United States Geological Survey (USGS) Earth Explorer website using Landsat 5: Thematic Mapper – TM (1992), Landsat 7: Enhanced Thematic Mapper – ETM+ (2001) and Landsat 8: Operational Land Imager – OLI (2020) for observing the LULC changes spanning three decades in the study area. All the three satellite images have a spatial resolution of 30 m and they were selected for almost similar date to avoid any discrepancies that might arise as different seasons have different

vegetative cover. The imagery downloaded was cloud-free and with reference to World Geodetic System – WGS datum 1984, present in the Universal Transverse Mercator – UTM Zone 43. Further details about the satellite images used in this study are provided in Table 3.2.

Table 3.2. Details of the Remotely Sensed Satellite Data

Satellite	Sensor	Resolution	Path / Row	Bands	Acquisition Date
Landsat 5	TM	30 m	148-149 / 36-37	7	31 – 10 – 1992
Landsat 7	ETM +	30 m	148-149 / 36-37	7	30 – 09 – 2001
Landsat 8	OLI	30 m	149 / 36-37	7	28 – 10 – 2020

3.3 Hydrological Modeling Using SWAT

The Jhelum river basin acquires a slightly tilted orientation towards North West spanning across the length and breadth of the Kashmir valley between 33^{o} 27' to 34^{o} 33' North latitude and 74^{o} 00' to 75^{o} 30' East longitude and covers an expanse of approximately 12,623.94 sq. km. The Jhelum river originates in the southern end of the valley as a spring in Verinag and is joined by a number of tributaries while flowing towards North including Bringi, Lidder, Vaishow, Ranbiara, Aripal, Romshi, Sindh, Sukhnag, Erin, Madhumati and Pohru rivers. It covers nearly 189.5 km length from the southernmost point in Verinag, taking a sharp westward turn after feeding the Wular lake till it finally leaves the Indian subcontinent to enter Pakistan. The basin is surrounded by the Pir Panjal mountain range from the south western side and the Karakoram mountain range from the north eastern side. The minimum and maximum elevations of the study area are 1152 and 5370 m above sea level respectively. The soil in the valley mostly consists of loam and also has a little clay content. The valley receives most of its precipitation from October to May [Dad et al. 2021] and experiences a temperate climate with the average mean temperature and precipitation being 7.31^{o}C and 1200.01 mm respectively. Figure 3.3 shows digital elevation model of the Jhelum river basin along with gridded climate stations obtained from SWAT global weather site and hydrological stations on the river. Unlike the trend analysis of hydrometeorological parameters of the Kashmir valley that utilized data from 3 available ground based meteorological stations from the study area, the hydrological model developed using SWAT used meteorological data from 13 stations that were not ground based but available from the National Centres for Environmental Prediction (NCEP) Climate Forecast System Reanalysis (CFSR) site (https://globalweather.tamu.edu/). This was done to increase the efficiency and reliability of the model developed because of more comprehensive data coverage from the study area which was not possible otherwise with the data from only 3 meteorological stations.

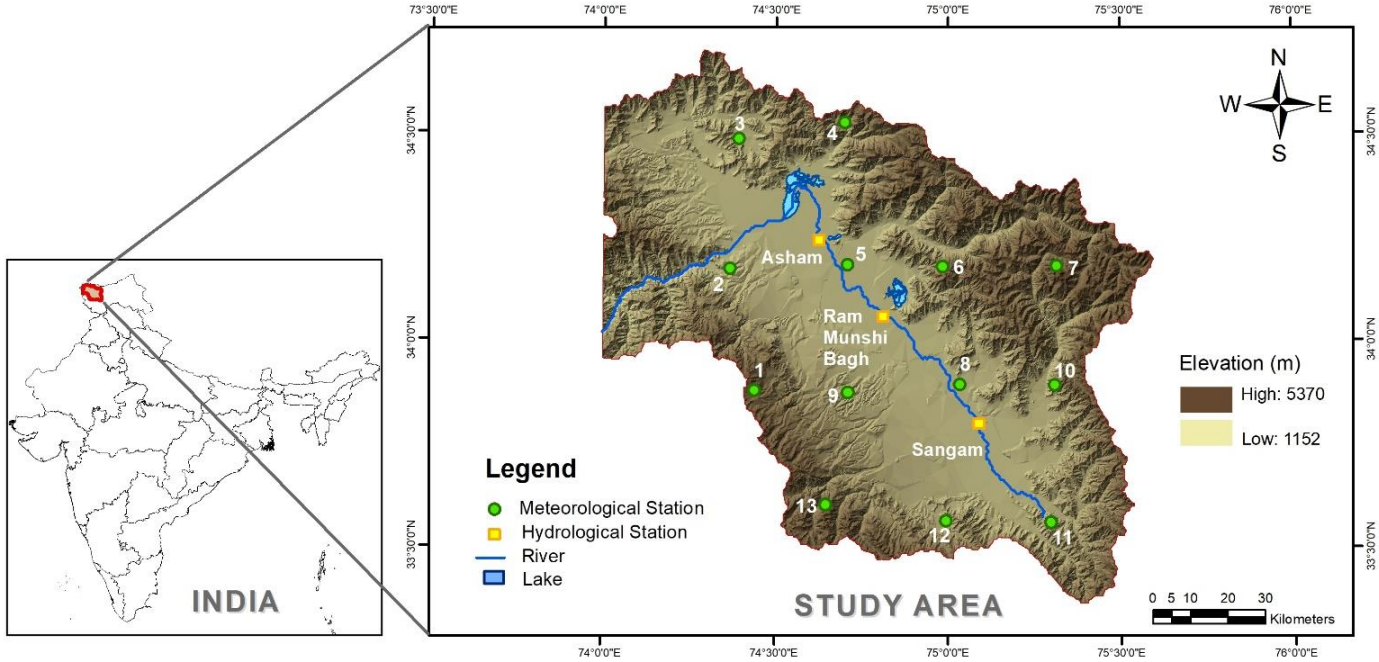

Figure 3.3. Location Map of the Study Area Showing Digital Elevation Model (DEM) of Kashmir Valley, Gridded Climate Stations and Hydrological Stations Used in the Development of SWAT Model

A lot of input data goes into developing a hydrological model using SWAT which includes both remotely sensed data as well as hydro-meteorological data obtained from the stations on ground. Geospatial data including the digital elevation model (DEM), land use land cover (LULC) and soil map are required initially after which weather data obtained from the meteorological stations is input. A detailed information and source of the data required for developing a SWAT model is presented in Table 3.3.

3.3.1 Land Use Land Cover

LULC has a huge impact on the runoff of a basin as the infiltration as well as the potential evapotranspiration characteristics of the catchment are altered because of changes in the land cover patterns. Forest cover and urbanized/barren lands for example illustrate sheer contrast response to infiltration and surface flow behaviour of the catchment area. Eight LULC types have been classified for the Jhelum river basin in this study and fed as input in the SWAT model after which the map is reclassified with the help of a four letter code recognized by the software for each land category. The details of the area covered by various LULC classes (namely; water bodies, forest cover, urban areas, snow cover, barren land, plantation and agricultural areas) in the study area and the change occurring in them from 1992 to 2020 are given in Table 3.4 and illustrated with the help of Figure 3.4 (a) and (b).

Table 3.3. Source and Details of Data Used in the Present Study

Data	Source	Scale
Digital Elevation Model [DEM]	NASA Shuttle Radar Topographic Mission https://earthexplorer.usgs.gov/	30 m
Land use land cover map	Landsat 5 TM, Landsat 8 OLI https://earthexplorer.usgs.gov/	30 m
Soil map	FAO-UNESCO Digital Soil Map https://www.fao.org/soils-portal/	1 : 5000000
Weather data	National Centres for Environmental Prediction (NCEP) Climate Forecast System Reanalysis (CFSR) https://globalweather.tamu.edu/	Daily gridded data (1984 – 2013)
Streamflow data	Irrigation and Flood Control (I&FC) Department Kashmir Division	Daily streamflow data for Asham station (1984 – 2013)

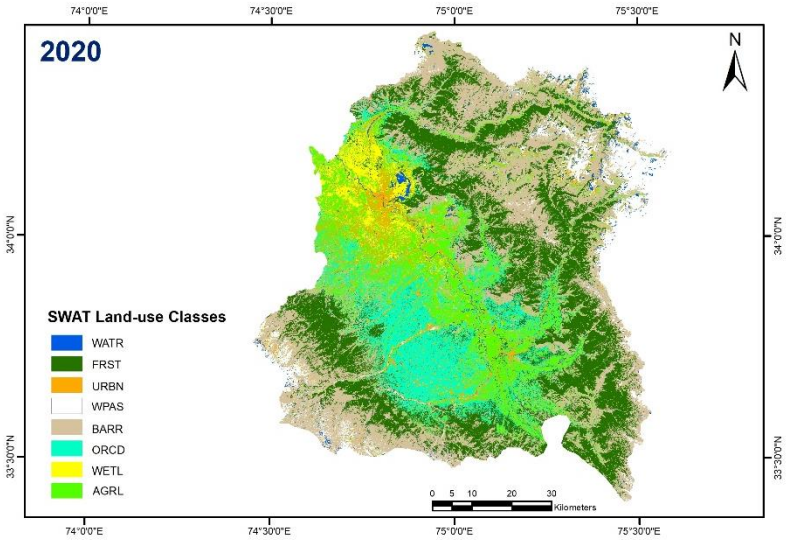

(a)

(b)

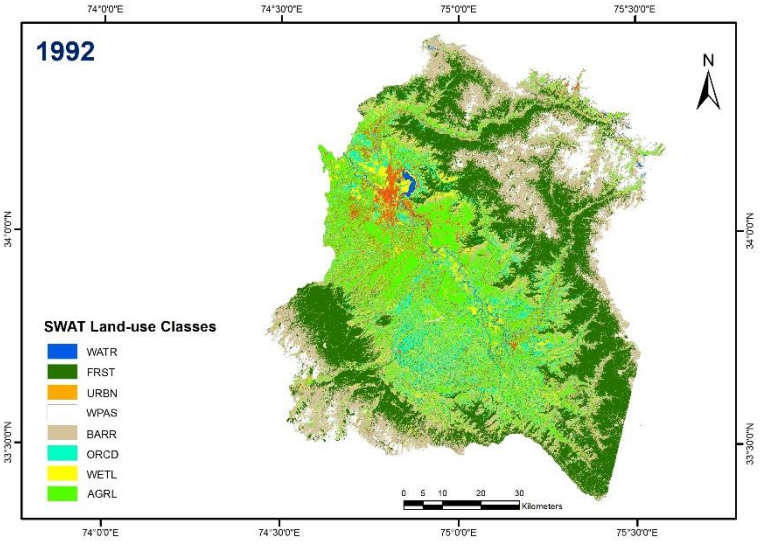

Figure 3.4. Classified LULC Maps of the Study Area During (a) 1992 and (b) 2020

Table 3.4. Area Covered by Various LULC Classes in the Jhelum River Basin and the Change Experienced ın Each Land Class from 1992 to 2020

SWAT Land use class	LULC class	Area 1992		Area 2020		Area change 1992 – 2020	
		sq. km	%	sq. km	%	sq. km	%
WATR	Water	51.00	0.63	47.54	0.58	- 3.46	- 6.78
FRST	Forest	2261.43	27.93	2188.56	27.03	- 72.87	- 3.22
URBN	Built up	358.68	4.43	416.98	5.15	58.30	16.25
WPAS	Snow	778.91	9.62	538.43	6.65	- 240.48	- 30.87
BARR	Barren	2112.45	26.09	2595.26	32.05	482.81	22.85
ORCD	Plantation	667.17	8.24	902.79	11.15	235.62	35.31
WETL	Marsh	666.36	8.23	378.11	4.66	-288.25	- 43.25
AGRL	Agriculture	1201.56	14.83	1029.91	12.72	- 171.65	- 14.28

3.3.2 Soil Map

Soil characteristics like composition, water content, density, texture, hydraulic conductivity, etc. are recorded by SWAT as they also affect the watershed properties. The digital soil map of the study area was acquired from the Food and Agricultural Organization (FAO) UNESCO having a scale of 1:5,000,000 after extraction from the available soil map of the world. After projecting the soil map on Universal Transverse Mercator (UTM) Zone 43, it was reclassified by providing a SWAT code for each soil class present in the study area as shown in Figure 3.5 (a). Due to the high variability of elevations in the study area encompassing mountain ranges, meadows, hilly regions as well as plains; it was divided into five slope classes for the model development as illustrated in Figure 3.5 (b).

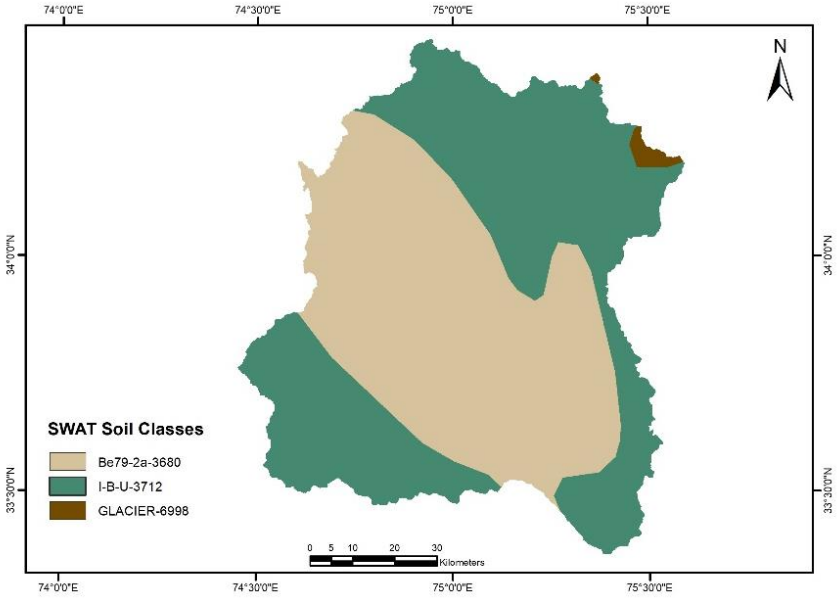

(a)

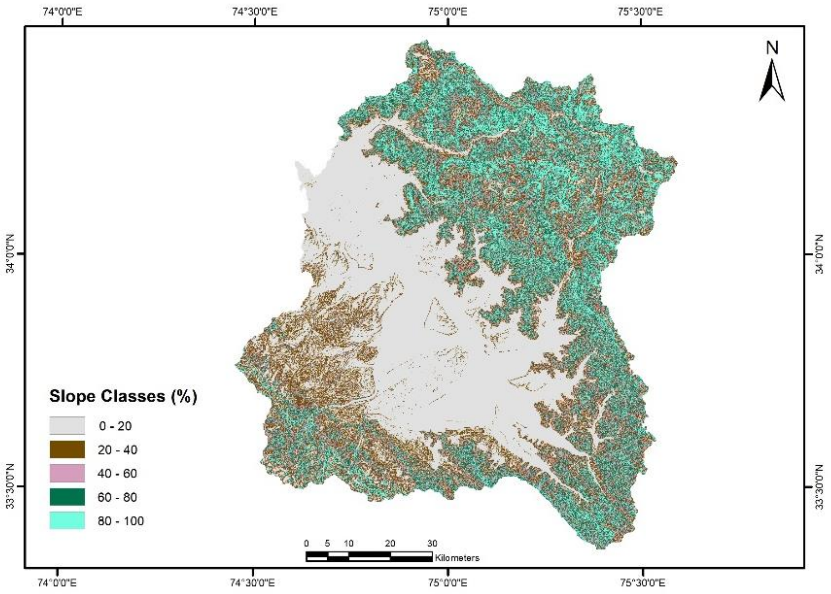

(b)

Figure 3.5. (a) Classified FAO Soil Map and (b) Classified Slope Map Of The Jhelum River Basin

3.3.3 Meteorological Data

Barring one climatological station at Gulmarg, rest of all the eight stations recording the weather data in Kashmir lie in low altitudes and are therefore not representative of the actual weather conditions of the area. Meteorological data in the form of minimum and maximum temperature, precipitation, relative humidity, wind speed and solar insolation in a basin on daily basis hold utmost importance for efficient hydrological modelling. As a result, good quality daily gridded meteorological data from 13 climatological stations from 1984 – 2013 was used in the present study which was obtained from National Centres for Environmental Prediction (NCEP) Climate Forecast System Reanalysis (CFSR) shown in Figure 3.3.

For the future hydro-meteorological forecasts, datasets from the General Circulation Models (GCMs) or Regional Climate Models (RCMs) have to be downscaled for higher resolution by either using a statistical or a dynamical approach because of bias

present in the climate models. Amongst various available statistical bias correction methods, Distribution Mapping (DM) outperforms the other techniques because of its ability to correct maximum statistical features while showing least variability and offering best fit with the observed overlapping mean daily temperatures and precipitation [Teutschbein and Seibert 2012, Smitha et al. 2018]. For the Indian subcontinent Norwegian Earth System Model 1 – Medium resolution (NorESM1-M) has been evaluated to perform well amongst others [Chaturvedi et al. 2012]. Therefore, DM technique was utilized for NorESM1-M model in the present study to depict future hydro-meteorological predictions in the Jhelum river basin under two greenhouse gas emission scenarios RCP 4.5 and RCP 8.5 which represent the medium and high radiative forcing scenarios respectively till the end of the 21st century. Details and source of the model used for future predictions is given in Table 3.5.

Table 3.5. Details of the RCM Used in the Present Study

Project	Model Name	Experiment	Ensemble	Source
CMIP5	NorESM1-M	RCP 4.5, RCP 8.5	r1i1p1	Norwegian Climate Centre (NorClim)

CHAPTER 4

METHODOLOGY

4.1 Trend Analysis of Hydro-Meteorological Parameters

All the data was subjected to four methods of homogeneity tests namely Pettitt test, Standard Normal Homogeneity test (SNHT), Buishand test and Von Neumann test after classifying it into monthly, seasonal and yearly averages. The reason for using multiple tests is that these tests make different assumptions to test the data for the presence of trend. Therefore, to be more confident about the homogeneity of the data being used 4 tests were conducted. The null hypothesis considered that the data was homogeneous and consistent for the given time series at 5% significance level while the p-value was provided using Monte Carlo simulations. The advantage of utilizing these tests is the flexibility they provide in applying to any data distribution. Almost all the time series for average monthly, seasonal and yearly data for precipitation, temperature and streamflow passed the homogeneity tests to be reviewed further for any statistically significant trends utilizing the non-parametric Mann-Kendall and Sen's slope estimator tests.

4.1.1 Mann-Kendall Trend Test:

The Mann-Kendall trend test is a non-parametric rank correlation test given for the ranks of the observations and their time sequence. For a time series $X = \{x_i : i = 1,2,3, \dots, n\}$, the test statistic S is given by:

$$S = \sum_{i=1}^{n-1} \sum_{j=i+1}^{n} a_{ij} \qquad (1)$$

where

$$a_{ij} = \text{sign}\,(x_j - x_i) = \text{sign}\,(R_j - R_i) = \begin{cases} 1 & x_i < x_j \\ 0 & x_i = x_j \\ -1 & x_i > x_j \end{cases} \quad (2)$$

and R_i and R_j are the ranks of observations x_i and x_j of the time series respectively. According to Kendall (1975), the observations considered independent and identically distributed random variables have mean and variance of the test statistic S calculated by the following equations:

$$E\,(S) = 0 \quad (3)$$

$$V_o(S) = \frac{n(n-1)(2n+5)}{18} \quad (4)$$

where n is the number of observations. The existence of tied ranks (equal observations) in the data results in a reduction of the variance of S to become:

$$V_o^*(S) = \frac{n(n-1)(2n+5)}{18} - \sum_{j-1}^{m} \frac{t_j(t_j-1)(2t_j+5)}{18} \quad (5)$$

where m is the number of groups of tied ranks, each with t_j tied observations. As the number of observations becomes large, Kendall (1975) stated that the distribution inclines to normality. The following equation is utilized to estimate the standard normal variate z at a significance level α, for the cases where n is greater than 10:

$$z = \begin{cases} \frac{S-1}{\sqrt{V_o(S)}} & , \quad S > 0 \\ 0 & , \quad S = 0 \\ \frac{S+1}{\sqrt{V_o(S)}} & , \quad S < 0 \end{cases} \quad (6)$$

Therefore, in a two-sided trend test, the null hypothesis H_o (which states that no trend exists in the time series) is accepted if $|z| \leq z_{\alpha/2}$ for a significance level α or that the other possible cases of alternate hypotheses exist where a positive value of z implies an 'upward trend' and a negative value insinuates a 'downward trend' [Kahya and Kalayci 2004].

4.1.2 Sen's Slope Estimator Test:

For the purpose of evaluating the slope of a linear trend (or the change per unit time), a non-parametric test called Sen's Slope Estimator Test was put forth by [Sen 1968] computed for N pairs of data given as:

$$Q_i = \frac{x_j - x_k}{j - k} \qquad for\ i = 1, \dots, N, \tag{7}$$

where x_j and x_k are data values at times j and k (j > k), respectively. For only one datum in each time period, $N = \frac{n(n-1)}{2}$ where n is the number of time periods and for multiple observations in one or more time periods, $N < \frac{n(n-1)}{2}$ where n is the total number of observations. The median of these N values of Q_i gives the Sen's Slope estimator computed as:

$$Q_{med} = \begin{cases} Q_{\frac{(N+1)}{2}} & ,\ if\ N\ is\ odd \\ \frac{Q_{(N)/2} + Q_{\frac{(N+2)}{2}}}{2} & ,\ if\ N\ is\ even \end{cases} \tag{8}$$

the Q_{med} sign reflects the data trend, while its value indicates the steepness of the trend line. The obtained value is tested by a two-sided test at $100(1-\alpha)\%$ confidence level.

4.1.3 Bravais-Pearson Correlation:

For the purpose of determining the correlation between meteorological parameters of the basin and the streamflow of River Jhelum, the Bravais-Pearson Linear Correlation Coefficient was utilized. Numerous studies have employed this method [Croitoru and Minea 2014, Minea and Croitoru 2017] that aids in establishing a linear relationship between the meteorological variables and the streamflow of a river basin and is computed as:

$$r(P,Q) = \frac{\sum_{i=1}^{n}(P_i - P_m)(Q_i - Q_m)}{\sum_{i=1}^{n}\sqrt{(P_i - P_m)}\ \sum_{i=1}^{n}\sqrt{(Q_i - Q_m)}} \tag{9}$$

where r is the Bravais-Pearson linear correlation coefficient, P and Q are the meteorological variable and river discharge, respectively; n is the total number of observations; P_i are the values of the meteorological variable series; Q_i are the values of the river discharge series; P_m and Q_m are the average values of meteorological variable and river discharge, respectively.

4.2 Land Use Land Cover Classification

The methodology used in the present study for the classification of satellite data of the study area was supervised classification in which the most commonly used approach is the maximum likelihood classification technique. In this approach, the analyst feeds each land use class with certain training samples to be recognized by the software for the whole study area. The software then tries to allot each pixel of the raster image to the land class which has the maximum probability / likelihood of having it and hence the name. In this study, ArcGIS (10.7.1) software was used to classify the valley into eight LULC classes namely water, forest, urban, snow, barren, plantation, marsh and agriculture. Further details about these land classes present in the study area can be found in Table 4.1. The classified raster images so obtained were also verified by comparing the uncertain classified points with the ground truth data available through high resolution Google Earth imagery. The final classified LULC images for the years 1992, 2001 and 2020 were thus acquired to be further evaluated for the changing extent of each land use class over a period of three decades spanning from 1992 to 2020.

Table 4.1. Description of the Land Use Land Cover Classes Used for Classification in the Study Area

S No.	Land Class	Description
1	Water	Water bodies such as lakes, flood channels, streams and rivers present in the study area form this land use class
2	Forest	Dense evergreen trees commonly found in the region at higher elevations of 2000 – 3100 m above sea level like Pine, Willow, Deodar, Poplar and Fir are included in this class
3	Urban	Residential / commercial and industrial areas including roads and similar man-made structures
4	Snow/Glacier	Glaciated areas and perennial snow covered high altitudes
5	Barren	Desolate, bare soiled or rocky lands bereft of vegetative cover form this category
6	Plantation	Cash crops mainly including apple, walnut, cherry, pear, almond, peach and apricot trees
7	Marsh	Swampy areas inhabiting aquatic vegetation and other wetlands unfit for human habitation
8	Agriculture	Fertile irrigated areas devoted to the cultivation of rice, vegetables, mustard and other locally grown crops

4.2.1 Accuracy Assessment

The land use land cover maps obtained after classification of the raw satellite images contain certain errors that need to be estimated for gauging the accuracy of the results thus attained. As a result, the accuracy assessment of the classified imagery is carried out using a statistical tool called error matrix that enables us to ascertain the accuracy of the classified pixels representative of each land class in the study area. Based on the random data points selected from the classified raster layer, the error matrix represented user's accuracy, producer's accuracy and the overall accuracy for the LULC maps generated. While the user's accuracy (commission error) provides information about the pixels assigned to a particular land class but originally belonging to other land classes, the producer's accuracy (omission error) informs about the pixels rightly being assigned to a particular land class in the classified raster image [Petropoulos et al. 2015, Pramit et al. 2020]. The user's and producer's accuracy is estimated using the following expressions:

User's accuracy $$\mathrm{UA} = \left({}^{n_{ii}}/_{n_{i\,row}} \right) \tag{10}$$

Producer's accuracy $$\mathrm{PA} = \left({}^{n_{ii}}/_{n_{i\,column}} \right) \tag{11}$$

where n_{ii} is the number of pixels accurately classified, $n_{i\,row}$ and $n_{i\,column}$ are the row and column totals respectively.

The overall accuracy denotes the pixels that are correctly classified in the final output raster and is expressed as;

$$\text{Overall accuracy} \quad \mathrm{OA} = \frac{\sum_{i=1}^{r} x_{ii}}{x} \tag{12}$$

where x_{ii} is the number of pixels that have been rightly classified present as the diagonal elements in the error matrix and x is the total number of pixels in the matrix.

Cohen's Kappa coefficient is another widely used accuracy assessment measure which takes into account the actual agreement between the classified and the reference data layers excluding the ones that get included by chance or random agreement [Congalton et al. 2002]. It is denoted by $\widehat{K}$ and mathematically given as;

$$\widehat{K} = \frac{n \sum_{i=1}^{r} x_{ii} \; - \; \sum_{i=1}^{r} x_{i+} \, x_{+i}}{n^2 \; - \; \sum_{i=1}^{r} x_{i+} \, x_{+i}} \tag{13}$$

where n is the total number of pixels in the error matrix, r is the number of rows in the matrix, x_{ii} is the total number of pixels in row i and column i, x_{i+} and x_{+i} are the marginal totals for row i and column i respectively.

Kappa coefficient was calculated for all the three classified LULC maps with the help of generated error matrix. The overall accuracy values of 88.1%, 86.9%, 88.8% and Kappa coefficient values equal to 0.86, 0.85 and 0.87 were acquired for the classified raster images of the years 1992, 2001 and 2020 respectively. These results are in coherence with the acceptable range adopted for considering the classified LULC maps as reliable as all the three values obtained for the classified maps (1992, 2001 and 2020) are greater than 0.80 [Congalton and Green 2019]. The error matrices generated for the classified LULC maps of the years 1992, 2001 and 2020 are illustrated using Tables 4.2, 4.3 and 4.4 respectively.

Table 4.2. Error Matrix Depicting the Accuracy of LULC Map (Landsat TM-1992) for the Study Area

Land class	W	F	U	S	B	P	M	A	RT	UA (%)
W	17	0	0	0	2	1	0	0	20	85
F	0	17	0	1	2	0	0	0	20	85
U	0	0	17	0	0	0	0	3	20	85
S	0	0	0	20	0	0	0	0	20	100
B	0	0	0	2	18	0	0	0	20	90
P	0	0	0	0	0	17	0	3	20	85
M	0	0	0	0	0	0	17	3	20	85
A	0	0	0	0	2	0	0	18	20	90
CT	17	17	17	23	24	18	17	27	160	
PA (%)	100.0	100.0	100.0	86.9	75.0	94.4	100.0	66.7		

Overall accuracy = 88.1%, Kappa coefficient ($\widehat{\boldsymbol{K}}$) = 0.86

Table 4.3. Error Matrix Depicting the Accuracy of LULC Map (Landsat ETM+ 2001) for Study area

Land class	W	F	U	S	B	P	M	A	RT	UA (%)
W	17	2	0	0	1	0	0	0	20	85
F	1	18	0	0	1	0	0	0	20	90
U	0	0	17	0	0	0	1	2	20	85
S	1	0	0	17	2	0	0	0	20	85
B	0	1	0	2	17	0	0	0	20	85
P	0	0	0	0	0	17	1	2	20	85
M	0	1	0	0	1	0	17	1	20	85
A	0	0	0	0	1	0	0	19	20	95
CT	19	22	17	19	23	17	19	24	160	
PA (%)	89.5	81.8	100.0	89.5	73.9	100.0	89.5	79.2		

Overall accuracy = 86.9%, Kappa coefficient (K^) = 0.85

Table 4.4. Error Matrix Depicting the Accuracy of LULC Map (Landsat OLI-2020) for the Study Area

Land class	W	F	U	S	B	P	M	A	RT	UA (%)
W	16	1	0	1	2	0	0	0	20	80
F	0	19	0	0	0	1	0	0	20	95
U	1	0	15	0	2	0	0	2	20	75
S	2	0	0	17	1	0	0	0	20	85
B	0	1	0	0	17	0	0	2	20	85
P	0	0	0	0	0	19	0	1	20	95
M	0	0	0	0	0	1	19	0	20	95
A	0	0	0	0	0	0	0	20	20	100
CT	19	21	15	18	22	21	19	25	160	
PA (%)	84.2	90.5	100.0	94.4	77.3	90.5	100.0	80.0		

Overall accuracy = 88.8%, Kappa coefficient (K^) = 0.87

Values in the diagonal represent correctly classified pixels for each land use land cover class.W – Water, F – Forest, U – Urban, S – Snow/Glacier, B – Barren, P – Plantation, M – Marsh, A – Agriculture

4.3 Soil and Water Assessment Tool (SWAT)

SWAT is a robust physical process based continuous time scale model that is efficiently capable of simulating soil, water and nutrient characteristics of large and complex watersheds. It provides a comprehensive report about various processes taking place in a watershed including the hydrology, sediment, nitrogen cycle, phosphorus cycle, plant growth, landscape nutrient losses, land use summary, etc. that can be utilized for impact assessment studies.

4.3.1 SWAT Model Set-up

The foremost requirement for setting up SWAT hydrological model over a river basin is the DEM to delineate the watershed. DEM having a resolution of 30 m was used in the present study and the outlet of the watershed was selected at Asham hydrological station because of the unavailability of hydrological data on the main river beyond that point owing to security reasons. 23 sub-basins were formed of the watershed covering an area of approximately 8096.801 sq. km on the basis of river network, confluence points of rivers with the main channel and river geometry as shown in Figure 4.1.

All the maps used in the present study were projected with reference to the World Geodetic System (WGS) – Datum 84, present in UTM Zone 43. LULC, soil and slope maps were loaded in SWAT to create an overlay of the datasets. 10% threshold level was selected for land use percentage over the sub-basin area, 5% for soil class percentage over land use area, 5% for slope class percentage over soil area along with 5 elevation bands were considered that developed 426 Hydrological Response Units (HRUs) in the watershed. Weather data on daily scale was imported to create SWAT database tables. Priestley-Taylor method was selected for PET calculation in the watershed. The model was run for a period of 30 years from 1984 to 2013 including a warm-up period of 3 years for generating efficient hydrological output

from the model. The average curve number for the watershed was 83.43. Daily streamflow data from the Asham hydrological station was obtained from Irrigation and Flood Control Department of Kashmir and was utilized for the calibration and validation of the developed SWAT model.

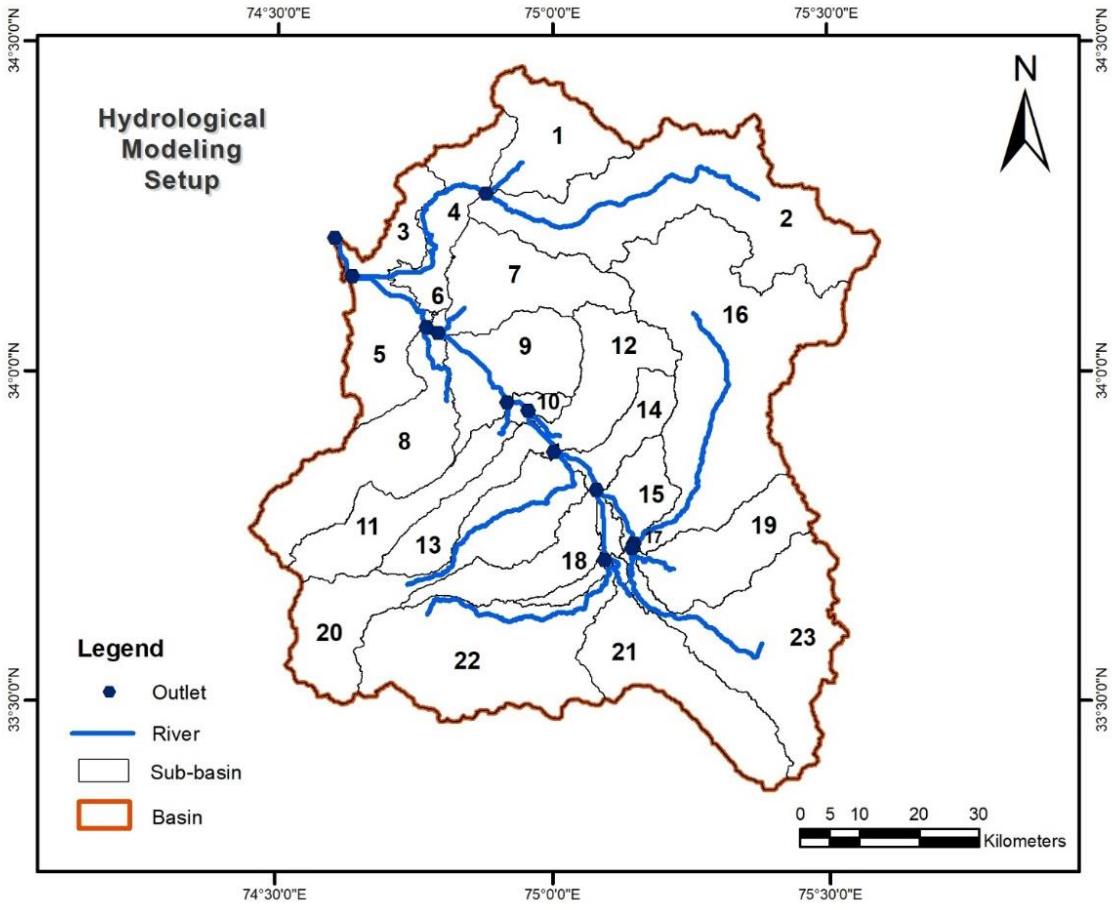

Figure 4.1. Hydrological Modelling Set-Up over the Jhelum River Basin with Delineated Watershed

4.3.2 Sensitivity Analysis, Calibration and Validation of the Model

Due to the large amount of input parameters being fed to the software, the uncertainty associated with the model is also high [Abbaspour 2008]. Sequential Uncertainty Fitting (SUFI-2) algorithm in SWAT Calibration Uncertainty Programme (SWAT-CUP) was used in the present study to find the hydrologically sensitive parameters in the watershed, calibrate and validate the model. Sensitivity analysis of a watershed requires prior knowledge of the area for the modeller to determine the set of suitable parameters that affect the water balance components and hence the efficiency of the model developed. Latin Hypercube sampling (using one factor at a time) was utilized and the list of sensitive parameters obtained for the watershed is summarized in Table 4.5.

Calibration of the model was done using the set of sensitive parameters by varying the range of input parameters after the first iteration run of the model. Daily streamflow data from Asham hydrological station was utilized to calibrate the model from 1984 to 1994 (using 1992 LULC) and 2000 to 2009 (using 2020 LULC). For analysing the combined impact of LULC and climate change on the streamflow of the Jhelum river basin, daily streamflow data was used to validate the model from 1995 to 1999 and 2010 to 2013, to observe the respective changes in the water balance components from 1984 to 2013.

Table 4.5. Sensitive Parameters of the Jhelum River Basin and their Best Fitted Values

Parameter name	Description	Range	Fitted value
V__SMTMP.bsn	Snow melt base temperature	4 – 17	16.93
V__GW_DELAY.gw	Groundwater delay (days)	0 – 80	74.79
R__SOL_K(..).sol	Saturated hydraulic conductivity	-0.2 – 0.5	0.07
V__TIMP.bsn	Snow pack temperature lag factor	0 – 1	0.005
R__OV_N.hru	Manning's "n" value for overland flow	0 – 1	0.13
R__SOL_AWC.sol	Available water capacity of the soil layer	0 – 0.35	0.10
V__TLAPS.sub	Temperature lapse rate	-6.4 to -6.3	-6.39
V__PLAPS.sub	Precipitation lapse rate	0 – 0.04	0.01
R__CN2.mgt	SCS runoff curve number	-0.2 – 0.2	0.05
V__SFTMP.bsn	Snowfall temperature	-1 – 6	2.53
V__ALPHA_BF.gw	Base-flow alpha factor (days)	0 – 0.3	0.006
V__SMFMN.bsn	Minimum melt rate for snow during the year (occurs on winter solstice)	0 – 5	0.07
V__SMFMX.bsn	Maximum melt rate for snow during year (occurs on summer solstice)	0 – 3	2.02

4.3.3 Future Climate Impact

The impact of future changes in the climate has been utilized in this study in the SWAT model to find out the future hydrological response of the basin in the form of changes in the groundwater level, evapotranspiration, potential evapotranspiration, surface runoff and water yield.

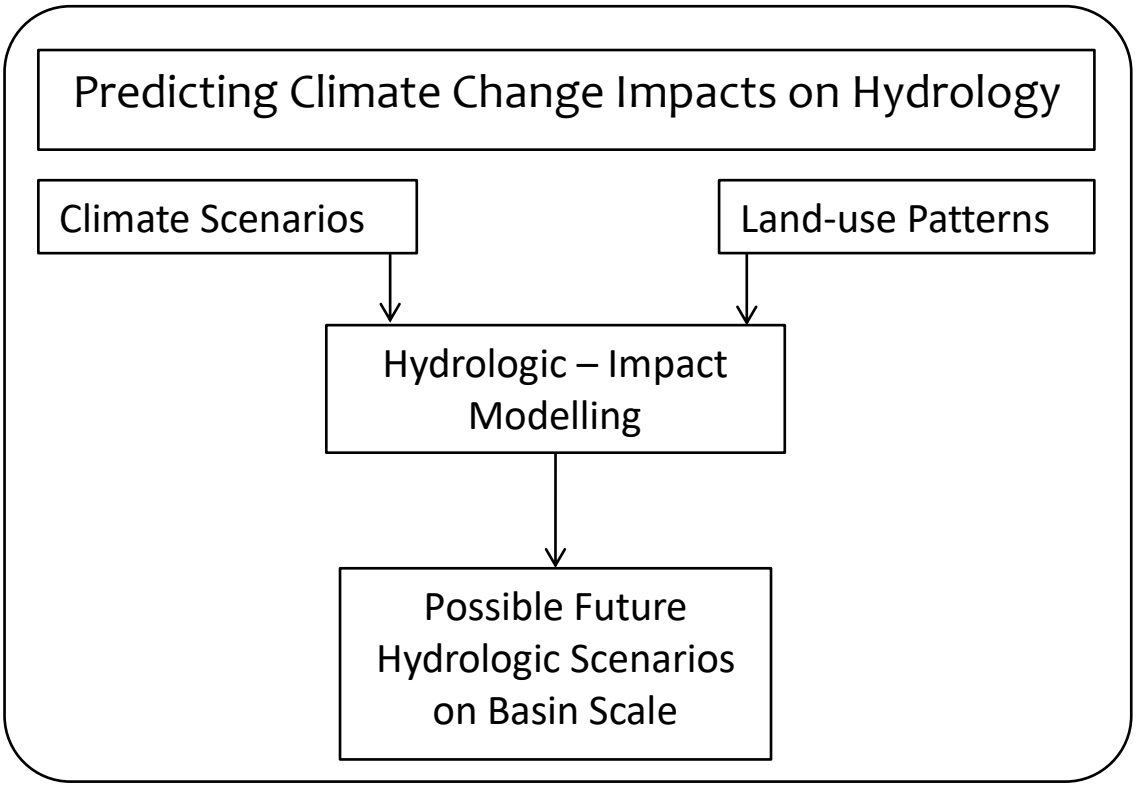

Figure 4.2. Methodology Adopted for Predicting the Future Hydrological Scenarios using SWAT Model

CHAPTER 5

RESULTS AND DISCUSSION

5.1 Trend Analysis of Climate Change Parameters

The changing trends of temperature and precipitation analyzed over a river basin and their relationship with the changing trend of the streamflow in the basin is an important study for observing the hydrological response of a catchment to climate change. Such studies aid in the proper planning and management of water resources apart from verifying the climate change impact occurring at regional level. The subsequent section gives a detailed account of the changing trends in temperature, precipitation and streamflow over the Jhelum river basin in Kashmir observed using the Mann-Kendal and Sen's Slope estimator tests. Additionally, the relationship between meteorological parameters and the streamflow has also been evaluated using the Bravais-Pearson correlation coefficient.

5.1.1 Temperature and Precipitation

The temperature and precipitation records procured for a period of 41 years spanning from 1980 – 2020 reflected an overall surge in the average annual temperature and a decline in the annual average precipitation recorded over the valley using the statistical trend results tested over a 95% significance level. The meteorological station at Qazigund recorded a rate of increase of 0.014 ^{o}C /year in the annual average temperature since 1980. It witnessed a marked statistically significant upward shift in the average temperature during Spring from 12.14 ^{o}C to 13.23 ^{o}C before and after the change point year of 1998 respectively. Figure 5.1 (a) shows the rate of increase of average temperature for Spring at Qazigund since 1980. The seasonal increase in average temperature for spring at Qazigund was found out to be 0.035 ^{o}C /year.

Considering the central meteorological station at Rambagh (Srinagar), the study area from the period spanning from 1980 to 2020 has experienced a range of annual average temperature from 12.39 ºC in the year 1986 to 14.72 ºC in 2001 and a mean value of 13.79 ºC.

The trend result of annual average temperature recorded for the Srinagar station (Figure 5.1 b) shows a statistically significant trend of increasing annual average temperature at a rate of 0.026 ºC/year. A change or break point in the year 1997 can be discerned from the plot (Figure 5.1 b) that exhibits an upward shift in the overall annual average temperature having an average value of 13.23 ºC before the breakpoint and averaging a value of 14.15 ºC after the breakpoint. Similar trends are revealed by the seasonal observations which are statistically significant at 95% significance level (since p value < 0.05) excluding summer. The seasonal rate of increase in temperature of 0.010 ºC/year was observed for summer, 0.031 ºC/year for winter, 0.036 ºC/year for spring and 0.024 ºC/year for autumn. The meteorological station at Gulmarg demonstrated noticeable trend results both seasonally as well as annually with an average annual upsurge rate of 0.012 ºC/year over the 41 year study period. Spanning the period from 1980 to 2020, Gulmarg being a hilly station experienced a varying range of annual average temperature ranging from 5.71 ºC in 2012 to 9.29 ºC in the year 1999 and a mean value of 7.13 ºC. Concurrently, the year 1997 like the other adjoining meteorological stations reveals an increase in the overall annual average temperature recorded from 6.69 ºC to 7.46 ºC before and after the changepoint year respectively (Figure 5.1 c). While the seasonal observations show a noticeable increasing trend during the winter and spring seasons, the summer and autumn seasons register a decreasing trend annually. Winter and Spring showed an increase of 0.014 ºC /year and 0.028 ºC /year in the seasonal temperature respectively while as a marginal decrease of 0.008 ºC /year and 0.002 ºC /year in seasonal average temperature was observed for Summer and Autumn respectively. Figure 5.2 illustrates the spatial distribution of annual and seasonal trends shown by average temperature at Qazigund, Ram Bagh and Gulmarg meteorological stations in the Jhelum river basin for the forty one year study period

from 1980 to 2020. The details of the seasonal as well as the annual statistical trend results acquired for the Mann-Kendall test and the Sen's Slope Estimator test for average temperature at the three meteorological stations have been presented in Table 5.1.

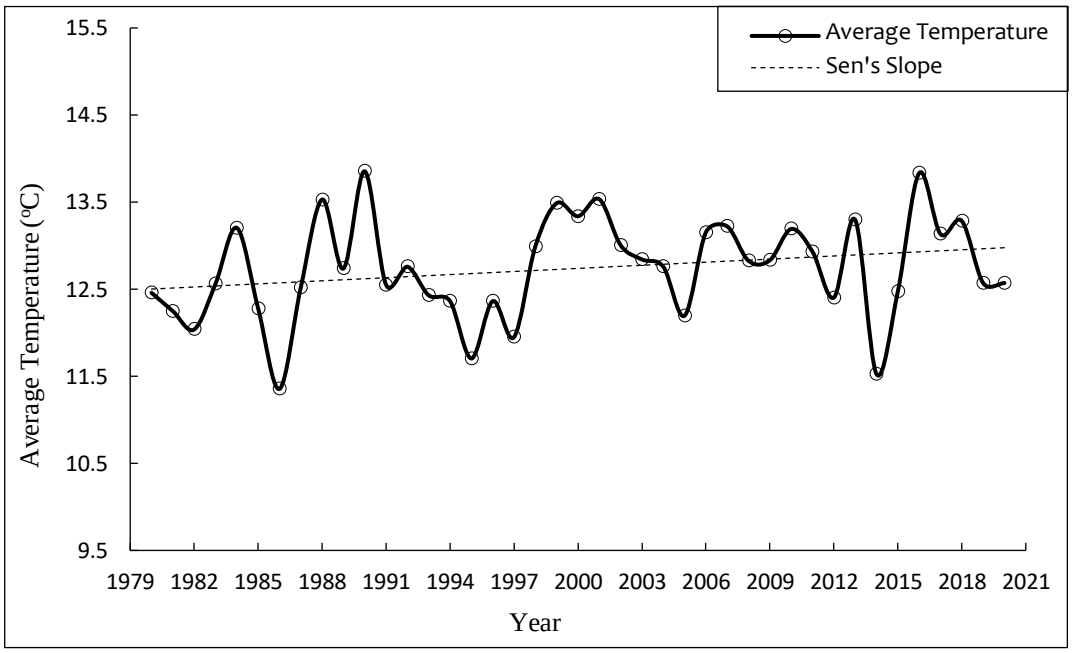

(a)

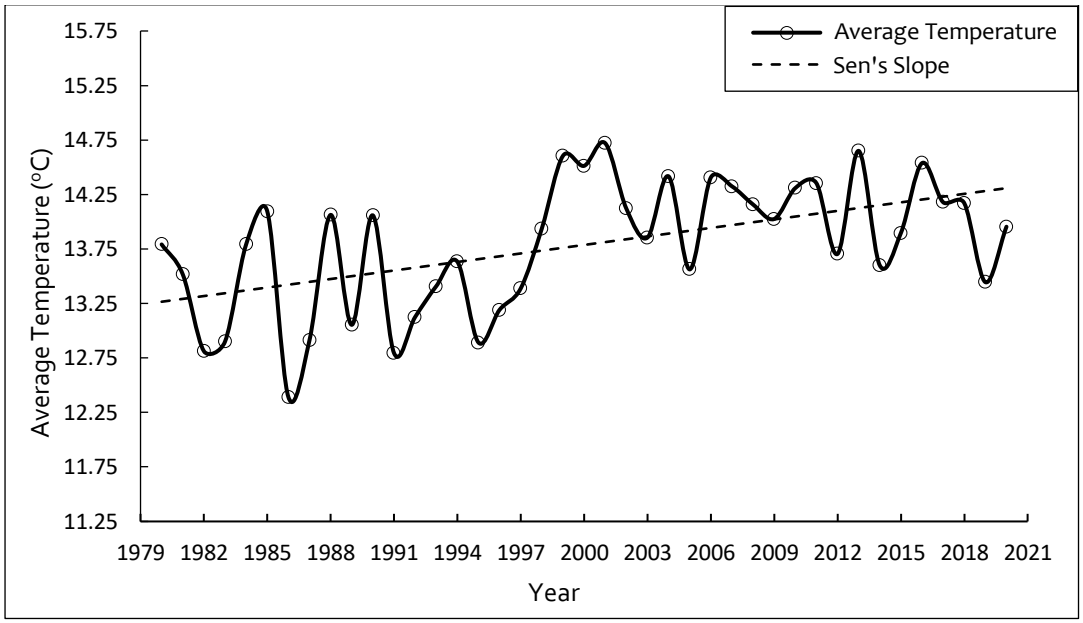

(b)

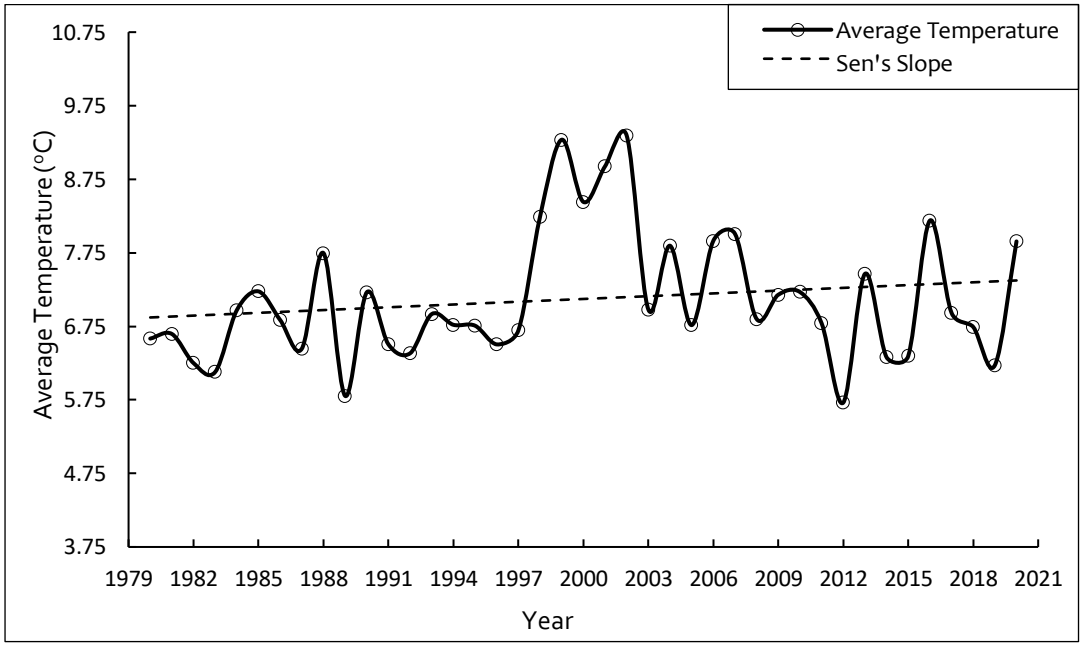

(c)

Figure 5.1. Trend Lines of Annual Average Temperature (T_{avg}) over a) Qazigund, b) Srinagar and c) Gulmarg from 1980 – 2020.

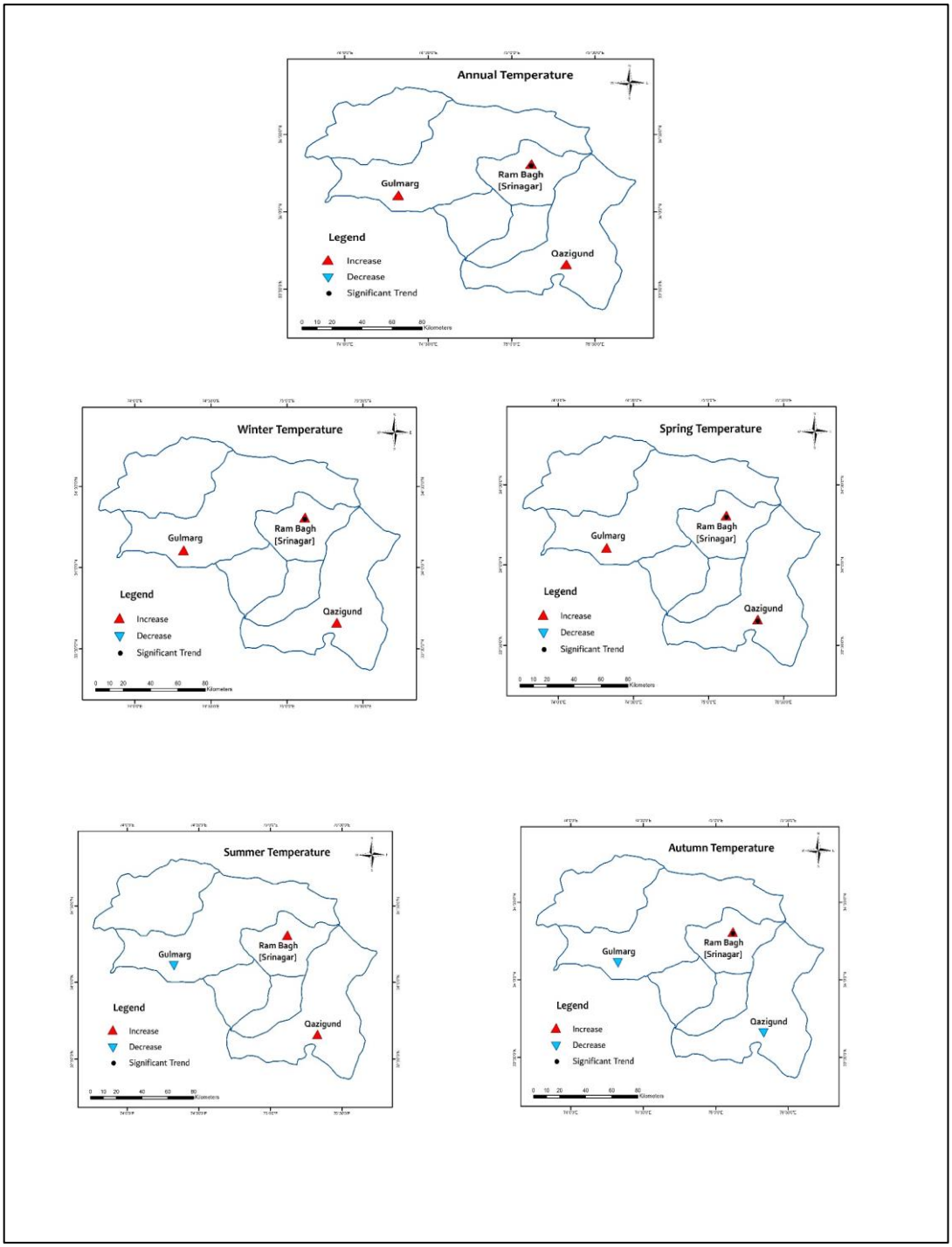

Figure 5.2. Spatial Distribution of Annual and Seasonal Trends of Average Temperature over the Jhelum River Basin from 1980 – 2020. (Black Dots Represent Significant Trends at 95% Significance Level)

The precipitation trends projected by the three meteorological stations at Qazigund, Ram Bagh and Gulmarg for the 41 year period from 1980 to 2020 at a significance level of 95% have been illustrated using Figure 5.3. Based on the results obtained by employing Mann-Kendall and Sen's Slope Estimator tests, the meteorological station at Qazigund registered the minimum downpour of 615.40 mm for the year 2016 while the maximum precipitation was recorded to be 1887.10 mm for the year 1996 and a mean annual value of 1198.71 mm with an overall annual rate of decrease being 5.43 mm/year from 1980 to 2020 (Figure 5.3 a). Although the station exhibited an increasing trend in precipitation received during the summer season with the average rate of increase being 0.68 mm/year; yet the effect is indemnified and subdued by the decreasing trend of results manifested by rest of the seasons recording the average rate of decrease in precipitation as 2.66 mm/year for winter, 4.25 mm/year for spring and 0.41 mm/year for the autumn seasons with a statistically significant trend shown by the spring season ($p < 0.05$). The rate of decrease in total annual precipitation received at the central station of the valley in Ram Bagh, Srinagar turned out to be 2.00 mm/year. Analyzing time series data of the station for the entire study period disclosed the range of total quantum of precipitation received since 1980 varies between a minimum value of 420.10 mm in 1999 to a maximum value of 1154.70 mm in the year 2015 and an average annual value of 718.44 mm (Figure 5.3 b). The rainfall distribution over the years has manifested a redistribution of shifting the downpour towards the winter and autumn seasons more, diverting away from the Spring and summer seasons which is evident by the fact that the rate of increase of total annual precipitation received shows an increasing trend of 0.31 mm/year in case of winter and 0.13 mm/year for the autumn season while as the rate of decrease of annual precipitation received illustrates a pronounced decreasing trend of 2.13 mm/year in case of spring and 0.06 mm/year for the summer season. Furthermore, while the precipitation seems merely redistributed, a closer observation reveals that the average annual depleting trend overshadows the increasing trend overall. The hilly meteorological station of Gulmarg documented receiving the minimum proportion of precipitation amounting to 491.40 mm during the year 2002

while as a maximum measure of 2380.30 mm for the year 1994 and a mean value of 1454.73 mm decreasing annually since 1980 at the rate of 13.30 mm/year showing a statistically significant trend at 95% significance level. Moreover, the year 1998 divulges a decreasing shift in the overall annual average precipitation recorded from 1741 mm to 1208 mm before and after the change point year respectively (Figure 5.3 c). Showcasing throughout a decreasing trend for all the seasons, the rate of decrease in the total precipitation was marked as 5.19 mm/year, 7.57 mm/year, 1.15 mm/year and 0.60 mm/year for the winter, spring, summer, and autumn seasons respectively with the trends illustrated by winter and spring seasons being statistically significant. Figure 5.4 illustrates the spatial distribution of annual and seasonal trends shown by precipitation at Qazigund, Ram Bagh and Gulmarg meteorological stations in the Jhelum River basin for the 41 year study period from 1980 to 2020. The details of the seasonal as well as the annual statistical trend results acquired for the Mann-Kendall test and the Sen's Slope Estimator test for precipitation at the three meteorological stations have been presented in Table 5.2.

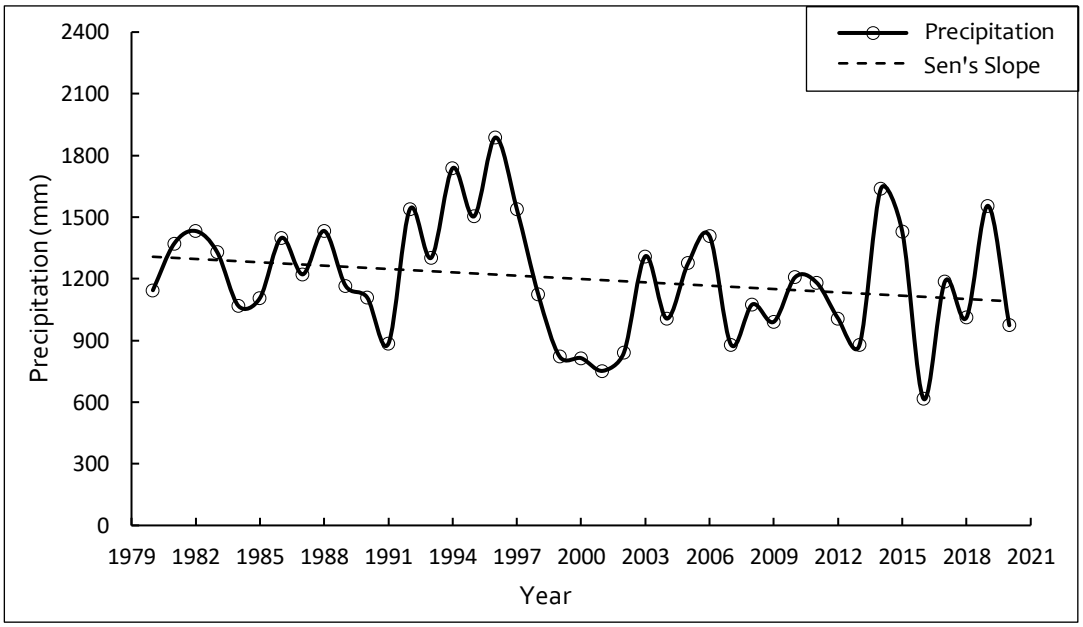

(a)

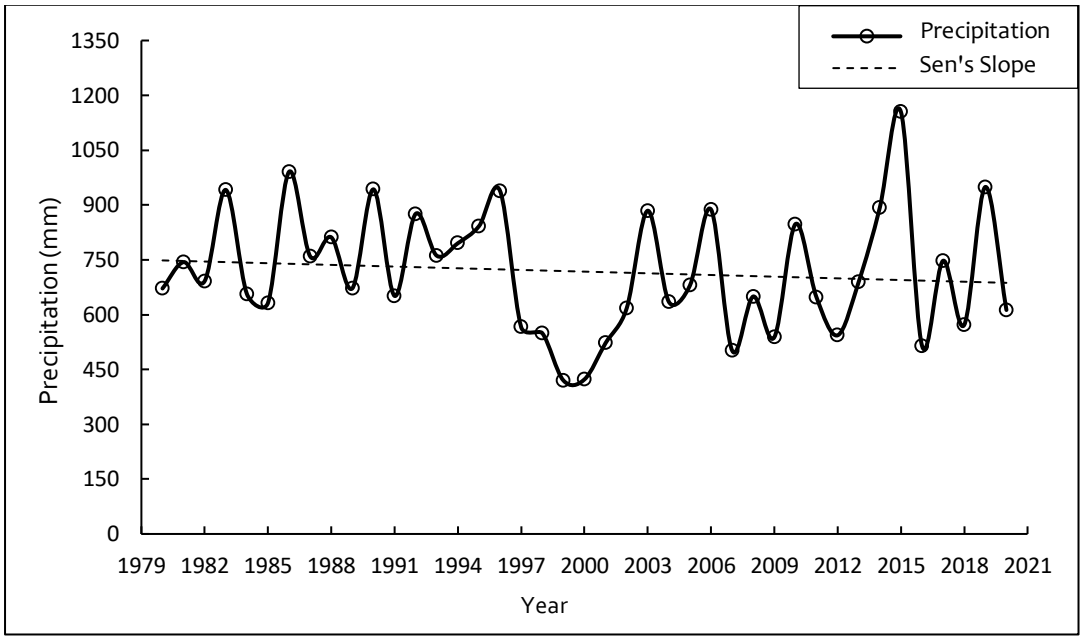

(b)

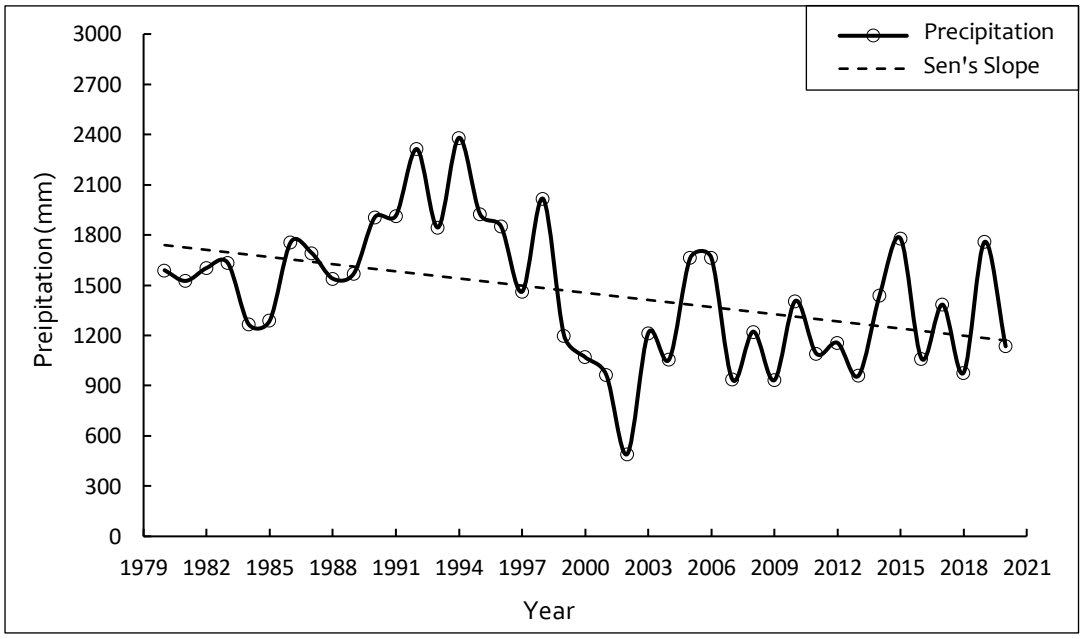

(c)

Figure 5.3. Trend Lines of Total Annual Precipitation (P_{avg}) over a) Qazigund, b) Srinagar and c) Gulmarg from 1980 – 2020.

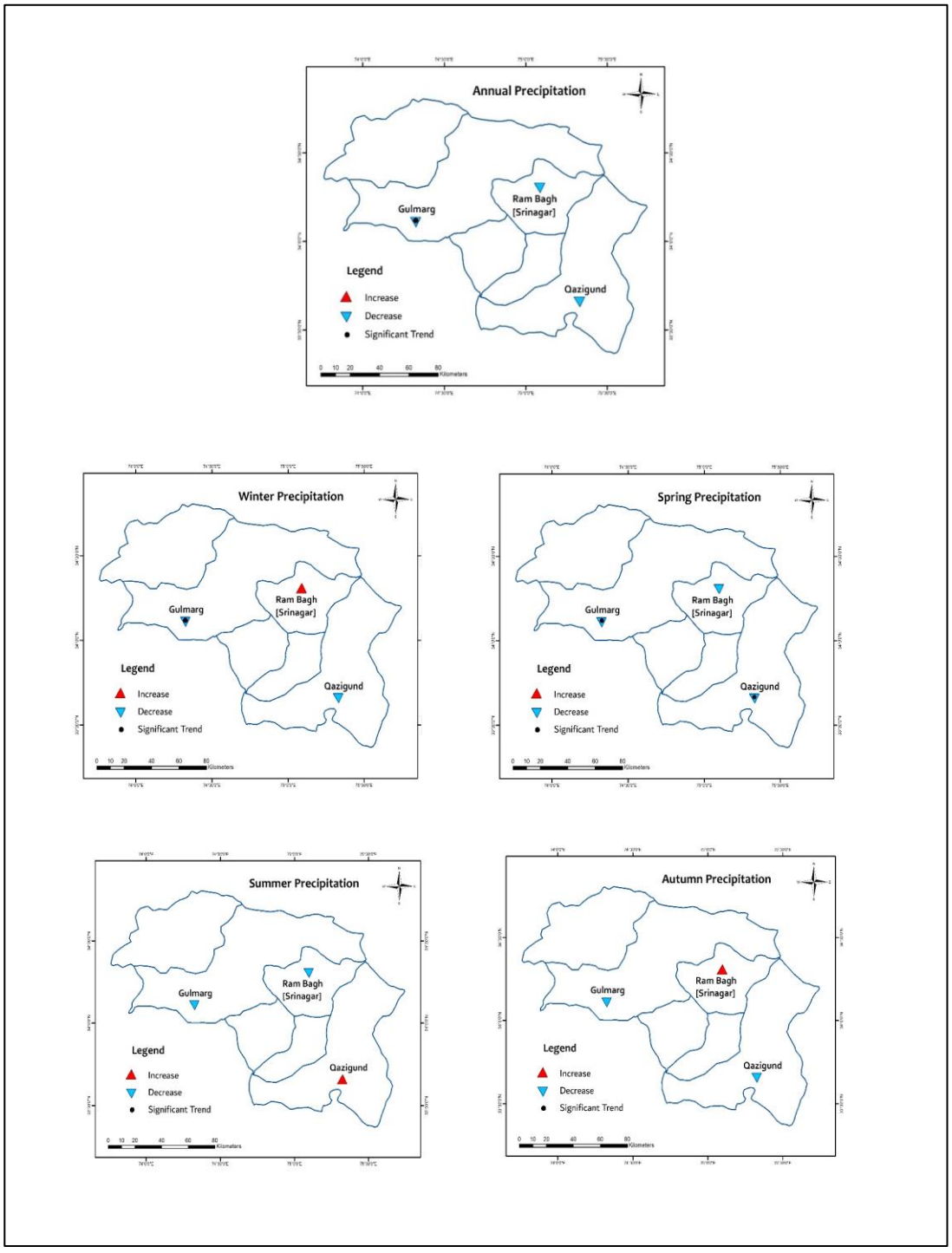

Figure 5.4. Spatial Distribution of Annual and Seasonal Trends of Precipitation over the Jhelum River Basin from 1980 – 2020. [Black Dots Represent Significant Trends at 95% Significance Level]

Table 5.1. Results of the Statistical Tests for Seasonal and Annual Average Temperature (T_{avg}) for Different Stations over 1980 – 2020

S No	Station	Test	Trends (Average Temperature)				
			Winter	Spring	Summer	Autumn	Annual
1	Qazigund	Z_s	0.160	**0.275**	0.017	-0.090	0.188
		Q_{med}	0.025	**0.035**	0.001	-0.007	0.014
2	Srinagar	Z_s	**0.277**	**0.259**	0.107	**0.343**	**0.334**
		Q_{med}	**0.031**	**0.036**	0.010	**0.024**	**0.026**
3	Gulmarg	Z_s	0.099	0.164	-0.063	-0.026	0.124
		Q_{med}	0.014	0.028	-0.008	-0.002	0.012

Bold values indicate statistically significant trends at 95% significance level

Table 5.2. Results of the Statistical Tests for Seasonal and Annual Precipitation (P_{avg}) for Different Stations over 1980 – 2020

S. No	Station	Test	Trends (Precipitation)				
			Winter	Spring	Summer	Autumn	Annual
1	Qazigund	Z_s	-0.105	**-0.244**	0.066	-0.016	-0.139
		Q_{med}	-2.663	**-4.250**	0.679	-0.405	-5.434
2	Srinagar	Z_s	0.024	-0.176	-0.012	0.017	-0.098
		Q_{med}	0.307	-2.128	-0.056	0.132	-1.998
3	Gulmarg	Z_s	**-0.217**	**-0.300**	-0.112	-0.059	**-0.256**
		Q_{med}	**-5.194**	**-7.567**	-1.153	-0.603	**-13.297**

Bold values indicate statistically significant trends at 95% significance level

5.1.2 Streamflow

Three main hydrological stations were considered over the time interval spanning 1980 – 2020 at the upstream (Sangam), central location (Rambagh) and the downstream (Asham) location. The stations were selected in such a way that their distribution over the valley elucidates the overall behaviour of the river. The Mann-Kendall and Sen's Slope estimator tests conducted for the average discharge of the river have shown decreasing trends in the seasonal as well as yearly discharge for all the three gauging stations.

The hydrological station at the upstream site of Sangam witnessed an average annual streamflow ranging from 35.85 m^3/s for the year 2001 to 239.50 m^3/s in the year 1996 and a mean value of 117.61 m^3/s since 1980. It has recorded an annual rate of decrease in the streamflow equal to 0.74 m^3/s /year for the 41 year study period (Figure 5.5 a). Furthermore, a prominent downward shift is delineated at the breakpoint year 1998, which enunciates an average streamflow of 148.63 m^3/s before the breakpoint and afterwards reducing to an average streamflow value of 90.82 m^3/s after the breakpoint year. The average streamflow values for all the seasons depict a downward shift in their streamflow for Sangam station with considerable depreciations shown by the spring and summer seasons declining from 200.17 m^3/s to 146.96 m^3/s and 220.46 m^3/s to 123.84 m^3/s at the rate of 1.87 m^3/s/year and 1.38 m^3/s/year for the spring and summer seasons respectively. Statistically significant declining trends at 95% significance level were exhibited by winter, spring and autumn seasons for the average streamflow recorded decreasing at the rate of 0.57 m^3/s/year and 0.86 m^3/s/year for the winter and autumn seasons respectively. The hydrological station at Ram Bagh in Srinagar has recorded a yearly average discharge value ranging from 50.77 m^3/s in the year 2001 to 236.13 m^3/s in the year 1995 and a mean value of 131.99 m^3/s. The rate of annual decline in the discharge of the river at Srinagar has been 0.48 m^3/s/year (Figure 5.5 b). Additionally, the statistical test results portray the year 1998 as the breakpoint year with an average

streamflow value of 153.47 m^3/s before the change point and a downward shift to the average streamflow of 113.43 m^3/s after the change point year. Also, while all the seasons registered a decreasing trend in the average annual discharge of the river, spring season presented a considerable depletion at the rate of 1.12 m^3/s/year against 0.45 m^3/s/year, 0.93 m^3/s/year and 0.54 m^3/s/year for winter, summer and autumn seasons respectively. The downstream hydrological station at Asham experienced a maximum decrease in its streamflow since 1980 dwindling annually at the rate of 1.14 m^3/s/year (Figure 5.5 c). In coherence with the Sangam and Ram Munshi Bagh stations, Asham hydrological station also marks a downward shift in its average streamflow for all the seasons insinuating maximum decline for the spring and summer seasons subsiding from 323.86 m^3/s to 249.27 m^3/s and 350.75 m^3/s to 241.09 m^3/s at a rate of 2.47 m^3/s/year and 2.67 m^3/s/year denoting the years 1992 and 1998 as breakpoint for the spring and summer seasons respectively while the trend showcased by spring season was statistically significant. Figure 5.6 illustrates the spatial distribution of annual and seasonal trends shown by average streamflow at Sangam, Ram Bagh and Asham hydrological stations in the Jhelum river basin for the forty one year study period from 1980 to 2020. The details of the seasonal as well as the annual statistical trend results acquired for the Mann-Kendall test and the Sen's Slope Estimator test for average streamflow at the three hydrological stations have been presented in Table 5.3.

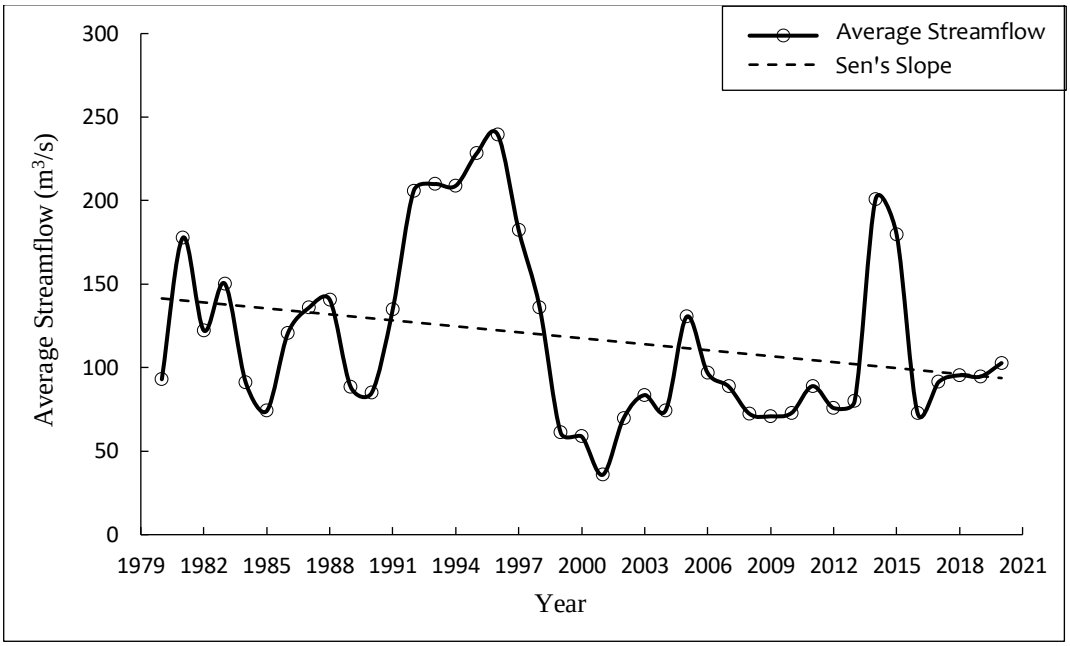
Average Streamflow
Sen's Slope
Average Streamflow (m3/s)
300
250
200
150
100
50
0
1979 1982 1985 1988 1991 1994 1997 2000 2003 2006 2009 2012 2015 2018 2021
Year

(a)

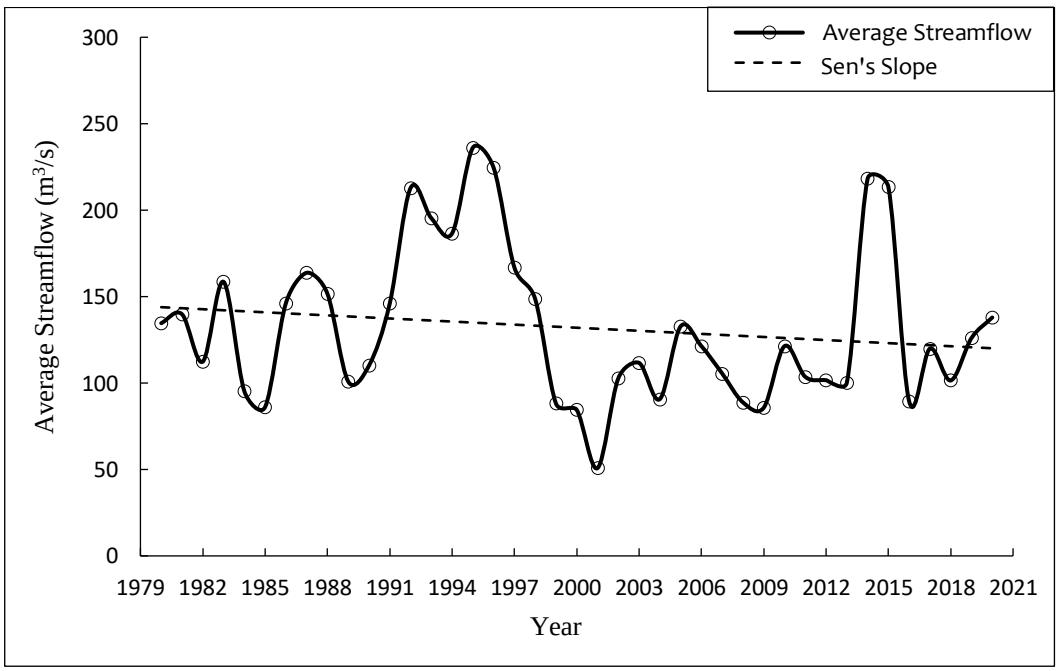
Average Streamflow
Sen's Slope
Average Streamflow (m3/s)
300
250
200
150
100
50
0
1979 1982 1985 1988 1991 1994 1997 2000 2003 2006 2009 2012 2015 2018 2021
Year

(b)

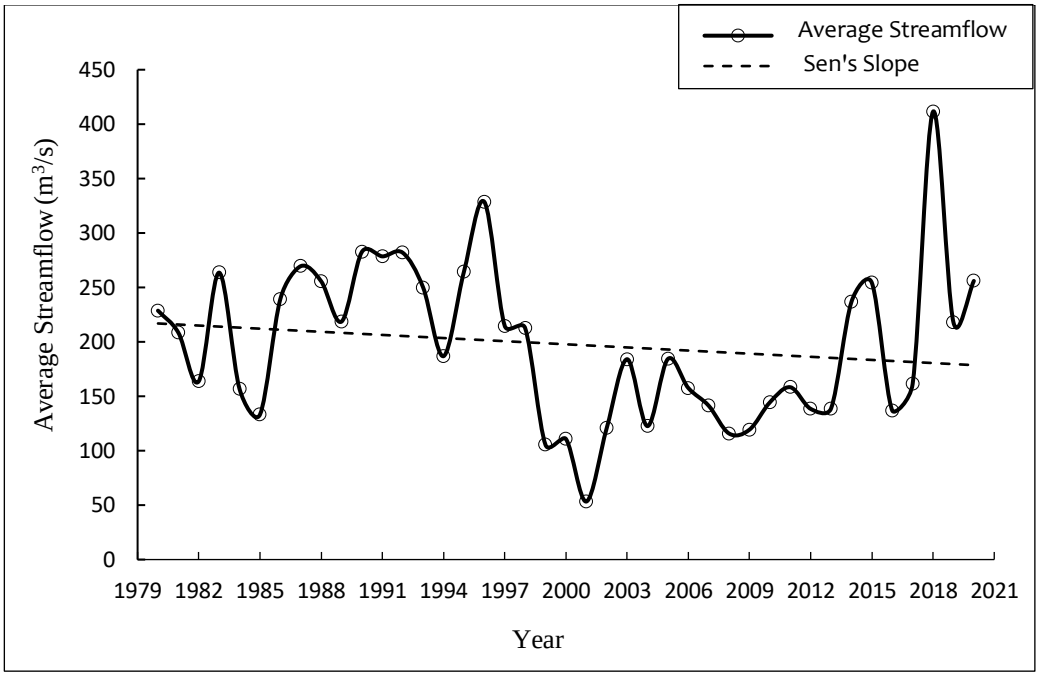

(c)

Figure 5.5. Trend Lines of Annual Average Streamflow (Q_{avg}) at a) Upstream (Sangam), b) Central (Ram Munshi Bagh) and c) Downstream (Asham) Hydrological Stations From 1980 – 2020.

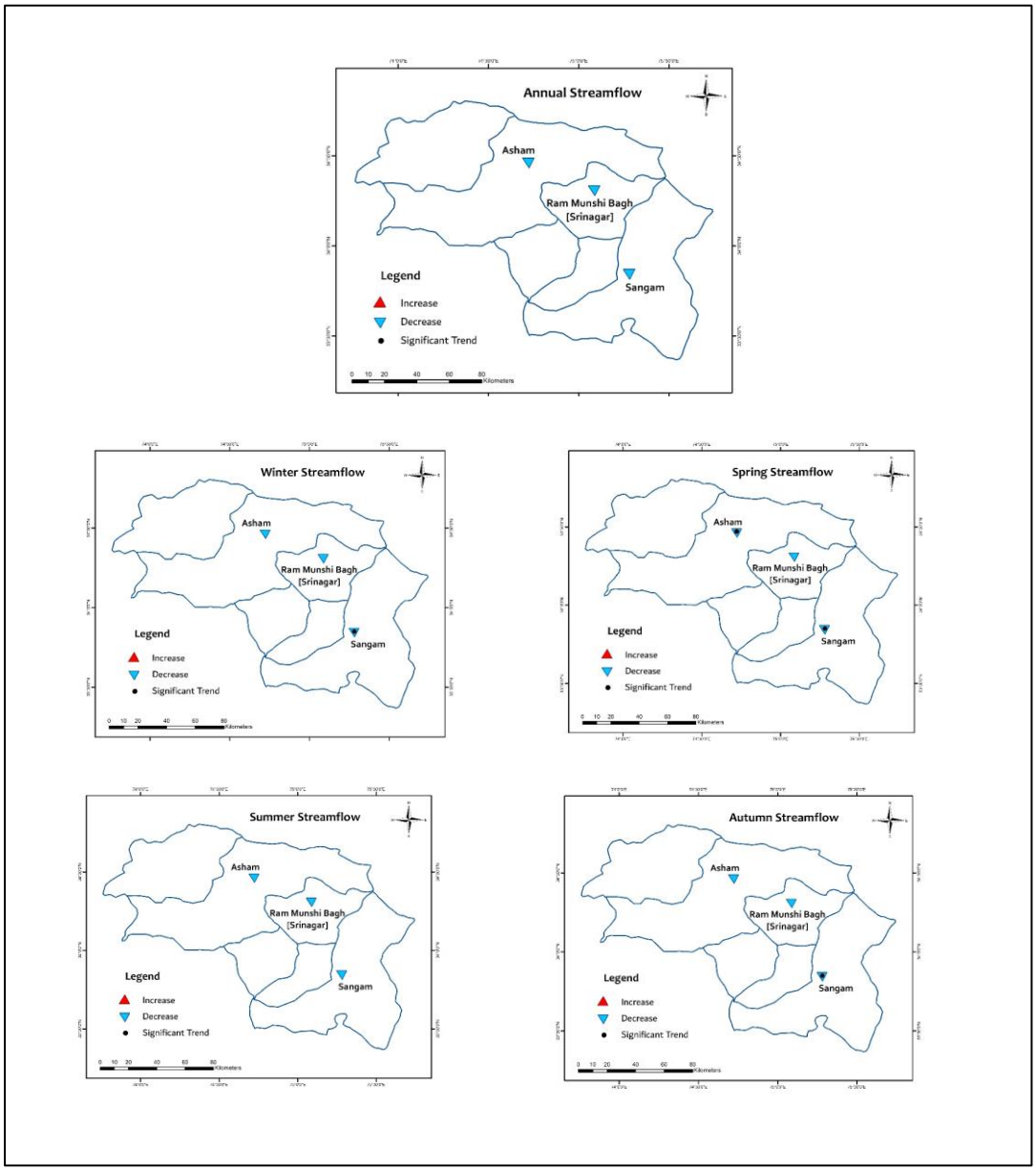

Figure 5.6. Spatial Distribution of Annual and Seasonal Trends of Average Streamflow of the Jhelum River Basin from 1980 – 2020. [Black Dots Represent Significant Trends at 95% Significance Level]

Table 5.3. Results of the Statistical Tests for Seasonal and Annual Average Discharge (Q_{avg}) for Different Stations over 1980 – 2020

S. No	Station	Test	Trends (Average Streamflow)				
			Winter	Spring	Summer	Autumn	Annual
1	Sangam	Z_s	**-0.320**	**-0.233**	-0.127	**-0.228**	-0.139
		Q_{med}	**-20.310**	**-66.092**	-48.785	**-30.211**	-26.277
2	Ram Munshi Bagh	Z_s	-0.183	-0.159	-0.095	-0.174	-0.115
		Q_{med}	-15.792	-39.409	-32.797	-18.939	-17.039
3	Asham	Z_s	-0.122	**-0.246**	-0.156	-0.158	-0.137
		Q_{med}	-16.549	**-87.428**	-94.276	-30.891	-40.345

Bold values indicate statistically significant trends at 95% significance level

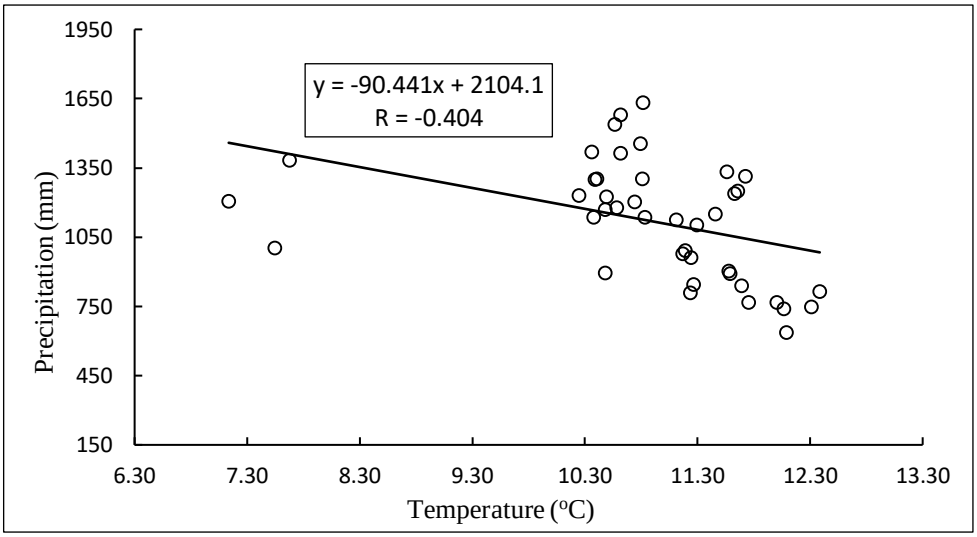
y = -90.441x + 2104.1
R = -0.404
Precipitation (mm)
1950
1650
1350
1050
750
450
150
6.30
7.30
8.30
9.30
10.30
11.30
12.30
13.30
Temperature (°C)

(a)

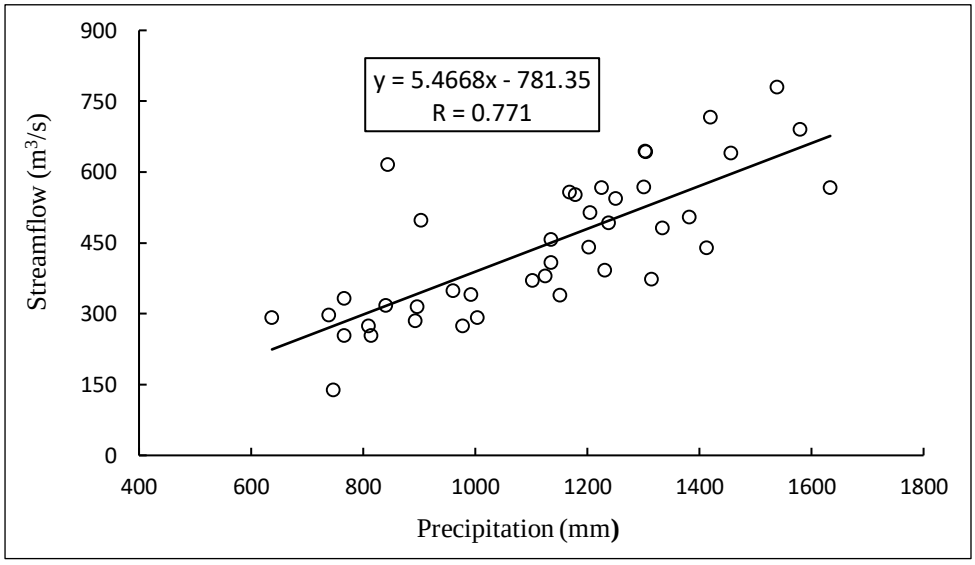
y = 5.4668x - 781.35
R = 0.771
Streamflow (m3/s)
900
750
600
450
300
150
0
400
600
800
1000
1200
1400
1600
1800
Precipitation (mm)

(b)

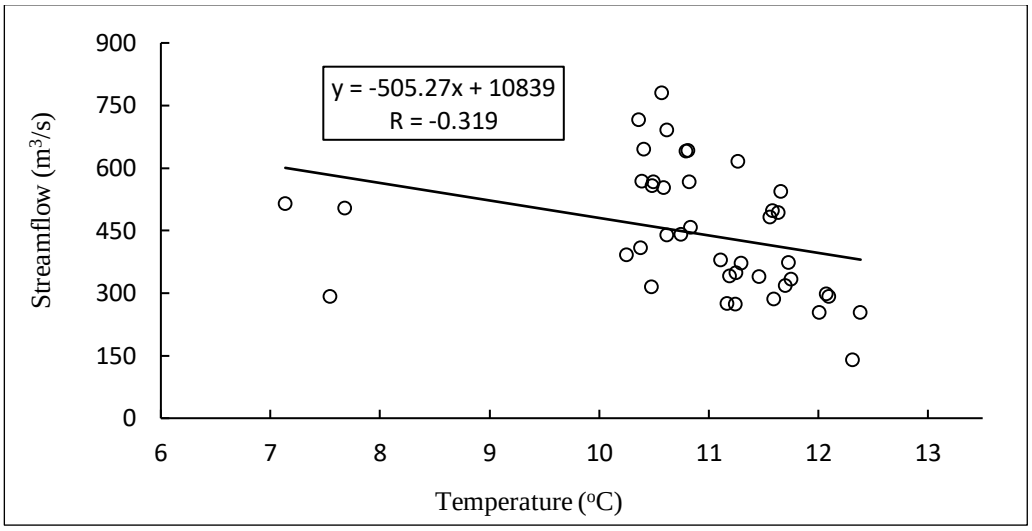

(c)

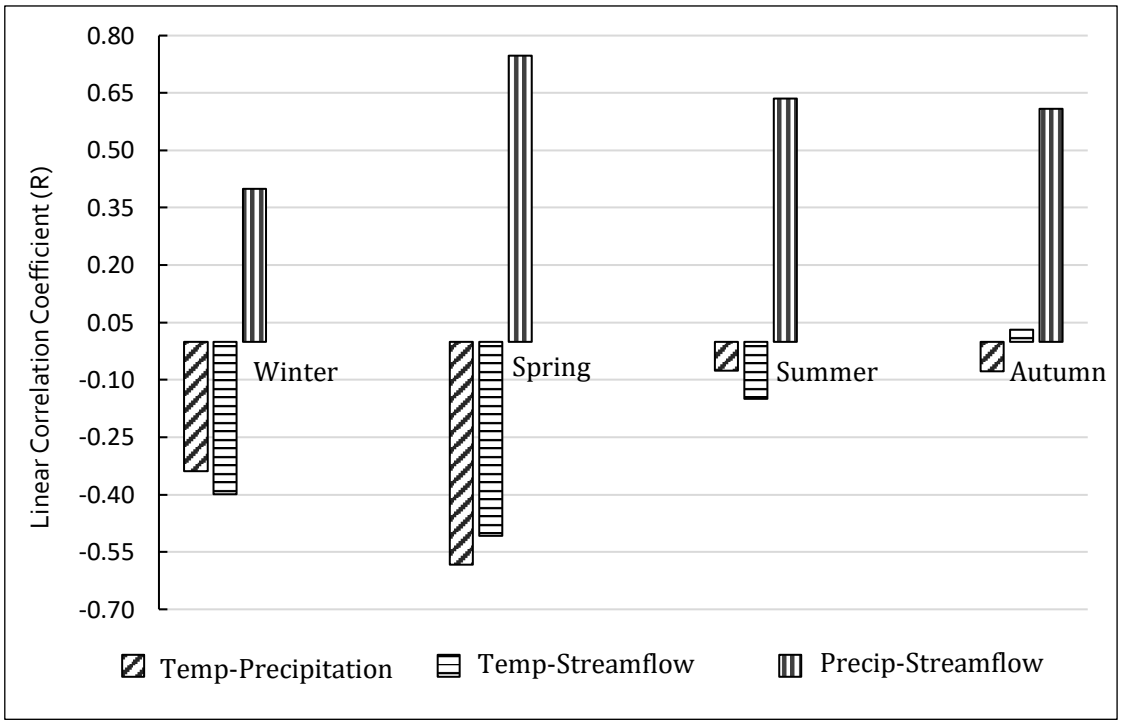

(d)

Figure 5.7. Plots Depicting Correlation Between a) Temperature – Precipitation, b) Precipitation – Streamflow, c) Temperature – Streamflow, and d) Seasonal Variation of Correlation for the Meteorological and Hydrological Parameters in the Jhelum River Basin from 1980 – 2020.

5.1.3 Relation between Meteorological Variables and Streamflow

Correlations were computed for quantifying the relationship between meteorological variables of the basin and discharge of the river. Thiessen Polygon method was employed over the basin to achieve better estimation of spatial distribution of temperature, precipitation and streamflow values based on calculated weighted average to generate annual and seasonal correlation scatter plots for the aforementioned parameters. The results of the scatter plots have been illustrated in Figure 5.7 which indicate negative correlation between both annual temperature and streamflow as well as for annual temperature and total annual precipitation. However, precipitation revealed strong positive correlation with streamflow having R value of 0.771. Additionally, while temperature – streamflow and temperature – precipitation showed negative correlations seasonally as well having R value of 0.51 and 0.58 respectively, the strongest correlation was noted between precipitation and streamflow for the spring season having R value of 0.75 followed by summer season. The reason behind this behaviour is the increased intensity and frequency of precipitation during the spring season that adds to the streamflow volume of the river in the form of snowmelt also which otherwise stacks up as snow cover and is retained on the glaciers during the winter season.

The outcomes of the present research are in coherence with various other researches conducted for different study areas around the world. Observations from some of the previous studies like Tabari and Talaee (2011), Domroes and El-Tantawi (2005), Mahmood and Jia (2017), and Marazi and Romshoo (2018) have all reported similar trends of increasing temperature, decreasing precipitation and streamflow at the regional scale for the past few decades. These studies have been conducted for varying geographical locations ranging from arid and semi-arid regions of Iran and Egypt to the mountainous upper Jhelum River basin and the glaciered Lidder valley of the Himalayas respectively. The comparison of trends in temperature, precipitation and discharge observed in the present study with various previous researches is shown in Figure 5.8 (a), (b) and (c).

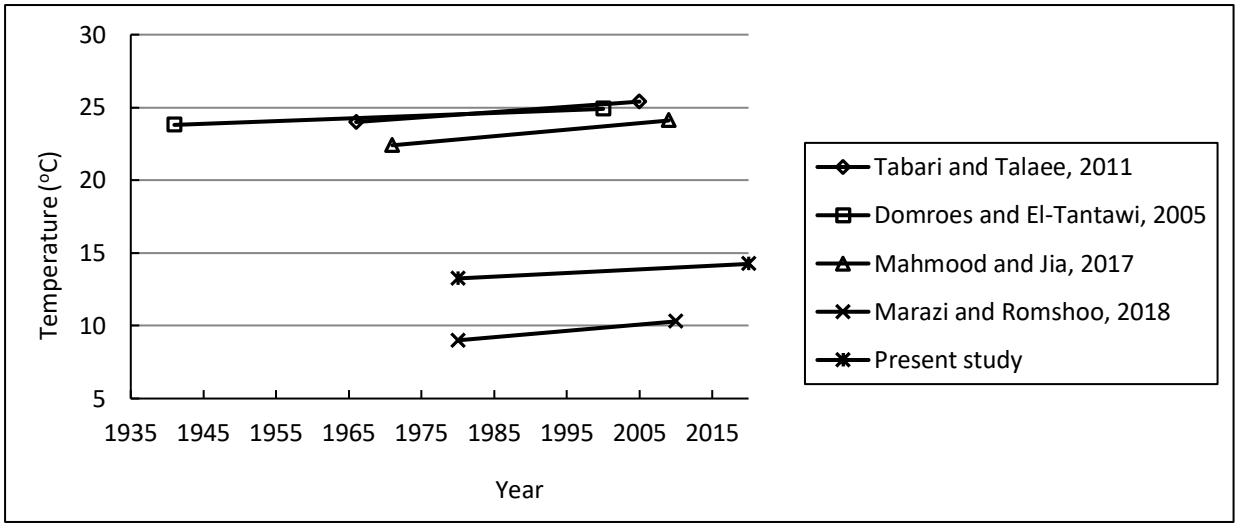
30
25
20
15
10
5
Temperature (°C)
1935 1945 1955 1965 1975 1985 1995 2005 2015
Year
Tabari and Talaee, 2011
Domroes and El-Tantawi, 2005
Mahmood and Jia, 2017
Marazi and Romshoo, 2018
Present study

(a)

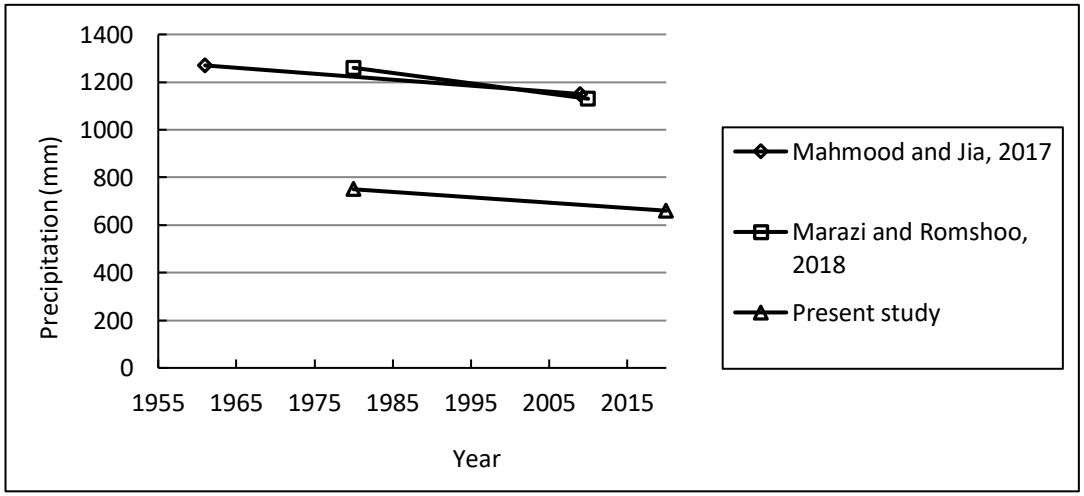
1400
1200
1000
800
600
400
200
0
Precipitation (mm)
1955 1965 1975 1985 1995 2005 2015
Year
Mahmood and Jia, 2017
Marazi and Romshoo, 2018
Present study

(b)

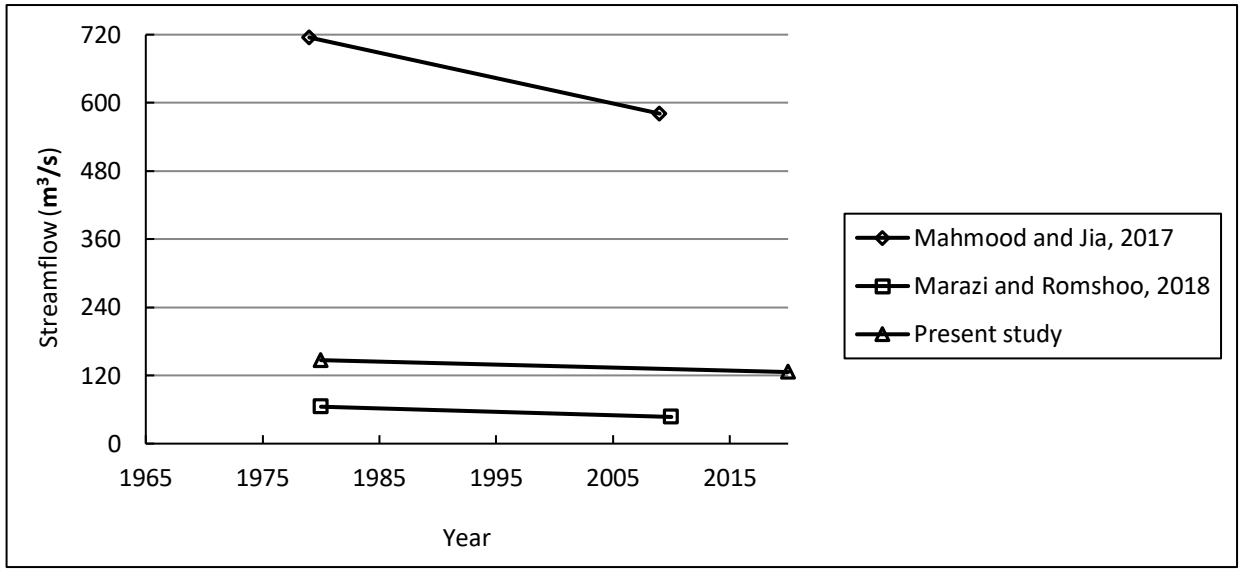

(c)

Figure 5.8. Comparison of Trend Results Obtained for Annual (a) Average Temperature, (b) Precipitation and (c) Streamflow for the Previous Studies with the Present Study.

5.2 Land Use Land Cover Change

Changing land use and land cover predominantly influence the natural environment whose far reaching impacts can not only be observed in the man-environment interaction areas but also near the uninhabited poles due to the global environmental change. The valley of Kashmir has experienced significant changes in its land use and land cover patterns during the three decade period spanning 1992 to 2020. These changes in individual land classes have been discussed in detail in the subsequent sections.

5.2.1 Water Bodies

The area covered by water bodies in the Kashmir valley has seen a considerable reduction from 1.16% to 0.97% and finally to 0.95% of the total area through the years 1992, 2001 and 2020 respectively. The change in the water covered areas from 1992 to 2020 can be observed in Figure 5.9. A major share of this change is attributed to the encroachment by the local dwelling communities and transforming the water covered areas for housing and agricultural purposes by landfilling them. The growing human intervention and unchecked over-exploitation of the water resources in the study area declined the total water covered area by 16.49% from 1992 to 2001, 2.06% from 2001 to 2020 with an overall decrease of 18.21% during the three-decade period from 1992 to 2020. Considerable transformation of the peripheral areas of lakes into marshes can be observed especially in the decade spanning 1992 to 2001 due to the poor implementation of government policies and unchecked urbanization in the vicinity of such water bodies. Such unabated changes have a direct negative impact on the hydrological response of the watershed, which sustains not only the human lives but also supports innumerable flora, and fauna of the area.

5.2.2 Forest cover

The Kashmir valley has witnessed a substantial reduction in the forest cover during the past three decades out of which a significant part was lost due to the territorial dispute that saw an escalated unrest during the 1990's where massive forested areas were burnt down [Gupta 2018]. Consequently, area covered by this resource has reduced from 36.75% in 1992 to 32.16% in 2001 and 31.76% in 2020 as illustrated by Figure 5.9. A major decline of 12.48% from 1992 to 2001 is observed, while 1.23% declined from 2001 to 2020 and a huge overall reduction of 13.56% has been experienced from 1992 to 2020. Although, illegal timber smuggling hugely reduced with the implementation of J&K Forest Conservation Act (1997), nonetheless official involvement has instead amply contributed in further deforestation. It is also estimated that deforestation accounts for 12 – 15% of the world's carbon emissions just behind the biggest contributor of burning fossil fuels [Van der Werf et al. 2009].

5.2.3 Urban area

The urban sprawl in the Kashmir valley has increased from 3.42% to 3.89% and 4.18% in 1992, 2001 and 2020 respectively. The total urban growth has witnessed 22.33% increase during the three-decade period from 1992 to 2020. Unplanned urbanization and encroaching the ecologically fragile river banks in addition to landfilling minor water channels and wetlands has negatively influenced the ecology of the study area that recently bore the brunt of overflowing flood waters in 2014 [Rashid & Anaeus 2020]. Prior to encroachment, these areas would soak up the excessive outpours saving the inhabitants from inundation.

5.2.4 Snow cover

The glacier and snow cover has reduced significantly from 6.87% in 1992 and 6.39% in 2001 to mere 4.85% in 2020. A reduction of 7.01% in snow cover has been

observed from 1992 to 2001 whereas a significant decline of 23.98% is witnessed from 2001 to 2020 as is illustrated in Figure 5.9. An overall decrease of 29.32% in the snow cover was observed during the three decades. A major part of this glacial retreat is attributed to the increased average temperatures around the world due to global warming which leads to melting away of snow reserves [Romshoo et al. 2015]. Unchecked human intervention owing to pilgrimage and tourism in these ecologically sensitive areas also contributes to the depletion of snow cover.

5.2.5 Barren land

The barren land class in the study area has observed a growth from 21.57% in 1992 to 24.54% in 2001 and 29.61% in 2020. The increasing shift towards the barren land has mostly been associated with the shrinking glaciers and unabated degradation of the forest areas [Gupta 2018]. Between 1992 and 2001, the gain in this land class has been 13.79% while the period from 2001 to 2020 saw a growth of 20.68% and a notable overall expansion of 37.32% from 1992 to 2020 is observed.

5.2.6 Plantation

Plantation cover of 10.19%, 10.37% and 11.67% of total area was observed in 1992, 2001 and 2020 respectively as shown in Figure 5.9. A discernable shift towards the cultivation of cash crops (especially fruit and dry fruit trees) has been observed in the valley. The study area recorded a slight increase of 1.78% in the area under horticulture from 1992 to 2001 while as a noticeable upturn of 12.52% has occurred between 2001 and 2020 due to the high economic benefits earned in this sector. The overall increase in the area covered by the plantation land has been 14.53% during the past three decades

5.2.7 Marsh area

Area under the marshes has shown variable trends for the three-decade period in the valley of Kashmir. While the decade of 1990's witnessed shrinking of the water bodies in the study area, most of them got transformed to marshy lands owing to unchecked anthropogenic activity in the immediate vicinity of the lakes; encroaching banks of rivers/lakes, dumping wastes and draining untreated sewage into them [Rashid & Anaeus 2020, Alam et al. 2020]. Such activities have depleted the natural expanse of the hydrological resource in addition to severely affecting its quality due to excessive sedimentation threatening the biodiversity of the region [Ganai et al. 2010]. While the decade spanning 1992 to 2001 had 3.97% and 5.89% of the area covered by marshes respectively, this value reduced to 4.49% in the year 2020 as shown in Figure 5.9. Although an overall increase of 13.21% has been registered in this land class from 1992 to 2020, yet a reduction of 23.69% is observed from 2001 to 2020 due to the relentless transformation of marshy areas into built-up and agricultural land classes [Rashid & Anaeus 2020]. Housing the wetlands has increased the vulnerability of its inhabitants who recently bore the brunt of 2014 flood of the Jhelum river. These marshes would earlier soak up the excess water during minor storms or atleast buffer their negative impacts

5.2.8 Agricultural area

As a substantial part of the economy of the study area, agriculture forms the chief source of occupation for the people in the valley [Rather et al. 2013, Ahmed et al. 2021]. From 16.08% of the total study area in 1992, the agricultural land receded to 15.80% in 2001 and 12.48% in 2020 as depicted in Figure 5.9. Although a marginal reduction of 1.74% from 1992 to 2001 is observed, a substantial decline of 20.99% from 2001 to 2020 is registered. The overall decrement for the three decade period in the agricultural area covered has been 22.37% from 1992 to 2020. This shift has been accredited to the transformation towards plantation / horticulture land class.

Considerable changes in the LULC were observed in the study area. In the present study, eight land use classes were mapped. The land cover change in the land use classes have been quantified and are presented in Table 5.4. The LULC classified maps for the year 1992, 2001 and 2020 are presented in Figure 5.9. A perusal of Figure 5.9 shows considerable LULC changes and transformation from one land use class to another that has occurred over the last three decades. An overall expansion of 9892.68 ha, 104258.06 ha, 19179.48 ha and 6796.72 ha is observed in the urban areas, barren lands, plantation and marshy areas respectively throughout the three decade period spanning 1992 to 2020 in Kashmir. However, a depletion in the expanse of water bodies, forested lands, glacial / snow cover and agricultural areas of 2740.35 ha, 64542.83 ha, 26088.46 ha and 46581.60 ha respectively is experienced concurrently. The changes in the land cover of various land use classes is presented in Figure 5.10 (a) and (b).

Table 5.4. Area Occupied by Various LULC Classes and Change Occurring in them from 1992 to 2020

Land use Class	1992		2001		2020		Change [1992 – 2001]		Change [2001 – 2020]		Overall change [1992 – 2020]	
	ha	%	ha	%	ha	%	ha	%	ha	%	ha	%
Water	15049.9	1.16	12568.1	0.97	12309.6	0.95	–2481.83	– 6.49	–258.52	–2.06	–2740.35	–18.21
Forest	476119	36.75	416690	32.16	411576	31.76	–9428.53	–2.48	–5114.30	–1.23	–64542.83	–3.56
Urban	44299.9	3.42	50417.8	3.89	54192.5	4.18	6117.89	13.81	3774.79	7.49	9892.68	22.33
Snow/Glacier	88989.1	6.87	82746.6	6.39	62900.6	4.85	–6242.54	–7.01	–9845.93	–3.98	–26088.46	–9.32
Barren	279397	21.57	317924	24.54	383655	29.61	38527	13.79	65731	20.68	104258.06	37.32
Plantation	132010	10.19	134362	10.37	151190	11.67	2351.45	1.78	16828	12.52	19179.48	14.53
Marsh	51439.3	3.97	73615.5	5.89	58236	4.49	24876.2	48.36	–8079.47	–3.69	6796.72	13.21
Agriculture	208275	16.08	204658	15.8	161693	12.48	–3617.13	–1.74	–42964.47	–20.99	–46581.60	–22.37

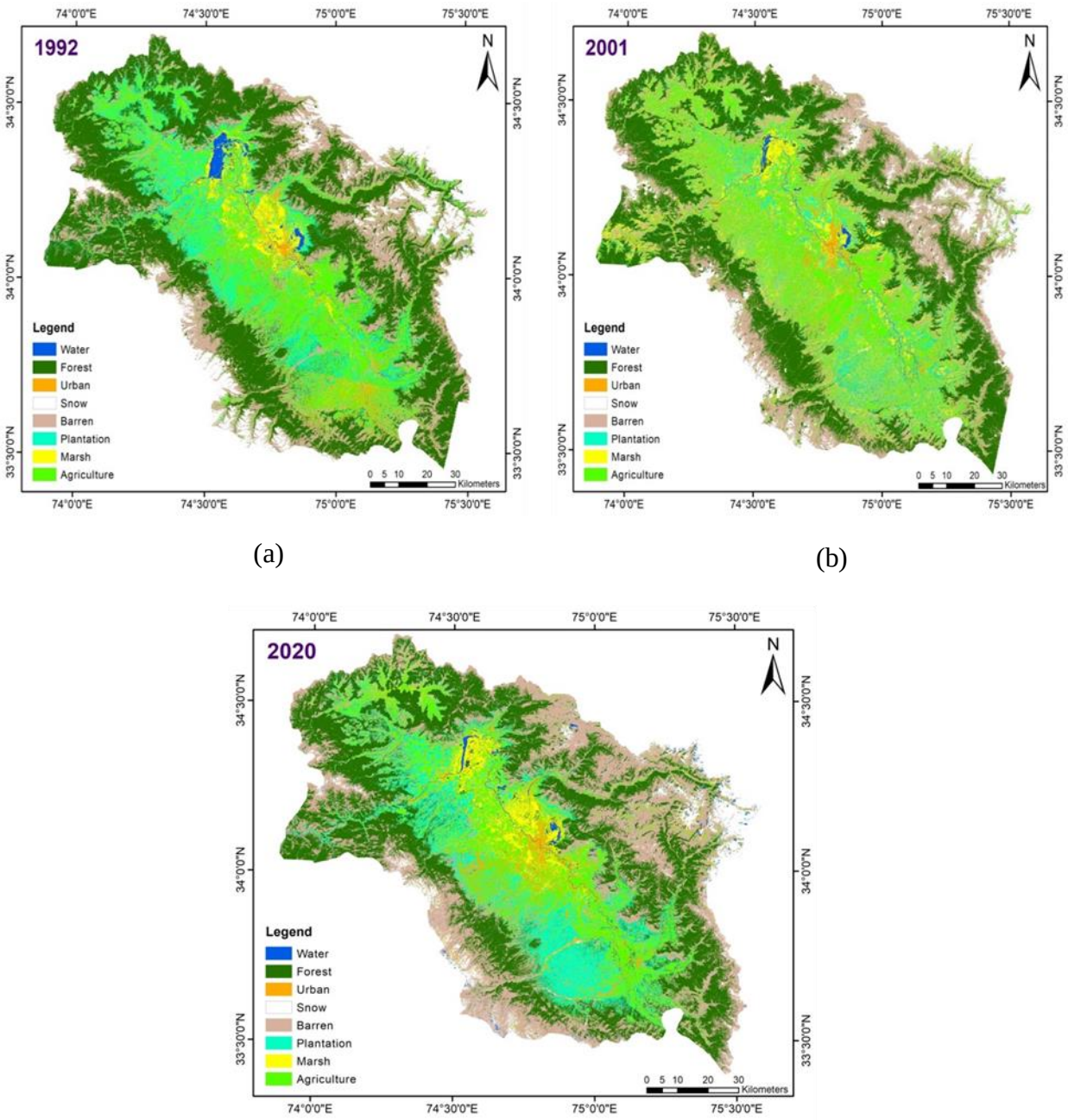

Figure 5.9. Classified LULC Maps of the Study Area for the Years (a) 1992, (b) 2001 and (c) 2020 Corresponding to Satellite Imagery Landsat TM, Landsat ETM+ and Landsat OLI Respectively.

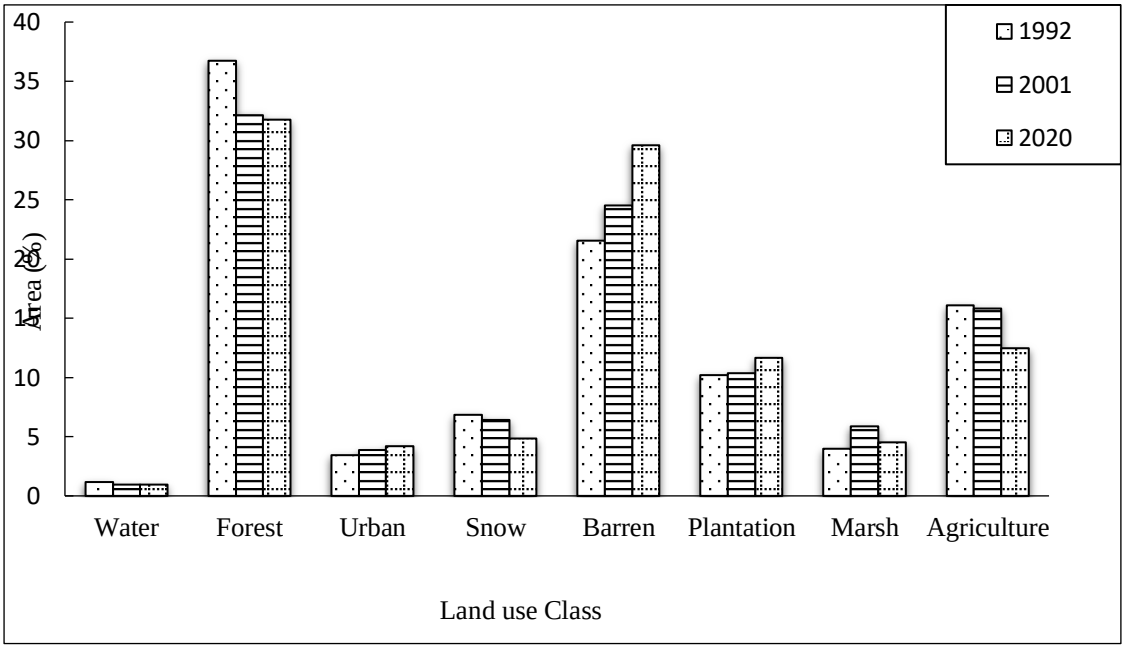

(a)

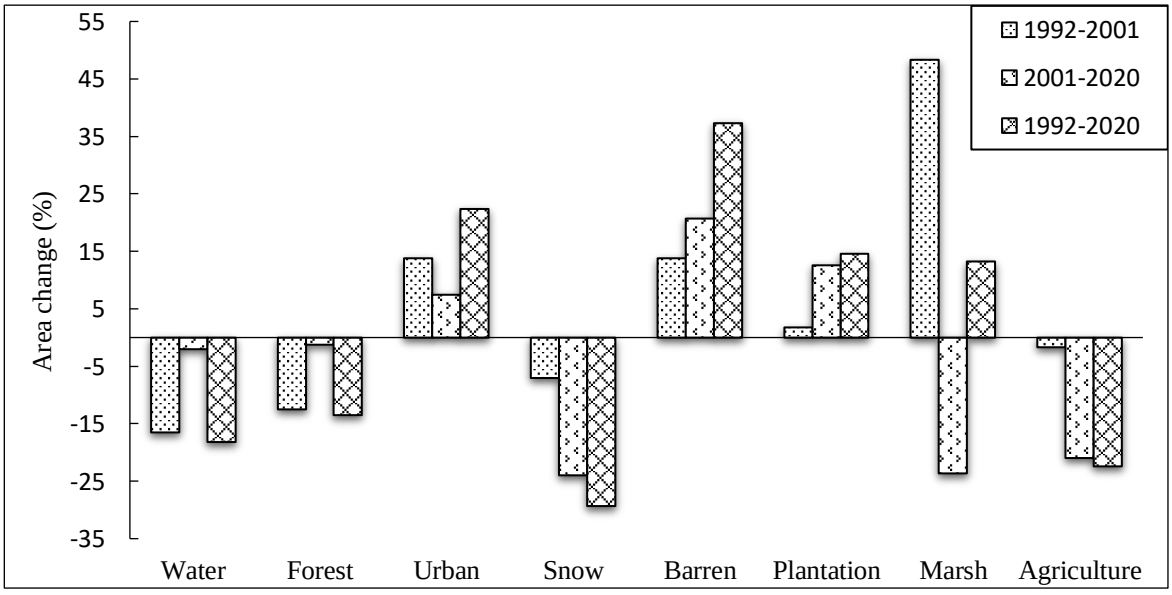

(b)

Figure 5.10. (a) Area (%) covered by LULC classes during 1992, 2001 and 2020 (b) Changes in area (%) for Individual LULC classes from 1992 to 2020.

Various researches carried out in the past on different parts of the study area have reported similar observations as observed in the present study. There has been a significant reduction in the areas covered by water, forest, snow/glacier and agriculture as observed by Alam et al. (2020), Fayaz et al. (2020), Romshoo et al. (2015) and Rasool et al. (2021) who have analyzed the northern, southern and central parts of the Kashmir valley in their respective studies. Increase in the areas covered by urban, barren and plantation is also reported in these research studies. A decrease in the marshy areas has been observed in the recent past attributed to the increasing urbanization in the low lying areas which has also been reported by Iqbal and Sajjad (2014), Fayaz et al. (2020) and Ganaie et al. (2020). These studies have also confirmed the transformation of forest and glacial areas to barren lands in addition to agricultural areas converting into plantation land class. Besides, substantial reduction in the area covered by water bodies is evident from the classified land cover maps illustrated in the present research that is in coherence with the previous studies carried out by the aforementioned authors. Comparison of these LULC change studies with the present study is depicted individually for each land class in Figures 5.11 (a-h).

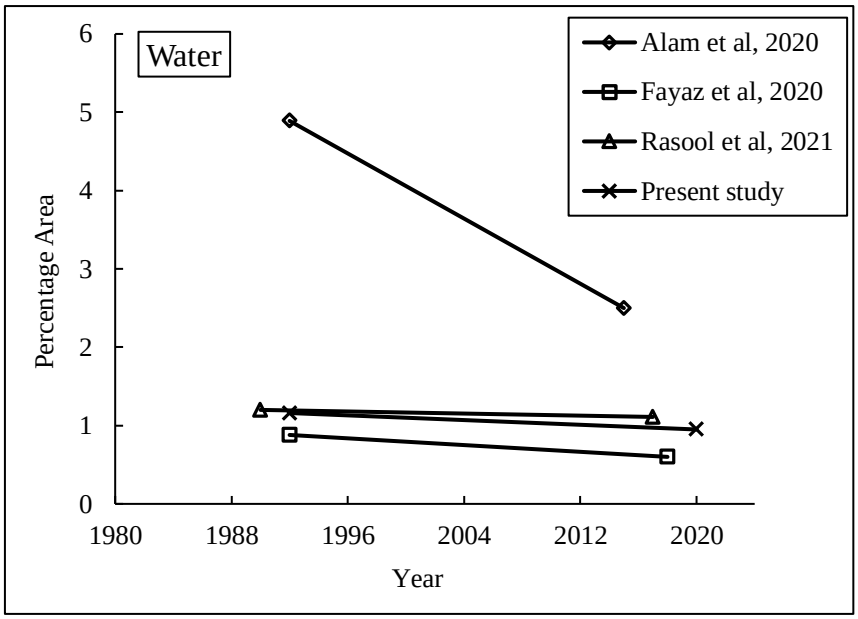

(a)

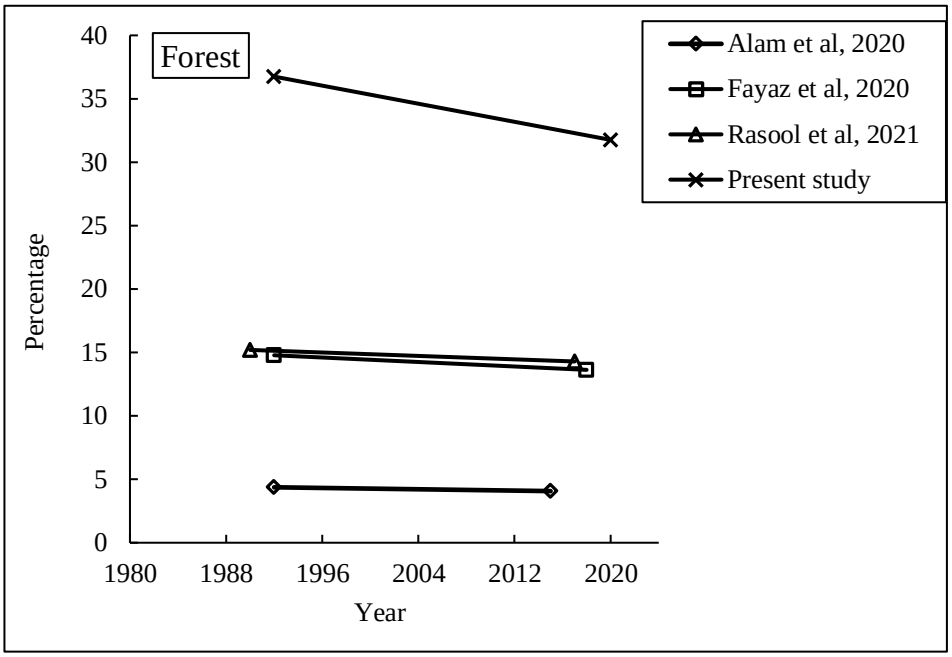
Forest
Alam et al, 2020
Fayaz et al, 2020
Rasool et al, 2021
Present study
Percentage
Year
0
5
10
15
20
25
30
35
40
1980
1988
1996
2004
2012
2020

(b)

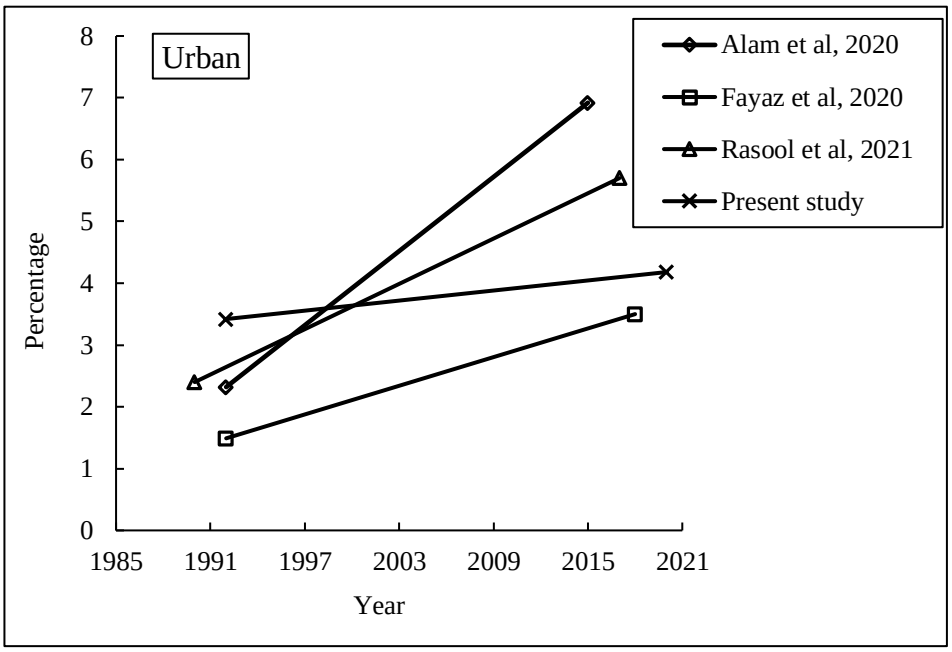
Urban
Alam et al, 2020
Fayaz et al, 2020
Rasool et al, 2021
Present study
Percentage
Year
0
1
2
3
4
5
6
7
8
1985
1991
1997
2003
2009
2015
2021

(c)

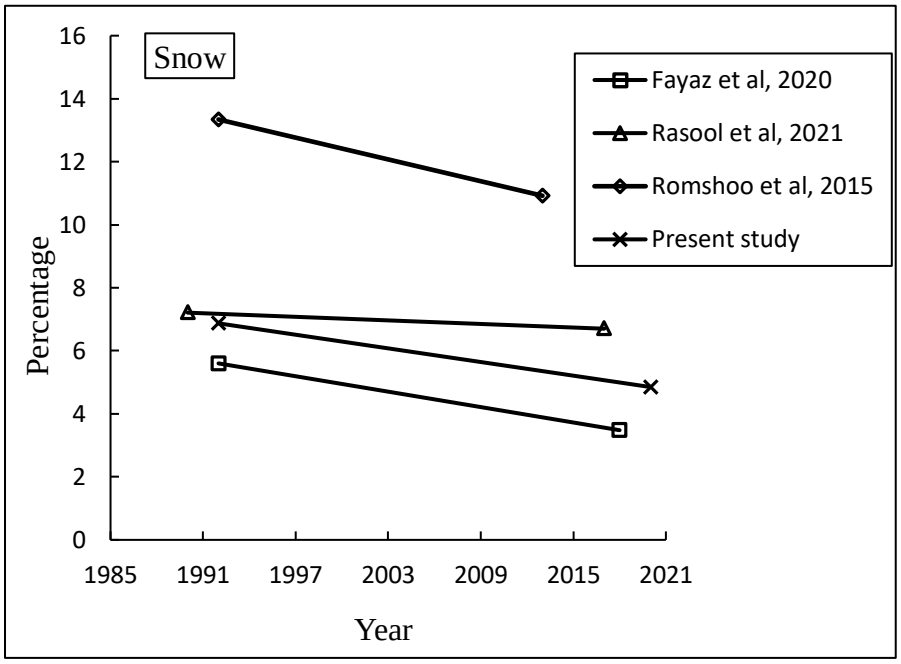
Snow
Fayaz et al, 2020
Rasool et al, 2021
Romshoo et al, 2015
Present study
Percentage
16
14
12
10
8
6
4
2
0
1985
1991
1997
2003
2009
2015
2021
Year

(d)

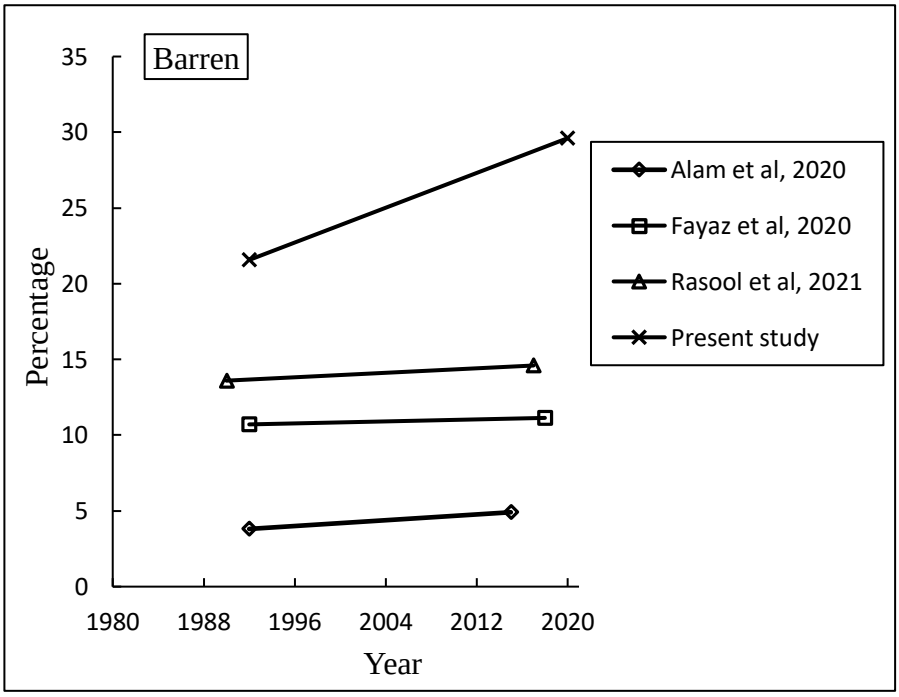
Barren
Alam et al, 2020
Fayaz et al, 2020
Rasool et al, 2021
Present study
Percentage
35
30
25
20
15
10
5
0
1980
1988
1996
2004
2012
2020
Year

(e)

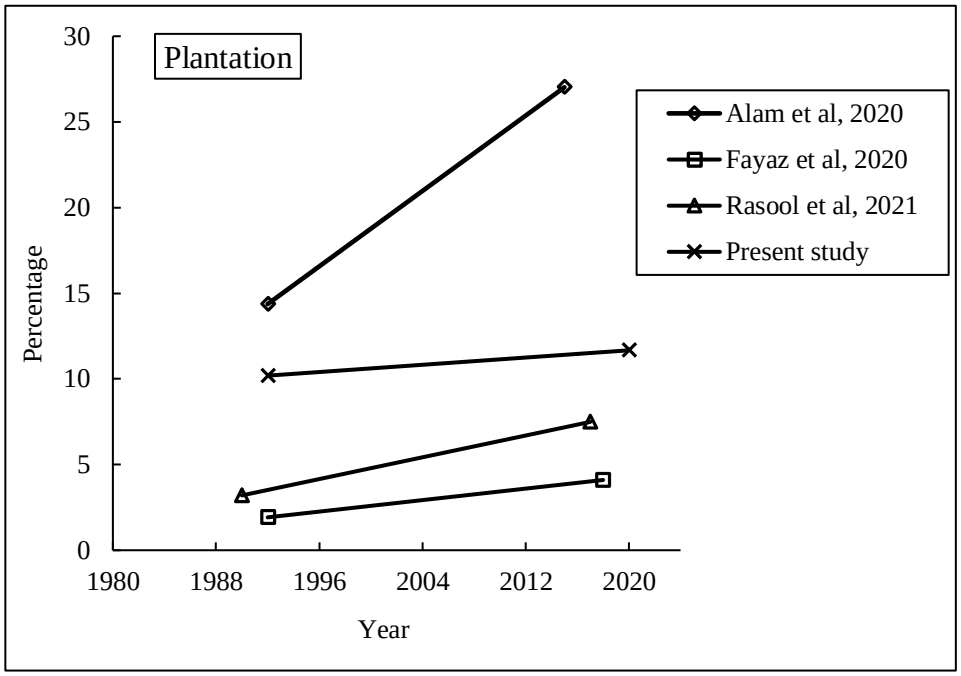
Plantation
Alam et al, 2020
Fayaz et al, 2020
Rasool et al, 2021
Present study
Percentage
Year
0
5
10
15
20
25
30
1980
1988
1996
2004
2012
2020

(f)

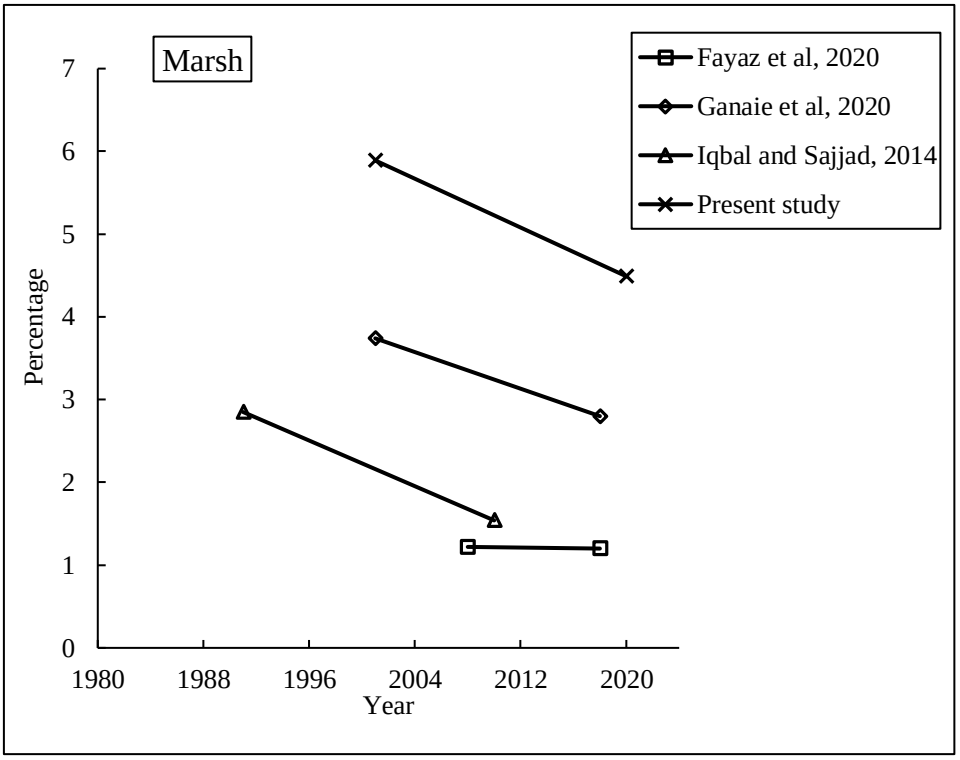
Marsh
Fayaz et al, 2020
Ganaie et al, 2020
Iqbal and Sajjad, 2014
Present study
Percentage
Year
0
1
2
3
4
5
6
7
1980
1988
1996
2004
2012
2020

(g)

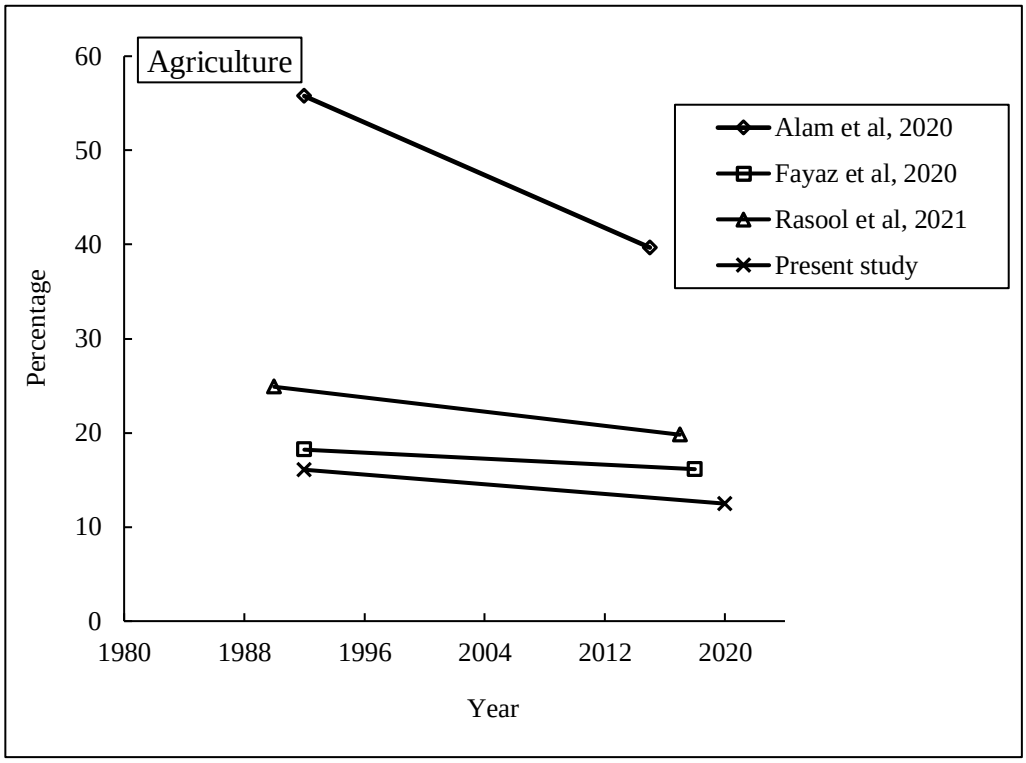

(h)

Figure 5.11. Comparison of Previous Studies Conducted on the Changing LULC Patterns in Different Parts of the Study Area with the Present Study.

5.3 Performance Evaluation of the Model

After setting the Nash-Sutcliffe efficiency (NSE) as the objective function, the values of the p-factor and r-factor determine the consonance between the observed and the simulated streamflow of the basin. Based on the initial iteration run of the model, 13 parameters for the Jhelum river basin were found to be sensitive that include SMTMP, GW_DELAY, SOL_K, TIMP, OV_N, SOL_AWC, TLAPS, PLAPS, CN2, SFTMP, ALPHA_BF, SMFMN and SMFMX as shown in Figure 5.12. While as the p-factor value closer to 1 indicates that most of the points lie within the 95PPU (Percent Prediction Uncertainty) band, the r-factor value closer to 0 signifies absolute match of the observed and the simulated points. t-stat and p-values determine the sensitivity of the parameters and a higher t-stat value along with closer to zero p-value for a watershed parameter indicate high sensitivity of the parameter [Arnold et al. 2012].

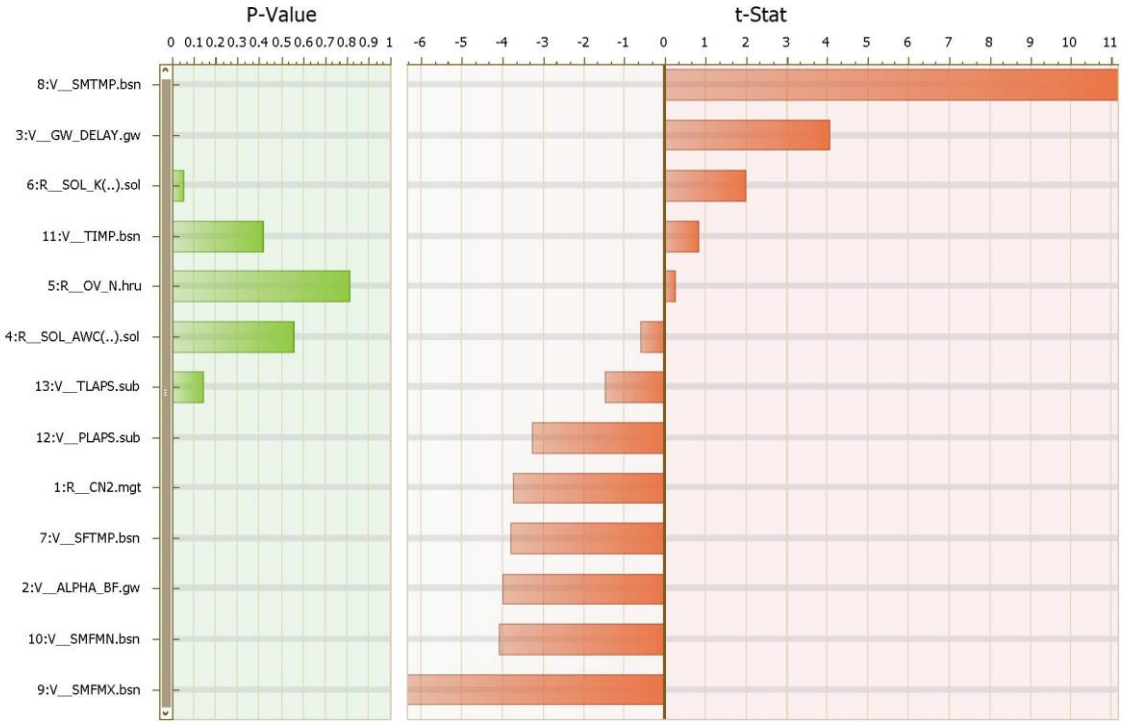

Figure 5.12. Sensitive Parameters of the Jhelum River Basin

The model performance is gauged based on the statistical parameters like R^2, NSE, PBIAS, KGE obtained after performing the calibration and validation of the model. The coefficient of determination R^2, Nash-Sutcliffe Efficiency NSE [Nash and Sutcliffe 1970], Percentage of bias PBIAS and Kling-Gupta Efficiency KGE [Gupta et al. 2009] for the model are calculated as:

$$R^2 = \left[\frac{\sum_{i=1}^{n}(O_i - O_m)(S_i - S_m)}{\sqrt{\sum_{i=1}^{n}(O_i - O_m)^2}\sqrt{\sum_{i=1}^{n}(S_i - S_m)^2}} \right]^2 \quad (14)$$

$$NSE = 1 - \frac{\sum_{i=1}^{n}(O_i - S_i)^2}{\sum_{i=1}^{n}(O_i - O_m)^2} \quad (15)$$

$$PBIAS = \frac{\sum_{i=1}^{n}(O_i - S_i)}{\sum_{i=1}^{n} O_i} \times 100 \quad (16)$$

$$KGE = 1 - \sqrt{(r-1)^2 + (\alpha - 1)^2 + (\beta - 1)^2} \quad (17)$$

Where, O_i and S_i is the observed and the simulated data, O_m and S_m is the mean observed and mean simulated data respectively, $\alpha = \frac{\sigma_s}{\sigma_m}$ and $\beta = \frac{\mu_s}{\mu_m}$, r is the linear regression coefficient between observed and simulated data, μ_s, μ_m are the averages of simulated and observed data σ_s, σ_m are the standard deviations of simulated and measured data respectively.

The hydrological model developed is considered to be satisfactory if NSE and R^2 are greater than 0.5 and $PBIAS$ is within ± 25 [Moriasi et al. 2015]. As a result, the statistical parameters signifying the efficiency of the model developed obtained in this study are considered satisfactory and have been presented in Table 5.5.

Table 5.5. Statistical Parameters Showing Model Performance During Calibration and Validation

Parameters	1992 LULC		2020 LULC	
	Calibration (1984 – 1994)	Validation (1995 – 1999)	Calibration (2000 – 2009)	Validation (2010 – 2013)
Average streamflow (m^3/s)	295.13 (276.63)	329.23 (297.81)	276.57 (223.41)	249.63 (238.91)
p – factor	0.79	0.79	0.85	0.65
r – factor	0.91	0.98	1.5	0.76
R^2	0.7	0.67	0.73	0.78
NSE	0.69	0.59	0.51	0.71
PBIAS	-6.3	-10.5	-13.3	5.5
KGE	0.79	0.79	0.63	0.81

Values in the brackets signify observed streamflow in m^3/s.

5.4 Model Calibration and Validation

The calibration and validation of the model was performed using two LULC's (1992 and 2020) and two sets of weather data (1984 to 1999 and 2000 to 2013) to observe the combined impact of LULC and climate change on the water balance components of the Jhelum river basin. The calibration and validation results obtained illustrated good coherence with the observed data. R^2 values of 0.71 and 0.74 were acquired for the two sets of models between the observed and the simulated data as shown in Figures 5.13 (a) and (b).

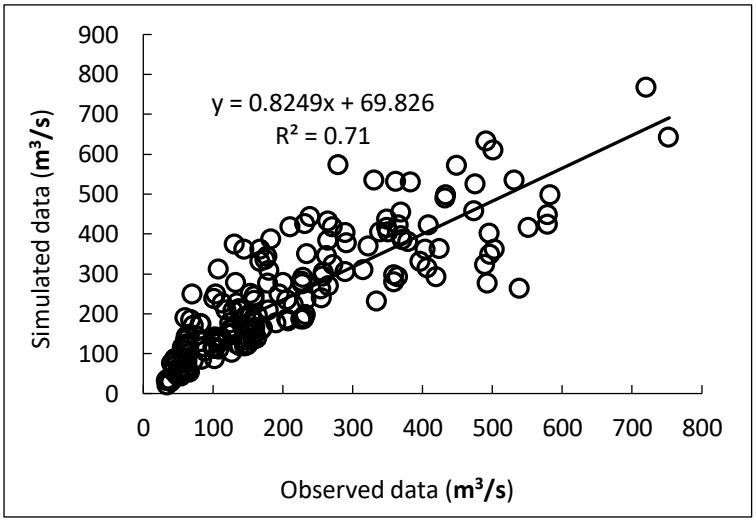

(a)

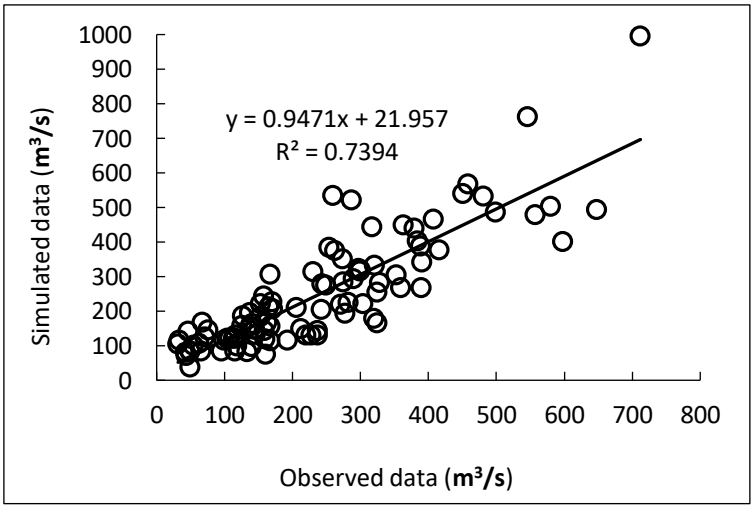

(b)

Figure 5.13. Correlation Between the Observed and Simulated Streamflow at Asham Station for (a) Calibration and (b) Validation Periods.

Calibration of the model was done for the time periods 1984 to 1994 and 2000 to 2009 using the 1992 and 2020 LULC respectively. The R^2, NSE, PBIAS and KGE values obtained for calibration periods was 0.7, 0.69, -6.3 and 0.79 for 1992 LULC and 0.73, 0.51, -13.3 and 0.63 for the 2020 LULC respectively. The average annual streamflow was 295.13 m^3/s and 276.63 m^3/s for the simulated and observed data of 1992 LULC while as 276.57 m^3/s and 223.41 m^3/s for 2020 LULC during calibration respectively. The R^2 value signifies correlation between the observed and simulated datasets and the NSE values reflect how closely does the average observed flow value approximates the estimated flow. KGE and PBIAS values are used to check the bias present in the results. KGE value closer to 1 reflects lesser variability and bias between the observed and the estimated flow values. Negative PBIAS values indicate an overestimation of the simulated flow values whereas positive PBIAS show an underestimated simulation by the model data.

Validation of the models developed was done from 1995 to 1999 and 2010 to 2013 without changing the range of the parameters used for final calibration. The R^2, NSE, PBIAS and KGE values obtained during validation were 0.67, 0.59, -10.5 and 0.79 for 1992 LULC and 0.78, 0.71, 5.5 and 0.81 for the 2020 LULC respectively. The average annual streamflow was 329.23 m^3/s and 297.81 m^3/s for the simulated and observed data of 1992 LULC while as 249.63 m^3/s and 238.91 m^3/s for 2020 LULC during validation respectively. Very good match was obtained between the observed and the simulated datasets and flow hydrographs acquired during the calibration and validation of the SWAT model have been illustrated using Figures 5.14 (a), (b), (c) and (d).

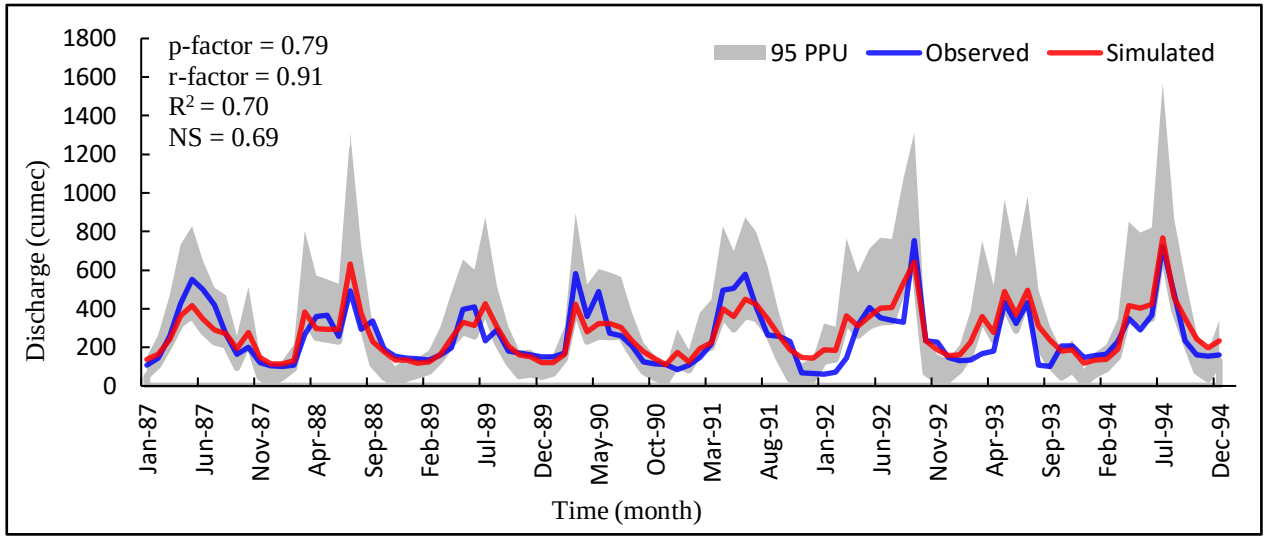
p-factor = 0.79
r-factor = 0.91
R2 = 0.70
NS = 0.69
95 PPU
Observed
Simulated
Discharge (cumec)
1800
1600
1400
1200
1000
800
600
400
200
0
Jan-87
Jun-87
Nov-87
Apr-88
Sep-88
Feb-89
Jul-89
Dec-89
May-90
Oct-90
Mar-91
Aug-91
Jan-92
Jun-92
Nov-92
Apr-93
Sep-93
Feb-94
Jul-94
Dec-94
Time (month)

(a)

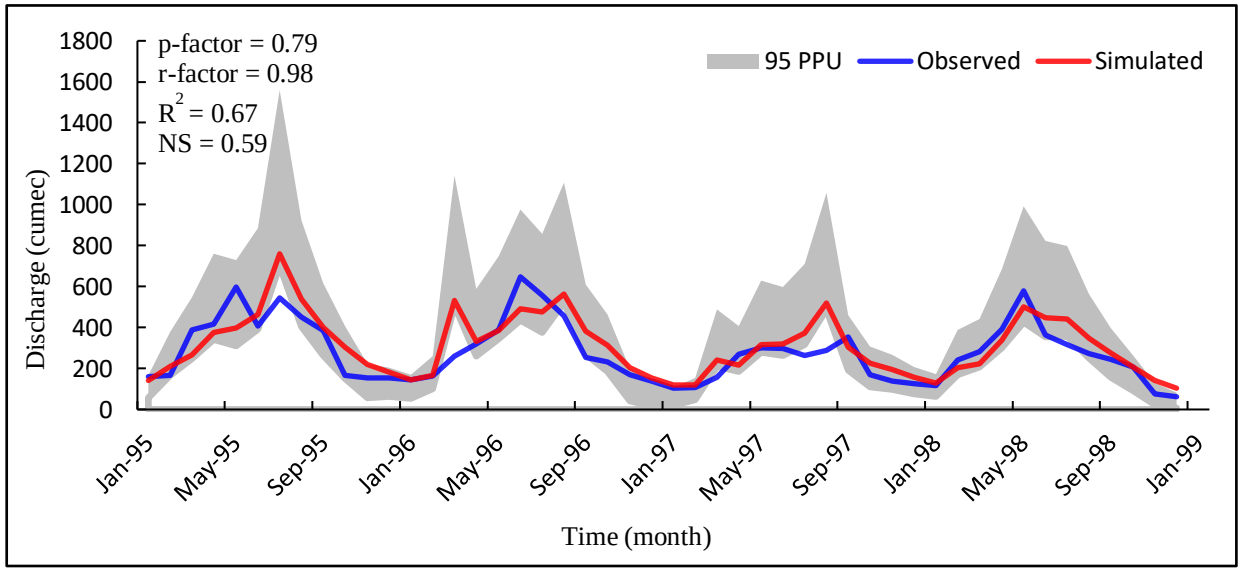
p-factor = 0.79
r-factor = 0.98
R2 = 0.67
NS = 0.59
95 PPU
Observed
Simulated
Discharge (cumec)
1800
1600
1400
1200
1000
800
600
400
200
0
Jan-95
May-95
Sep-95
Jan-96
May-96
Sep-96
Jan-97
May-97
Sep-97
Jan-98
May-98
Sep-98
Jan-99
Time (month)

(b)

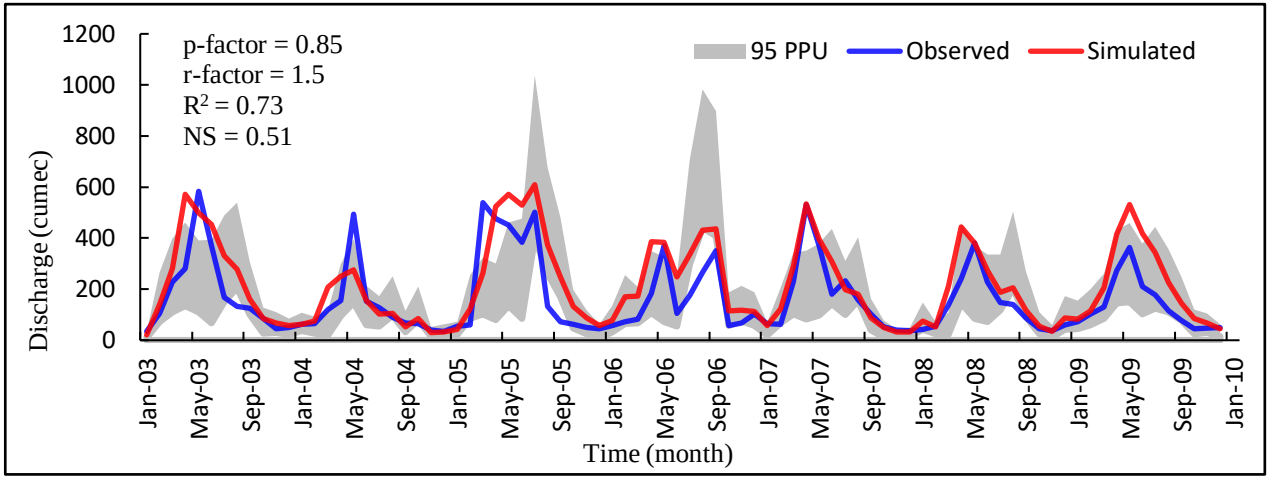

(c)

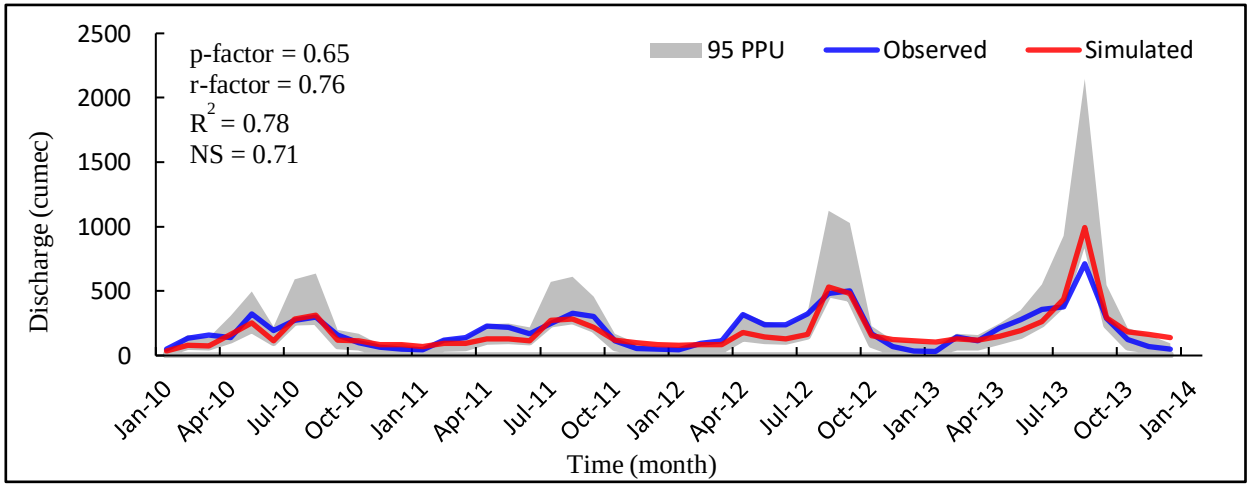

(d)

Figure 5.14. Flow Hydrographs for (a), (c) Calibration and (b), (d) Validation Periods

5.4.1 Combined Impact of LULC and Climate Change from 1984 to 2013

To observe the combined impact of LULC and climate change on streamflow response of the Jhelum river basin, two models were developed for the time periods 1984 to 1999 (using 1992 LULC) and 2000 to 2013 (using 2020 LULC). After proper calibration and validation of the data for the respective time periods, a comprehensive report was generated signifying the changes occurred in various hydrological parameters like evapotranspiration (ET), streamflow, potential evapotranspiration (PET), groundwater level, surface runoff and water yield. Streamflow has shown a reduction of 15.47% from 312.16 m^3/s to 263.85 m^3/s at the Asham hydrological station. Similarly, groundwater has decreased 20.81% from 315.76 mm to 250.04 mm in the basin from 1984 to 2013. Surface runoff and water yield have also reduced 12.17% and 15.51% from 778.28 mm to 692.34 mm and 1221.07 mm to 1031.66 mm respectively. While as evapotranspiration and potential evapotranspiration have increased from 13.94% and 6.74% from 310.50 mm to 353.80 mm and 1076.80 mm to 1149.40 mm respectively. These changes are a result of rapid urbanization in the watershed along with deforestation that has a huge impact on the surface infiltration and evapotranspiration characteristics (Table 3.4). Apart from surface properties, temperature in the basin has also seen a constant escalation as discussed in Section 5.4.2.1, that can be attributed as a source of intensified evapotranspiration in the watershed for the three decade period from 1984 to 2013. Snow/glacier cover has also suffered a major reduction of 30.87% in the basin that feeds major tributaries of the Jhelum river and hence contributed in reducing the streamflow of Jhelum. Changes experienced in the water balance components due to the combined influence of land use land cover and climate change from 1984 to 2013 are summarized in Table 5.6.

Table 5.6. Combined Influence of Climate and LULC Change on the Water Balance Components of Jhelum River Basin

Water balance components	Scenario I [1984 – 1999]	Scenario II [2000 – 2013]	Change (%)
Streamflow (m^3/s)	312.16	263.85	-15.47
Groundwater (mm)	315.76	250.04	-20.81
Surface runoff (mm)	788.28	692.34	-12.17
ET (mm)	310.50	353.80	13.94
PET (mm)	1076.80	1149.40	6.74
Water Yield (mm)	1221.07	1031.66	-15.51

5.4.2 Future Climate Change Impact

5.4.2.1 Temperature and Precipitation

NorESM1-M model was used in the present study after correction of bias present in the output to predict the future temperature and precipitation of the river basin. Distribution mapping was employed to analyse two radiative forcings RCP 4.5 and RCP 8.5 and the results obtained have been summed up in Table 5.7. In comparison with the observed mean annual temperature of 7.31^{o}C in the basin from 1984 to 2013, RCP 4.5 projected a surge in the temperature of 1.51^{o}C and 2.14^{o}C while as RCP 8.5 projected an increment of 2.27^{o}C and 4.34^{o}C towards the middle and end of 21st century respectively. Future projections for precipitation in the basin predicted a reduction throughout in comparison with the annual observed precipitation of 1200.01 mm for the three decade period. RCP 4.5 estimated a reduction of 7.05% and 6.81% while as RCP 8.5 projected a decline of 9.96% and 12.04% towards the middle and end of 21st century respectively. Future projections of temperature and precipitation based on RCP 4.5 and RCP 8.5 scenarios in comparison with the observed annual base values in the Jhelum river basin have been illustrated using Figures 5.15 (a), (b), (c) and (d).

Table 5.7. Predicted Average Annual Temperature and Precipitation During Mid and Late Century Under RCP 4.5 and RCP 8.5 in the Jhelum River Basin

Duration	RCP 4.5		RCP 8.5	
	Temperature (^{o}C)	Precipitation (mm)	Temperature (^{o}C)	Precipitation (mm)
2041 - 2070	8.82 (1.51)	1115.4 (-7.05%)	9.58 (2.27)	1080.46 (-9.96%)
2070 - 2100	9.45 (2.14)	1118.26 (-6.81%)	11.65 (4.34)	1055.53 (-12.04%)

Values in brackets signify changes in the average annual temperature and precipitation from the observed mean annual values respectively

5.4.2.2 Projected Streamflow Response of the Basin

With the help of bias corrected data from NorESM1-M model using DM technique, the developed SWAT model for the Jhelum river basin was run separately for mid and end of the 21st century to capture the future influence of climate change on the streamflow response. Considering the baseline observation period of three decades from 1984 to 2013, RCP 4.5 projected an increase in the streamflow of 20.67% and 23.81% against the mean annual average of 274.41 m^3/s while as RCP 8.5 estimated a lower increment of 17.16% and 7.86% during the middle and end of the 21st century as shown in Table 5.8. Comparison of future projections of streamflow between RCP 4.5 and RCP 8.5 has been illustrated using Figures 5.16 (a), (b) and (c).

Table 5.8. Predicted Average Annual Streamflow During Mid and Late Century under RCP 4.5 and RCP 8.5 in the Jhelum River Basin

Duration	RCP 4.5	RCP 8.5
	Streamflow (m^3/s)	Streamflow (m^3/s)
2041 - 2070	331.14 (20.67%)	321.50 (17.16%)
2070 - 2100	339.74 (23.81%)	295.97 (7.86%)

Values in brackets signify changes in the average annual streamflow from the observed mean annual value

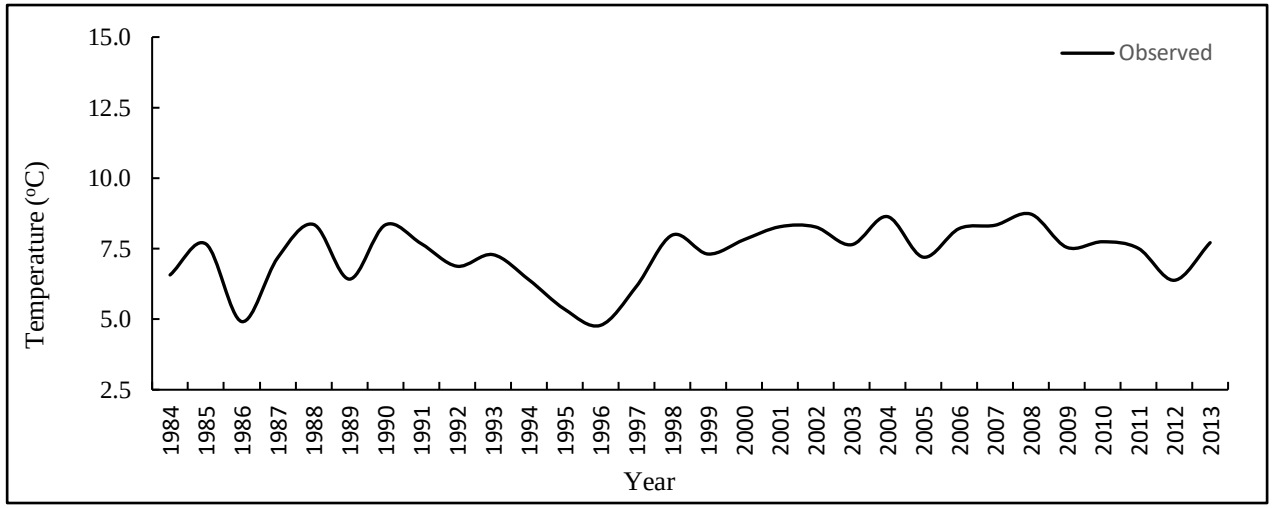
15.0
12.5
10.0
7.5
5.0
2.5
Temperature (°C)
Observed
1984 1985 1986 1987 1988 1989 1990 1991 1992 1993 1994 1995 1996 1997 1998 1999 2000 2001 2002 2003 2004 2005 2006 2007 2008 2009 2010 2011 2012 2013
Year

(a)

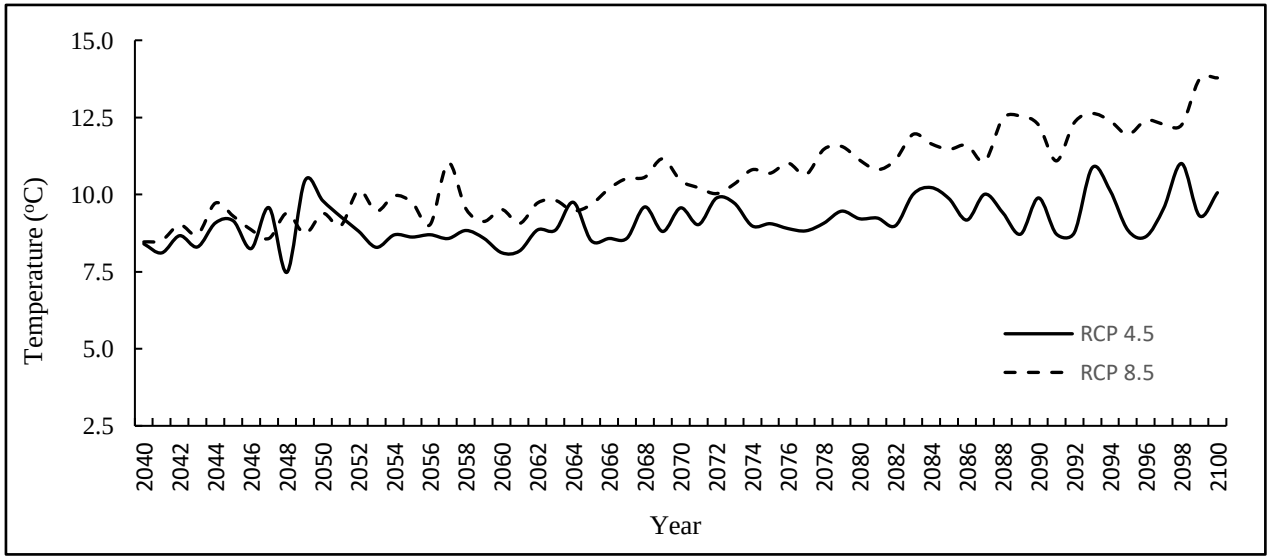
15.0
12.5
10.0
7.5
5.0
2.5
Temperature (°C)
RCP 4.5
RCP 8.5
2040 2042 2044 2046 2048 2050 2052 2054 2056 2058 2060 2062 2064 2066 2068 2070 2072 2074 2076 2078 2080 2082 2084 2086 2088 2090 2092 2094 2096 2098 2100
Year

(b)

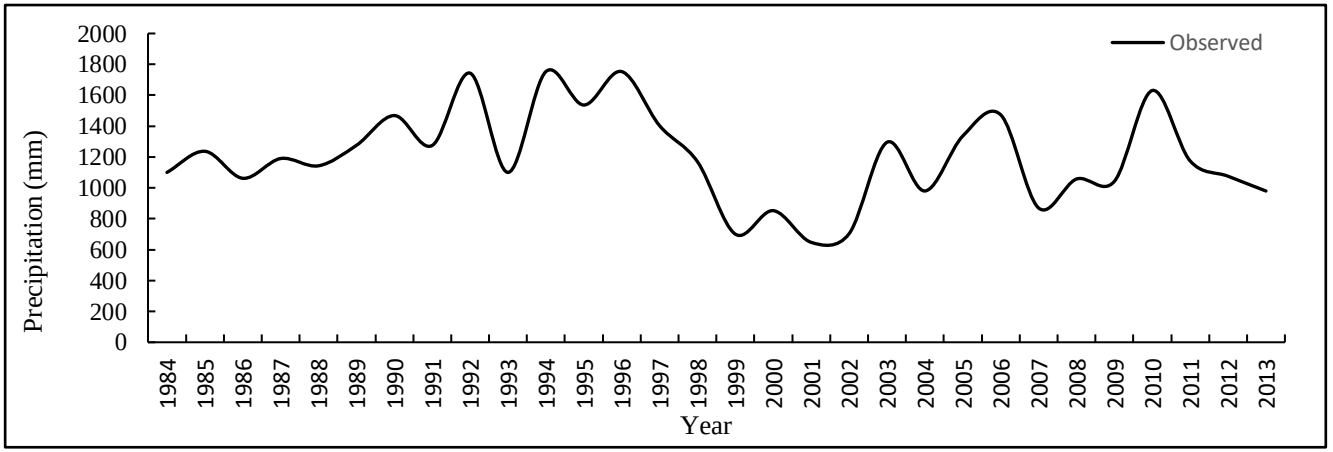

(c)

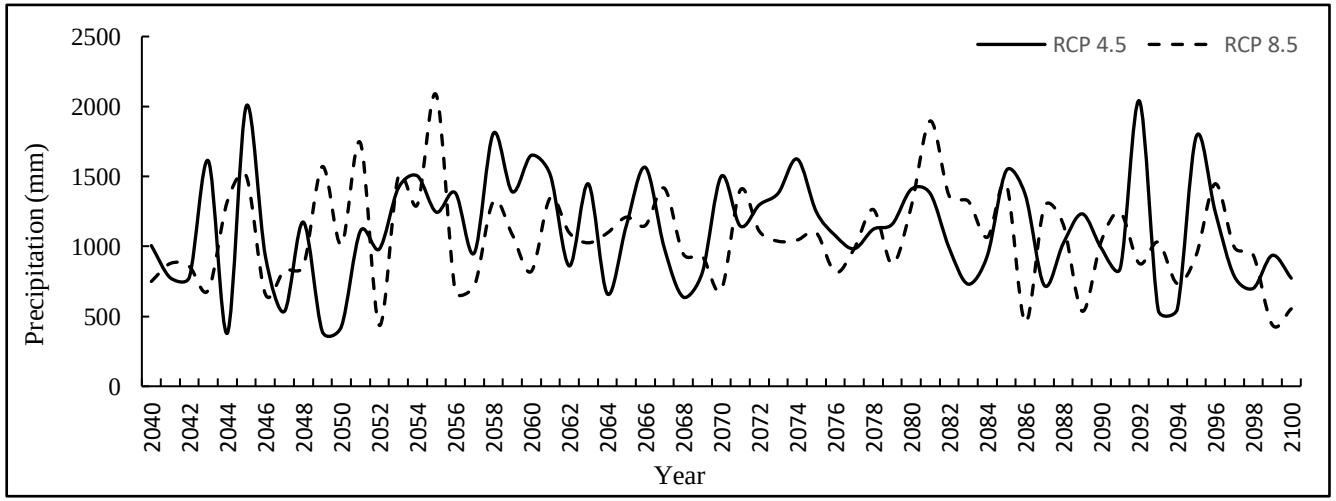

(d)

Figure 5.15. Observed and Comparison of Future Projections under RCP 4.5 and RCP 8.5 of Annual (a), (b) Mean Temperature and (c), (d) Precipitation from 1984 to 2013 and 2041 till the end of 21st Century

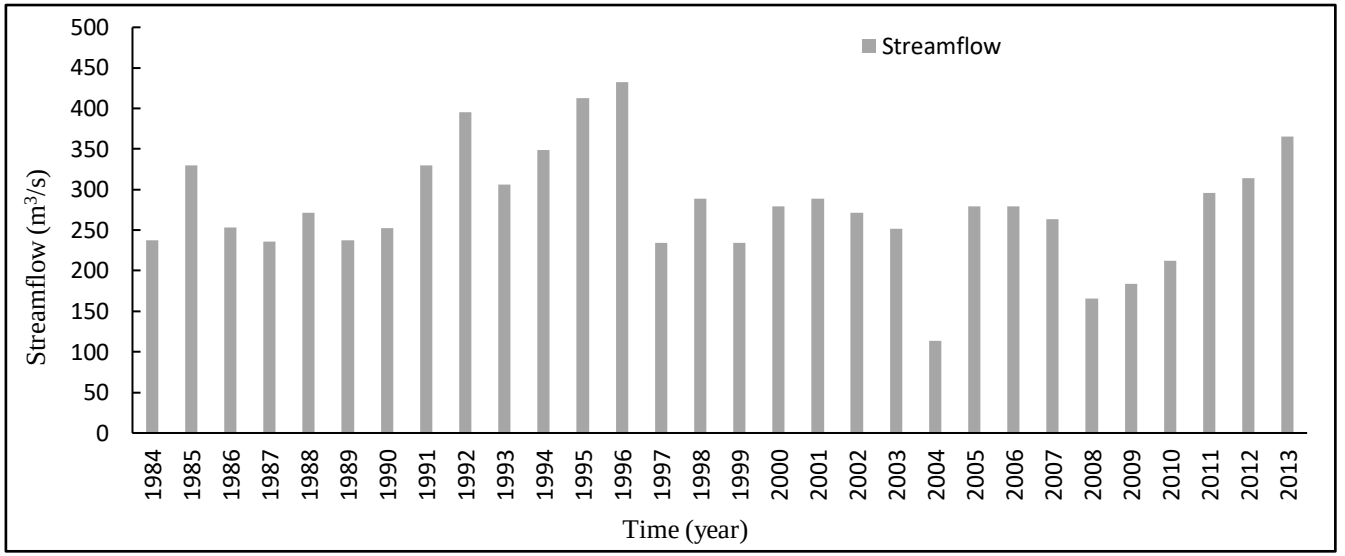
Streamflow
Streamflow (m3/s)
500
450
400
350
300
250
200
150
100
50
0
1984 1985 1986 1987 1988 1989 1990 1991 1992 1993 1994 1995 1996 1997 1998 1999 2000 2001 2002 2003 2004 2005 2006 2007 2008 2009 2010 2011 2012 2013
Time (year)

(a)

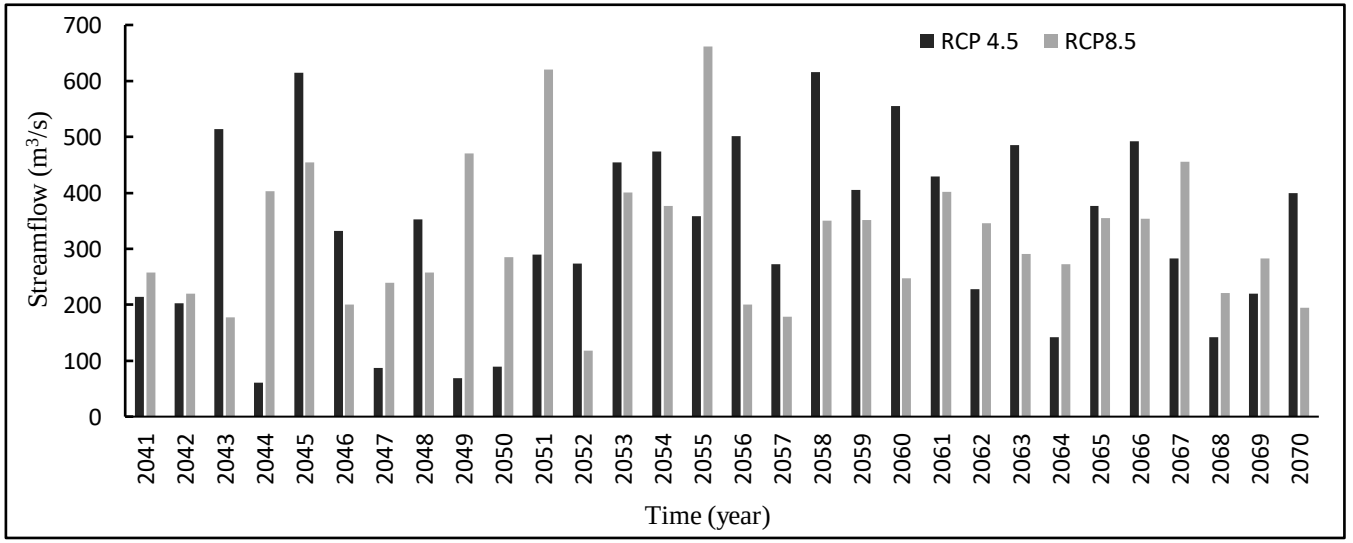
RCP 4.5
RCP8.5
Streamflow (m3/s)
700
600
500
400
300
200
100
0
2041 2042 2043 2044 2045 2046 2047 2048 2049 2050 2051 2052 2053 2054 2055 2056 2057 2058 2059 2060 2061 2062 2063 2064 2065 2066 2067 2068 2069 2070
Time (year)

(b)

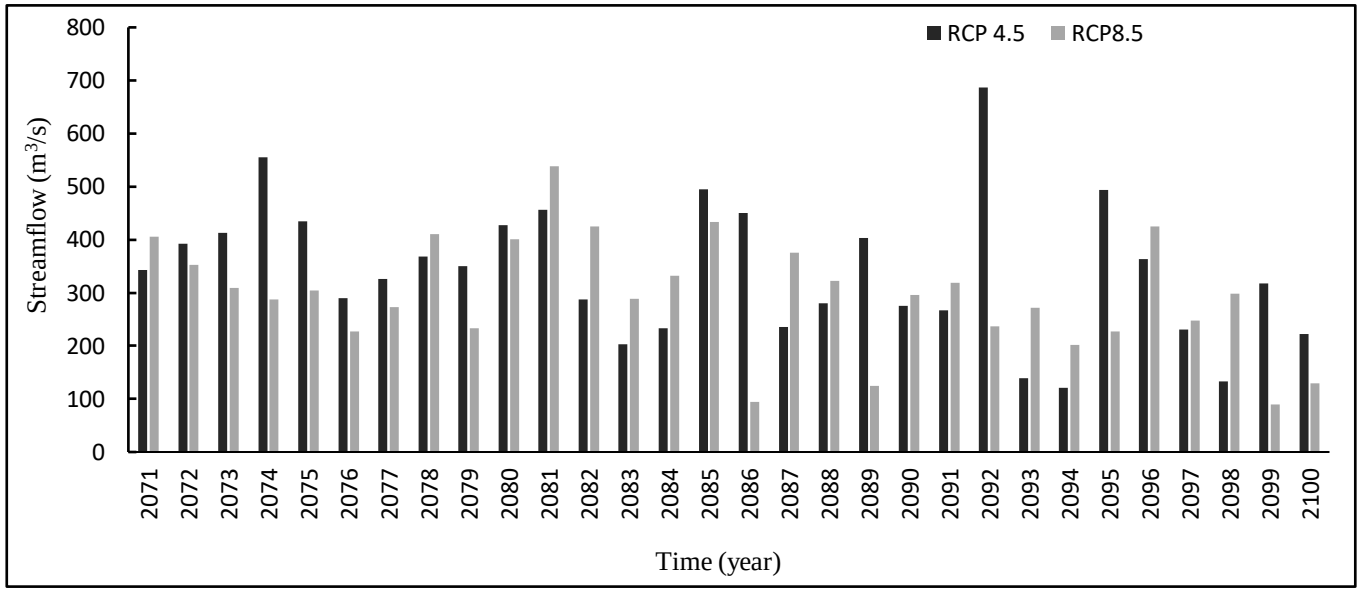

(c)

Figure 5.16. Observed Mean Annual Streamflow and Comparison of Future Projections of Mean Annual Streamflow under RCP 4.5 and RCP 8.5 from 1984 to 2013 and 2041 until the End of 21st Century.

The water balance components depicted variable patterns for the future projections. Groundwater exhibited a declining trend from 16.6% to 16.3% from mid (1941 – 1970) towards the end of the 21st century (1971 – 2100) but an increment of 16.6% against the baseline observed mean annual value of 282.90 mm (from 1984 to 2013) under RCP 4.5 emission scenario. While as RCP 8.5 projected a sharp decrement from 11.9% to -15.3% in the groundwater recharge for the mid and end of 21st century respectively. In comparison with the baseline mean annual surface runoff value of 740.31 mm (1984 – 2013), RCP 4.5 emission scenario estimated an increase of 11.0% and 15.4% and RCP 8.5 projected an increase of 8.2% and 7.4% towards the middle and end of 21st century respectively. Evapotranspiration showed a regular increasing trend against the mean annual value of 332.15 mm to 13.2% and 15.0% under RCP 4.5 and similarly 18.1% and 25.7% under RCP 8.5 towards the mid and end of the 21st century. Water yield will likely increase from the mean annual value of 1126.37 mm to 14% and 16.7% under RCP 4.5 scenario but projects a declining trend from 10.7% to 2.0% under RCP 8.5 emission scenario towards the middle and end of 21st century.

These forecasted fluctuations in the water balance components can be attributed to the high variability shown by precipitation patterns under medium and high emission scenarios as is depicted in Figure 5.15 (d) until the end of the 21st century. The likelihood of increased surface runoff and water yield under medium emission scenario is ascribed to the higher projected annual mean temperatures as depicted in Figure 5.15 (b) that leads to melting of the glaciers and contributes to increased streamflow. Such changes also induce conditions for increased evapotranspiration as predicted by the hydrological model under two emission scenarios. In case of the high emission scenarios water yield, groundwater recharge and runoff shows a notable decline whereas evapotranspiration projects a likely increase by the end of the 21st century. The increased rate of evapotranspiration and higher mean annual temperatures in the later half of the century can be a source for the reduced runoff, groundwater recharge and water yield contrary to expected pattern of increased glacier melt because of higher mean annual temperatures. The catchment response

in terms of the changing water balance components under two emission scenarios against the observed mean annual values (from 1984 to 2013) till the end of the 21st century are presented in Table 5.9.

Certain previous studies conducted on different watersheds have reported similar trends in the future projections of temperature, precipitation and the catchment response owing to LULC and climate change. Shah et al. (2020) predicted the future catchment response to the changes in climate in highly glaciered Indus river basin and reported similar increasing trends in temperature, precipitation and streamflow until the end of 21st century. Chanapathi and Thatikonda (2020) evaluated the present and future influence of land use land cover and climate change on Krishna river basin and projected 50% increase in the surface runoff, streamflow and water yield in the basin under RCP 4.5 that doubles under RCP 8.5. Similarly, Welde and Gebremariam (2017) studied the hydrological response of Tekeze watershed in Ethiopia and noted an increase in the mean annual streamflow and sediment yield to be around 7.31% and 21.8% respectively attributed to erratic rainfall patterns during the wet season. Trang et al (2017) assessed the combined impact of LULC and climate change on the transboundary river basin covering Laos, Cambodia and Vietnam and concluded that discharge and water availability is expected to increase along with temperature and precipitation under RCP 4.5 and RCP 8.5 emission scenarios using multiple climate models. Though some variable trends were shown by these hydro-meteorological parameters during dry and wet seasons, yet the overall results reflected a surge throughout.

Table 5.9. Predicted Average Annual Values of Water Balance Components During the Middle and Late Century Under RCP 4.5 and RCP 8.5 in the Jhelum River Basin

Scenario	Groundwater (mm)	Surface runoff (mm)	ET (mm)	PET (mm)	Water Yield (mm)
Observed 1984 – 2013	282.90	740.31	332.15	1113.1	1126.37
1941 – 1970 [RCP 4.5]	330.05 (16.6%)	822.38 (11.0%)	376.16 (13.2%)	1010.12 (-9.2%)	1284.42 (14.0%)
1971 – 2100 [RCP 4.5]	329.18 (16.3%)	854.36 (15.4%)	382.06 (15.0%)	1035.82 (-6.9%)	1315.32 (16.7%)
1941 – 1970 [RCP 8.5]	316.59 (11.9%)	801.23 (8.2%)	392.34 (18.1%)	1045.08 (-6.1%)	1247.06 (10.7%)
1971 – 2100 [RCP 8.5]	239.45 (-15.3%)	795.53 (7.4%)	417.50 (25.7%)	1146.47 (2.9%)	1149.04 (2.0%)

CHAPTER 6

CONCLUSIONS

The conclusions inferred from this study have been enumerated and discussed as follows:

1. The average annual temperature registered an overall increase spanning all meteorological stations with the rate of increase being 0.014 ^{o}C/year at Qazigund, 0.026 ^{o}C/year at Rambagh, and 0.012 ^{o}C/year at Gulmarg.
2. The total annual precipitation decreased at all the meteorological stations. The trends observed revealed a significant divergence in the spring and summer downpours towards the winter and autumn seasons. The rate of decrease in the total annual precipitation recorded 5.434 mm/year at Qazigund, 1.998 mm/year at Rambagh and a prominent decline of 13.297 mm/year at Gulmarg meteorological station.
3. The average annual streamflow of the River Jhelum also showed a decreasing trend at the rate of 26.277 cusec/year at Sangam, 17.039 cusec/year at Ram Munshi Bagh and 40.345 cusec/year at Asham hydrological station.
4. Correlation analysis showed negative correlations between temperature – precipitation and temperature – streamflow while as a strong positive correlation was found out between precipitation and streamflow of the basin.
5. A strong positive correlation between precipitation and streamflow for the spring season followed by the summer season stems from the fact that the increased intensity and frequency of downpour during the spring season enhances the river discharge substantially, amplifying with the snowmelt from

the glaciers which otherwise stacks up during the winter season as snow cover and is reserved on the glaciers.

6. The years 1997-1998 mark a significant breakpoint over almost all the trend results obtained, depicting a downward shift in the total annual precipitation received by the valley and the average annual streamflow of the river while as recording a surge in the average annual temperature.

7. Unchecked and unplanned urbanization in addition to extensive anthropogenic intervention in the ecologically sensitive areas has led to degradation of the natural resources in the study area.
8. An overall expansion of 9892.68 ha (22.33%), 104258.06 ha (37.32%), 19179.48 ha (14.53%) and 6796.72 ha (13.21%) is discerned in the urban areas, barren lands, plantation and marshy areas respectively throughout the three decade period spanning 1992 to 2020 in Kashmir.
9. However, a depletion in the expanse of water bodies, forested lands, glacial / snow cover and agricultural areas of 2740.35 ha (18.21%), 64542.83 ha (13.56%), 26088.46 ha (29.32%) and 46581.60 ha (22.37%), respectively is also observed.
10. Conversion of areas covered by forest, glacier and water bodies to barren lands and marshes has taken place which can be attributed to timber smuggling, encroachment around lakes, housing wetlands, growing population and poor implementation of government policies.
11. Transformation of agricultural farming land to plantation was observed in the study area as people have resorted towards horticulture as it is economically more beneficial.
12. Amongst other changes in the LULC patterns of the basin, significant reduction in the snow cover (-30.87%) and expansion of built-up area (+16.25%) and barren land (+22.85%) has been noted.
13. The combined impact of LULC and climate change has resulted in reduction in streamflow (-15.47%), groundwater (-20.81%), surface runoff (-12.17%)

and water yield (-15.51%) while as increase in the evapotranspiration (+13.94) of the basin from 1984 to 2013.

14. The projected changes in future temperature show 1.51^{o}C and 2.14^{o}C rise under RCP 4.5 while as 2.27^{o}C and 4.34^{o}C increment under RCP 8.5 during the mid and end of the 21st century in the basin.
15. Future precipitation changes project reductions of 7.05% and 6.81% under RCP 4.5 where as a decline of 9.96% and 12.04% under RCP 8.5 is estimated during the mid and end of the 21st century in the basin.
16. Changes in the future streamflow patterns project an increase of 20.67% and 23.81% under RCP 4.5 while as an increment of 17.16% and 7.86% against the baseline mean annual streamflow of 274.41 m^3/s in the basin for mid and end of the 21st century.

The outcome of present study gives a lucid picture of the present circumstances and a glimpse for the probable future events unfolding in our environment because of unprecedented changes in the climate. There have been prominent changes in the hydro-meteorological parameters in the valley of Kashmir that has been illustrated in this study using different methods such as trend analysis and hydrological modeling. The decreasing trend shown annualy by the streamflow of Jhelum river basin during the past four decades is alarming and requires immediate attention of hydrologists, policy makers and planners. This awareness is also needed to be disseminated among the general masses because of the expected worsening of the situation in the coming years.

The present study tried to incorporate a comprehensive analysis of the hydrological response of the Jhelum river basin as an impact assessment study of the changing climate and land use land cover change. However, the future hydrological response of the basin was predicted using future climate model data only. Therefore, further studies can be conducted in this area by predicting the future land use land cover scenarios of the basin and finding out the future possible combined impact on the hydrological response of the basin.

From the sustainability point of view this study has obtained several noteworthy results that provide a glimpse of the future with unwanted changes in our environment because of the prevailing changes induced by the mankind in their reckless usage and exploitation of the natural resources. As a result, keeping in view the sustainability aspect this study is valuable for the scientific community in particular and the common masses in general to disseminate more awareness about the drastic consequences of our actions and take steps that reduce the harm being done to the environment. This study also provides valuable information for better policy development and management of the water resources for the hydrologists.

REFERENCES

Abbaspour, K. C. (2008). SWAT calibration and uncertainty programs. *A User Manual. Eawag Zurich, Switzerland*, *20*.

Abdulkareem, J. H., Pradhan, B., Sulaiman, W. N. A., & Jamil, N. R. (2018a). Review of studies on hydrological modelling in Malaysia. *Modeling Earth Systems and Environment*, *4*(4), 1577-1605.

Abdulkareem, J. H., Sulaiman, W. N. A., Pradhan, B., & Jamil, N. R. (2018b). Long-term hydrologic impact assessment of non-point source pollution measured through Land Use/Land Cover (LULC) changes in a tropical complex catchment. *Earth Systems and Environment*, *2*(1), 67-84.

Ahmed, R., Ahmad, S. T., Wani, G. F., Ahmed, P., Mir, A. A., & Singh, A. (2021). Analysis of landuse and landcover changes in Kashmir valley, India—a review. *GeoJournal*, 1-13.

Alam, A., Bhat, M. S., & Maheen, M. (2020). Using Landsat satellite data for assessing the land use and land cover change in Kashmir valley. *GeoJournal*, *85*(6), 1529-1543.

Arnold, J. G., Moriasi, D. N., Gassman, P. W., Abbaspour, K. C., White, M. J., Srinivasan, R., Santhi, C., Harmel, R. D., van Griensven, A., Van Liew, M. W., Kannan, N. & Jha, M. K. (2012). SWAT: Model use, calibration, and validation. *Transactions of the ASABE*, *55*(4), 1491-1508.

Asadieh, B., & Krakauer, N. Y. (2017). Global change in streamflow extremes under climate change over the 21st century. *Hydrology and Earth System Sciences*, *21*(11), 5863-5874.

Ashraf A., Hanif-ur-Rehman, (2019). "Upstream and Downstream Response of Water Resource Regimes to Climate Change in the Indus River Basin", *Arabian Journal of Geosciences*, 12:516.

Azari, M., Moradi, H. R., Saghafian, B., & Faramarzi, M. (2016). Climate change impacts on streamflow and sediment yield in the North of Iran. *Hydrological Sciences Journal*, *61*(1), 123-133.

Barnett T. P., Adam J.C., Lettenmaier D. P., (2005). "Potential Impacts of a Warming Climate on Water Availability in Snow-Dominated Regions", *Nature – Reviews*, Vol 438.

Basnyat, P., Teeter, L. D., Lockaby, B. G., & Flynn, K. M. (2000). The use of remote sensing and GIS in watershed level analyses of non-point source pollution problems. *Forest Ecology and Management*, *128*(1-2), 65-73.

Belvederesi, C., Dominic, J. A., Hassan, Q. K., Gupta, A., & Achari, G. (2020). Predicting river flow using an AI-based sequential adaptive neuro-fuzzy inference system. *Water*, *12*(6), 1622.

Bolch, T. (2017). Asian glaciers are a reliable water source. *Nature*, *545*(7653), 161-162.

Buras, A., & Menzel, A. (2019). Projecting tree species composition changes of European forests for 2061–2090 under RCP 4.5 and RCP 8.5 scenarios. *Frontiers in Plant Science*, *9*, 1986.

Campbell, J. B., & Wynne, R. H. (2011). *Introduction to Remote Sensing*. Guilford Press.

Chanapathi, T., & Thatikonda, S. (2020). Investigating the impact of climate and land-use land cover changes on hydrological predictions over the Krishna river basin under present and future scenarios. *Science of the Total Environment*, *721*, 137736.

Chaturvedi, R. K., Joshi, J., Jayaraman, M., Bala, G., & Ravindranath, N. H. (2012). Multi-model climate change projections for India under representative concentration pathways. *Current Science*, 791-802.

Congalton, R. G., & Green, K. (2019). *Assessing the accuracy of remotely sensed data: principles and practices*. CRC press.

Congalton, R. G., Plourde, L., & Bossler, J. (2002). Quality assurance and accuracy assessment of information derived from remotely sensed data. *Manual of geospatial science and technology*, 349-361.

Croitoru A. E., Minea I. (2014). "The Impact of Climate Changes on Rivers Discharge in Eastern Romania", *Theoretical and Applied Climatology*, 120(3-4), 563–573.

Dad, J. M., Muslim, M., Rashid, I., & Reshi, Z. A. (2021). Time series analysis of climate variability and trends in Kashmir Himalaya. *Ecological Indicators*, *126*, 107690.

Dai, A., Zhao, T., & Chen, J. (2018). Climate change and drought: a precipitation and evaporation perspective. *Current Climate Change Reports*, *4*(3), 301-312.

Deng, X., Shi, Q., Zhang, Q., Shi, C., & Yin, F. (2015). Impacts of land use and land cover changes on surface energy and water balance in the Heihe River Basin of China, 2000–2010. *Physics and Chemistry of the Earth, Parts A/B/C*, *79*, 2-10.

Diallo, Y., Hu, G., & Wen, X. (2009). Applications of remote sensing in land use/land cover change detection in Puer and Simao Counties, Yunnan Province. *Journal of American Science*, *5*(4), 157-166.

Domroes, M., & El-Tantawi, A. (2005). Recent temporal and spatial temperature changes in Egypt. *International Journal of Climatology: A Journal of the Royal Meteorological Society*, *25*(1), 51-63.

Drogue, G., Pfister, L., Leviandier, T., El Idrissi, A., Iffly, J. F., Matgen, P., ... & Hoffmann, L. (2004). Simulating the spatio-temporal variability of streamflow response to climate change scenarios in a mesoscale basin. *Journal of Hydrology*, *293*(1-4), 255-269.

Elmahdy, S., Mohamed, M., & Ali, T. (2020). Land use/land cover changes impact on groundwater level and quality in the northern part of the United Arab Emirates. *Remote Sensing*, *12*(11), 1715.

Enderle, D. I., & Weih Jr, R. C. (2005). Integrating supervised and unsupervised classification methods to develop a more accurate land cover classification. *Journal of the Arkansas Academy of Science*, *59*(1), 65-73.

Fayaz, A., ul Shafiq, M., Singh, H., & Ahmed, P. (2020). Assessment of spatiotemporal changes in land use/land cover of North Kashmir Himalayas from 1992 to 2018. *Modeling Earth Systems and Environment*, 1-12.

Fowler H.J., Archer D. R.,(2005). "Conflicting Signals of Climate Change in the Upper Indus Basin", *Journal of Climate,* Vol 19 – 4276.

Fu G., Charles S. P., Chiew F. H. S., (2007). "A Two-Parameter Climate Elasticity of Streamflow Index to Assess Climate Change Effects on Annual Streamflow", *Water Resources Research,* Vol 43 – W11419.

Gajbhiye S., Meshram C., Mirabbasi R., Sharma S. K., (2015). "Trend Analysis of Rainfall Time Series for Sindh River Basin in India", *Theoretical and Applied Climatology,* 125(3-4), 593–608.

Ganaie, T. A., Jamal, S., & Ahmad, W. S. (2020). Changing land use/land cover patterns and growing human population in Wular catchment of Kashmir Valley, India. *GeoJournal*, 1-18.

Gassman, P. W., Sadeghi, A. M., & Srinivasan, R. (2014). Applications of the SWAT model special section: overview and insights. *Journal of Environmental Quality*, *43*(1), 1-8.

Gazi, M. Y., Rahman, M. Z., Uddin, M. M., & Rahman, F. A. (2020). Spatio-temporal dynamic land cover changes and their impacts on the urban thermal environment in the Chittagong metropolitan area, Bangladesh. *GeoJournal*, 1-16.

Gocic M., Trajkovic S., (2013). "Analysis of Changes in Meteorological Variables Using Mann-Kendall and Sen's Slope Estimator Statistical Tests in Serbia", *Global and Planetary Change,* 100, 172–182.

Grecchi, R. C., Gwyn, Q. H. J., Bénié, G. B., Formaggio, A. R., & Fahl, F. C. (2014). Land use and land cover changes in the Brazilian Cerrado: A multidisciplinary approach to assess the impacts of agricultural expansion. *Applied Geography*, *55*, 300-312.

Gujree I., Wani I., Muslim M., Farooq M., Meraj G., (2017). "Evaluating the Variability and Trends in Extreme Climate Events in the Kashmir Valley using PRECIS RCM Simulations", *Modeling Earth Systems and Environment*, 3(4), 1647–1662.

Güler, M., Yomralıoğlu, T., & Reis, S. (2007). Using landsat data to determine land use/land cover changes in Samsun, Turkey. *Environmental monitoring and assessment*, *127*(1), 155-167.

Guo, H., Hu, Q., & Jiang, T. (2008). Annual and seasonal streamflow responses to climate and land-cover changes in the Poyang Lake basin, China. *Journal of Hydrology*, *355*(1-4), 106-122.

Gupta, H. V., Kling, H., Yilmaz, K. K., & Martinez, G. F. (2009). Decomposition of the mean squared error and NSE performance criteria: Implications for improving hydrological modelling. *Journal of hydrology*, *377*(1-2), 80-91.

Gupta, S. (2018). Forests, state and people: a historical account of forest management and control in J&K. In *Contesting Conservation* (pp. 121-141). Springer, Cham.

Haider, H., Zaman, M., Liu, S., Saifullah, M., Usman, M., Chauhdary, J. N., & Waseem, M. (2020). Appraisal of climate change and its impact on water resources of Pakistan: a case study of Mangla Watershed. *Atmosphere*, *11*(10), 1071.

Iqbal, M., & Sajjad, H. (2014). Watershed prioritization using morphometric and land use/land cover parameters of Dudhganga Catchment Kashmir Valley India using spatial technology. *J Geophys Remote Sens*, *3*, 115.

Ismail H., Rowshon M. K., Hin L. S., Abdullah A. F. B., Nasidi N. M., (2020). "Assessment of Climate Change Impact on Future Streamflow at Bernam River Basin Malaysia", *Earth and Environmental Science*, 540, 012040.

Jeelani G., Feddema J. J., Veen C. J., Stearns L., (2012). "Role of Snow and Glacier Melt in controlling River Hydrology in Lidder Watershed (Western Himalaya) Under Current and Future Climate", *Water Resources Research*, Vol 48 – W12508,.

Jensen, J. R. (1986). *Introductory digital image processing: a remote sensing perspective*. Univ. of South Carolina, Columbus.

Jiang, Q., Qi, Z., Tang, F., Xue, L., & Bukovsky, M. (2020). Modelling climate change impact on streamflow as affected by snowmelt in Nicolet River Watershed, Quebec. *Computers and Electronics in Agriculture*, *178*, 105756.

Jodar-Abellan, A., Valdes-Abellan, J., Pla, C., & Gomariz-Castillo, F. (2019). Impact of land use changes on flash flood prediction using a sub-daily SWAT model in five Mediterranean ungauged watersheds (SE Spain). *Science of the Total Environment*, *657*, 1578-1591.

Kahya E., Kalayci S., (2004). “Trend Analysis of Streamflow in Turkey”, *Journal of Hydrology*, 289, 128 – 144.

Kantakumar, L. N., & Neelamsetti, P. (2015). Multi-temporal land use classification using hybrid approach. *The Egyptian Journal of Remote Sensing and Space Science*, *18*(2), 289-295.

Kendall M. G., “Rank Correlation Methods”, *Griffin* – 1948.

Kundzewicz Z. W., Kanae S., Seneviratne S. I., Handmer J., Nicholls N., Peduzzi P., Sherstyukov B., (2014). “Flood Risk and Climate Change: Global and Regional Perspectives.” *Hydrological Sciences Journal,* 59(1), 1–28.

Lee T. M., Markowitz E. M., Howe P. D., Ko C. Y., Leiserowitz A. A., (2015). “Predictors of Public Climate Change Awareness and Risk Perception Around the World”, *Nature Climate Change,* 5(11) 1014-1020.

Mahmood R., Jia S., (2017). “Spatial and temporal hydro-climatic trends in the transboundary Jhelum River basin”, *Journal of Water and Climate Change*, 8(3), 423–440.

Mango, L. M., Melesse, A., McClain, M. E., Gann, D., & Setegn, S. G. (2010). A modeling approach to determine the impacts of land use and climate change scenarios on the water flux of the upper Mara River.

Marazi A., Romshoo S. A., (2018). “Streamflow Response to Shrinking Glaciers under Changing Climate in the Lidder Valley, Kashmir Himalayas”, *Journal of Mountain Science,* 15(6), 1241–1253.

Meraj G., Romshoo S. A., Yousuf A. R., Altaf S., Altaf F., (2015a). “Assessing the Influence of Watershed Characteristics on the Flood Vulnerability of Jhelum Basin in Kashmir Himalaya: reply to comment by Shah 2015”, *Natural Hazards,* 78(1), 1–5.

Meraj G., Romshoo S. A., Yousuf A. R., Altaf S., Altaf F., (2015b). “Assessing the Influence of Watershed Characteristics on the Flood Vulnerability of Jhelum Basin in Kashmir Himalaya”, *Natural Hazards*, 77(1), 153–175.

Metzger, J. C., Landschreiber, L., Gröngröft, A., & Eschenbach, A. (2014). Soil evaporation under different types of land use in southern African savanna ecosystems. *Journal of Plant Nutrition and Soil Science*, *177*(3), 468-475.

Minea I., Croitoru A. E., (2017). “Groundwater Response to Changes in Precipitations in North-Eastern Romania”, *Environmental Engineering and Management Journal,* 16(3), 643–651.

Moriasi, D. N., Gitau, M. W., Pai, N., & Daggupati, P., (2015). Hydrologic and water quality models: Performance measures and evaluation criteria. *Transactions of the ASABE*, *58*(6), 1763-1785.

Nash, J. E., & Sutcliffe, J. V. (1970). River flow forecasting through conceptual models part I—A discussion of principles. *Journal of hydrology*, *10*(3), 282-290.

Neitsch, S. L., Arnold, J. G., Kiniry, J. R., & Williams, J. R. (2011). *Soil and water assessment tool theoretical documentation version 2009*. Texas Water Resources Institute.

Nie, W., Yuan, Y., Kepner, W., Nash, M. S., Jackson, M., & Erickson, C. (2011). Assessing impacts of Landuse and Landcover changes on hydrology for the upper San Pedro watershed. *Journal of Hydrology*, *407*(1-4), 105-114.

Nilawar, A. P., & Waikar, M. L. (2019). Impacts of climate change on streamflow and sediment concentration under RCP 4.5 and 8.5: A case study in Purna river basin, India. *Science of the total environment*, *650*, 2685-2696.

Olivera, F., & DeFee, B. B. (2007). Urbanization and Its effect on runoff in the Whiteoak Bayou Watershed, Texas 1. *JAWRA Journal of the American Water Resources Association*, *43*(1), 170-182.

Owuor, S. O., Butterbach-Bahl, K., Guzha, A. C., Rufino, M. C., Pelster, D. E., Díaz-Pinés, E., & Breuer, L. (2016). Groundwater recharge rates and surface runoff response to land use and land cover changes in semi-arid environments. *Ecological Processes*, *5*(1), 1-21.

Petropoulos, G. P., Kalivas, D. P., Georgopoulou, I. A., & Srivastava, P. K. (2015). Urban vegetation cover extraction from hyperspectral imagery and geographic information system spatial analysis techniques: case of Athens, Greece. *Journal of Applied Remote Sensing*, *9*(1), 096088.

Pramit, V., Aditya, R., Srivastava, P. K., & Raghubanshi, A. S. (2020). Appraisal of kappa-based metrics and disagreement indices of accuracy assessment for parametric and nonparametric techniques used in LULC classification and change detection. *Modelling Earth Systems and Environment*, *6*(2), 1045-1059.

Purkis, S. J., & Klemas, V. V. (2011). *Remote sensing and global environmental change*. John Wiley & Sons.

Rasool, R., Fayaz, A., ul Shafiq, M., Singh, H., & Ahmed, P. (2021). Land use land cover change in Kashmir Himalaya: Linking remote sensing with an indicator based DPSIR approach. *Ecological Indicators*, *125*, 107447.

Rather, N. A., Lone, P. A., Reshi, A. A., & Mir, M. M. (2013). An analytical study on production and export of fresh and dry fruits in Jammu and Kashmir. *International Journal of Scientific and Research Publications*, *3*(2), 1-7.

Romshoo S. A., Altaf S., Rashid I., Dar R. A., (2017a). "Climatic, geomorphic and anthropogenic drivers of the 2014 extreme flooding in the Jhelum basin of Kashmir, India", *Geomatics, Natural Hazards and Risk,* 9(1), 224–248.

Romshoo S. A., Dar R. A., Rashid I., Marazi A., Ali N., Zaz S. N., (2015a). "Implications of Shrinking Cryosphere Under Changing Climate on the Streamflow in the Lidder Catchment in the Upper Indus Basin, India", *Arctic, Antarctic, and Alpine Research,* 47(4), 627–644.

Romshoo, S. A., Dar, R. A., Rashid, I., Marazi, A., Ali, N., & Zaz, S. N. (2015b). Implications of shrinking cryosphere under changing climate on the streamflows in the Lidder catchment in the Upper Indus Basin, India. *Arctic, antarctic, and alpine research*, *47*(4), 627-644

Schiermeier Q., (2018). "Droughts, Heatwaves and Floods: How to Tell When Climate Change is to Blame.", *Nature,* 560 (7716), 20–22.

Sen P. K., (1968). "Estimates of the Regression Coefficient Based on Kendall's Tau", *Journal of the American Statistical Association,* 63, 1379 – 1389.

Shafiq M., Ashraf I., Islam Z., Ahmed P., Dimri A., P., (2020). "Response of Streamflow to Climate Variability in the source region of Jhelum River Basin in Kashmir Valley, India", *Natural Hazards,* 104, 611-637.

Shah, M. I., Khan, A., Akbar, T. A., Hassan, Q. K., Khan, A. J., & Dewan, A. (2020). Predicting hydrologic responses to climate changes in highly glacierized and mountainous region Upper Indus Basin. *Royal Society open science*, *7*(8), 191957.

Smitha, P. S., Narasimhan, B., Sudheer, K. P., & Annamalai, H. (2018). An improved bias correction method of daily rainfall data using a sliding window technique for climate change impact assessment. *Journal of Hydrology*, *556*, 100-118.

Tabari H., Somee B. S., Zadeh M. R., (2011a). "Testing for Long-term Trends in Climatic Variables in Iran", *Atmospheric Research,* 100(1), 132–140.

Tabari, H., & Talaee, P. H. (2011b). Analysis of trends in temperature data in arid and semi-arid regions of Iran. *Global and Planetary Change*, *79*(1-2), 1-10.

Tan M. L., Samat N., Chan N. W., Lee A. J., Li C., (2019) "Analysis of Precipitation and Temperature Extremes over the Muda River Basin, Malaysia", *Water,* 11(2) 283.

Teutschbein, C., & Seibert, J. (2012). Bias correction of regional climate model simulations for hydrological climate-change impact studies: Review and evaluation of different methods. *Journal of hydrology*, *456*, 12-29.

Trang, N. T. T., Shrestha, S., Shrestha, M., Datta, A., & Kawasaki, A. (2017). Evaluating the impacts of climate and land-use change on the hydrology and

nutrient yield in a transboundary river basin: A case study in the 3S River Basin (Sekong, Sesan, and Srepok). *Science of the Total Environment*, *576*, 586-598.

Tripathi, A., & Mishra, A. K. (2017). Knowledge and passive adaptation to climate change: An example from Indian farmers. *Climate Risk Management*, *16*, 195-207.

Van der Werf, G. R., Morton, D. C., DeFries, R. S., Olivier, J. G., Kasibhatla, P. S., Jackson, R. B. & Randerson, J. T. (2009). CO_2 emissions from forest loss. *Nature geoscience*, *2*(11), 737-738.

Wani R. A., (2014). "Historical Temporal Trends of Climatic Variables Over Kashmir Valley and Discharge Response to Climate Variability in Upper Jhelum Catchment", *Advances in Geographical and Environmental Sciences*, 103–112.

Weih, R. C., & Riggan, N. D. (2010). Object-based classification vs. pixel-based classification: Comparative importance of multi-resolution imagery. *The International Archives of the Photogrammetry, Remote Sensing and Spatial Information Sciences*, *38*(4), C7.

Welde, K., & Gebremariam, B. (2017). Effect of land use land cover dynamics on hydrological response of watershed: Case study of Tekeze Dam watershed, northern Ethiopia. *International Soil and Water Conservation Research*, *5*(1), 1-16.

Xu R., Hu H., Tian F., Li C., Khan M. Y. A., (2018) "Projected Climate Change Impacts on Future Streamflow of the Yarlung Tsangpo-Brahmaputra river", *Hydrology and Earth System Sciences*.

Yaseen, M., Waseem, M., Latif, Y., Azam, M. I., Ahmad, I., Abbas, S., Sarwar, M. K., & Nabi, G. (2020). Statistical Downscaling and Hydrological Modelling-Based Runoff Simulation in Trans-Boundary Mangla Watershed Pakistan. *Water*, *12*(11), 3254.

Yifru, B. A., Chung, I. M., Kim, M. G., & Chang, S. W. (2021). Assessing the effect of land/use land cover and climate change on water yield and groundwater recharge in East African Rift Valley using integrated model. *Journal of Hydrology: Regional Studies*, *37*, 100926.

Zaz S. N., Romshoo S. A., Krishnamoorthy R. T., Viswanadhapalli Y., (2019) " Analyses of Temperature and Precipitation in the Indian Jammu and Kashmir Region for the 1980–2016 Period: Implications for Remote Influence and Extreme Events", *Atmospheric Chemistry and Physics*, 19(1), 15–37.